Low Firing Temperature Absorption Chiller System

by

KEVIN A. GOODHEART

A thesis submitted in partial fulfillment
of the requirements for the degree of

MASTER OF SCIENCE

(MECHANICAL ENGINEERING)

at the

UNIVERSITY OF WISCONSIN – MADISON

DECEMBER 2000

Approved by

_____

Professor Sanford A. Klein
December 12, 2000

ABSTRACT

Two types of the absorption chillers, the single and half effect cycles, can operate using low temperature hot water. The advantage of the single effect over the half effect cycle is the higher COP but the single effect has a narrower temperature operating range. The half effect has the capability of using lower hot water temperature but the lower COP increases operating cost and requires investing a larger cooling tower. A detailed computer model was written for the single and half effect cycles based on heat transfer coefficients for the inside and outside tubes of each component [generator, absorber, condenser, and evaporator], energy, mass, salt balances, and rate equations. The single effect component model was calibrated with known data from a US absorption chiller manufacturer. The cooling tower was modeled using the analogy approach, calibrated and validated with performance data from a cooling tower manufacturer. Capacity and dollars per ton were used to determine lower limits on the firing temperature. The results show that at 225^{o}F (107 C) at 2000 gpm (7570 L/min) of hot water, the cost to maintain capacity starts to change for the single effect cycle. At 205^{o}F (99 C) the cost to maintain capacity increases rapidly. The half effect cycle can maintain capacity at temperatures as low as 185^{o}F (82 C) hot water at 2000 gpm (7570 L/min) without a large increase in capital investment. The capital cost for the half effect chiller system is 200 $/ton (57 $/kW) more than the single effect, using hot water temperatures above 200 ^{o}F (93 C). The single effect cycle can only be competitive with an electric centrifugal chiller if the heat source is free or a combination of high electrical cost with a low cost of heat.

The half effect cycle can be competitive with the single effect if the waste heat is free and the temperature is below 200^{o}F (93 C) or has a low flow rate in the range of 1000 gpm (3785 L/min).

ACKNOWLEDGMENTS

The first acknowledgment is to recognize Ken Schultz for making this project possible and being available to answer questions and supply information on absorption chillers. I would like to thank the Trane Company for their financial support for the project [The facts and findings expressed in this thesis do not necessarily reflect the views held by the Trane Company].

My second acknowledgment is to recognize the importance of using EES in modeling systems. With this model I can solve for the capacity given the UA of the generator and in a second I can solve for the UA of the generator given the capacity. The above procedure is done by changing the arrangement of how 700 equations are solved. I came to this lab with a set of books and a HP calculator and I am leaving this lab with a set of books and the ability to model systems using EES. It has been a great pleasure to work with Sanford Klein the developer of EES on this project and as his student in Thermodynamics. Without EES I would not have had the inspiration to examine the different facets of an absorption chiller and an absorption chiller system.

I would also like to acknowledge William Beckman the director of the Solar Energy lab for making it possible to have this place to study and learn. The way in which he asks questions is encouraging because it promotes one to "think" about what they are doing.

I would like to thank my colleagues in the lab for letting me use the same computer, listening to my problems, hearing my cheers when something worked, and all around making my time in the SEL lab a memorable occasion.

And finally

Gratiam soli agere volo
quia facit dies tempus degendos
quod litteras in annis
meas faciet obsoletas futuris

Latin translation by Rüdiger Spahl

TABLE OF CONTENTS

LIST OF FIGURES

LIST OF TABLES

NOMENCLATURE

Subscripts

1,7,8,23,24,24t25l,25v,30,31,1a,1b,11,25,40,41,50,51 representative state points for the absorption chiller

30sat	saturated steam inside the generator
11p	equilibrium temperature entering the absorber
7p	equilibrium temperature entering the generator
a	absorber
ab	absorption chiller
ab,ct	absorption chiller cooling tower
a,i, a,o	air inside and outside
a,eff	air effective
c	condenser
e	evaporator
ec	electric chiller
ec,ct	electric chiller cooling tower
f	film
fan,nom,i	nominal fan speed
g	generator
ft	finned tube
hs	heat source
hr	heat recovery
i	inside
l	liquid
o	outside
sat	saturated
st	smooth tube
s,eff	saturated effective
v	vapor
w	water

Variables

d	Diamter [ft], discount rate
D	Ratio of down payment to initial investment
C	Capital cost [$]
C_h	break-even cost of the heat source [$]
C_{min}	Minimum specific heat of water [Btu/lb_m-F]
C_s	Effective specific heat, which is a change in enthalpy divided by a change temperature along a saturation line [Btu/lb_m-F].

C_w	Specific heat of water [Btu/lb_m-F]
f_{abs}	Fraction of LC absorber tubes in half-effect cycle
f_{gen}	Fraction of LT generator tubes in the half-effect cycle
F_o	Rated volume flow rate of hot water [gpm]
F	Volume flow rate of hot water [gpm]
g	Gravitational constant [ft/s^2]
h	Enthalpy [Btu/lb_m] / heat transfer coefficient [Btu/hr-ft^2-F]
K	Overall heat transfer coefficient [Btu/hr-F]
K_o	Rated overall heat transfer coefficient [Btu/hr-F]
LCC	Life cycle cost [$]
Le	Length of tubes
LMTD	Log mean temperature difference
$\dot{m}$	Mass flow rate [lb_m/hr]
m	Annual mortgage interest rate
M_s	Ratio of first year cost (maintenance, insurance) to initial investment
NC	Number of tubes in a column
N_{cells}	Number of cells in the cooling tower
N_D	Depreciation lifetime [years]
N_e	Period of economic analysis [year]
N_L	Term of the loan [years]
$N_{min,}$	Year of mortgage payments min(N_L or N_e) [years]
N'_{min}	Years which depreciation contributes min(N_D or N_e).
Nu	Nusselt Number
NTU	Heat transfer units
P_1	Ratio of life cycle fuel cost savings to first year fuel cost [~ N_e/2]
P_2	Life cycle expenditures because of the capital investment. [~ 0.8-1.2]
P	Pressure [psia]
P_{elec}	Electric Power consumption [hp]
P_{fan}	Fan Power [hp]
Pr	Prandtl Number
Q	Heat transfer rate [Btu/hr]
R	Resistance of tubes [Btu/hr-ft^2-F].
Re_D	Reynolds number in pipe
Re_f	Film Reynolds number
R_v	Ratio of the resale value
Subcool	Subcooling at the outlet of the absorpber [^oF]
Spill	Fraction of spill out of the evaporator
T	Temperature [^oF]
$\overline{t}$	Effective income tax rate.
t	Property tax based on assessed value
Tube	Number of tubes
UA	Overall heat transfer coefficient [Btu/hr-F]
V	Ratio of assessed valuation of the system in first year to the initial investment
w	Humidity ratio of the air [lbm_w/$lbm_{dry,a}$]
x	LiBr concentration

Greek

Γ	Film flow rate [lb_m/ft-hr]
ε	Effectiveness of heat exchanger [0.-1.]
μ	Viscosity of the solution [lb_m/ft-hr]
φ	Spraying density [lb_m/hr-ft]
η	efficiency of equipment
γ	Ration of air flow to nominal air flow

CHAPTER 1

INTRODUCTION

The purpose of this project is examine the performance of a current single-effect absorption chiller and determine what design changes are needed so that the chiller can operate using low temperature hot water. For example, if there is a hot water source at 205^{o}F with a flow rate of 1000 gpm, what changes are needed to a machine that normally operates at 230^{o}F and 1000 gpm to obtain the same capacity. The second phase of the project involves designing a half-effect cycle to operate on low-temperature hot water. The performance characteristics of the half-effect cycle are examined by changing the hot water flow rate, the cooling water temperature, and the flow arrangements of the cooling and heat source flow. The half-effect and single-effect cycles are compared to see which one is more competitive for a specified fuel source temperature.

1.1 Why Absorption?

Absorption units are able to generate a cooling effect with a heat source. The heat source can come in the form of natural gas, solar, coal, co-generation, or an industrial waste stream. A main advantage of absorption units is their ability to utilize waste heat streams that would be otherwise discarded.

1.2 What is Absorption?

The standard vapor compression refrigeration system is a condenser, evaporator, throttling valve, and a compressor. Figure 1-1 is a schematic of the components and flow arrangements for the vapor compression cycle.

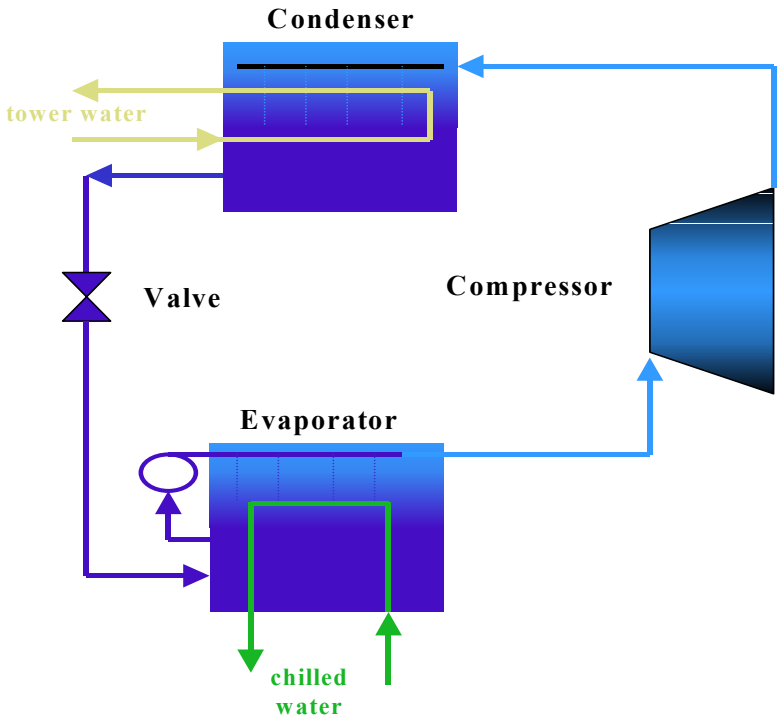

Figure 1-1. Schematic of a centrifugal chiller.

Absorption refrigeration systems replace the compressor with a generator and an absorber. The generator is a shell and tube heat exchanger, which sprays a LiBr-H_2O solution over heated tubes to boil off the water [refrigerant]. The refrigerant vapor then enters the condenser. The absorber is a shell and tube heat exchanger that draws in the water vapor from the evaporator and sprays the LiBr-H_2O solution from the generator over cooling water tubes to absorb the water vapor. During the absorption process a portion of the heat is transferred to the cooling water, which comes from the cooling tower. In Figure 1-2 the generator and absorber replace the compressor in Figure 1-1.

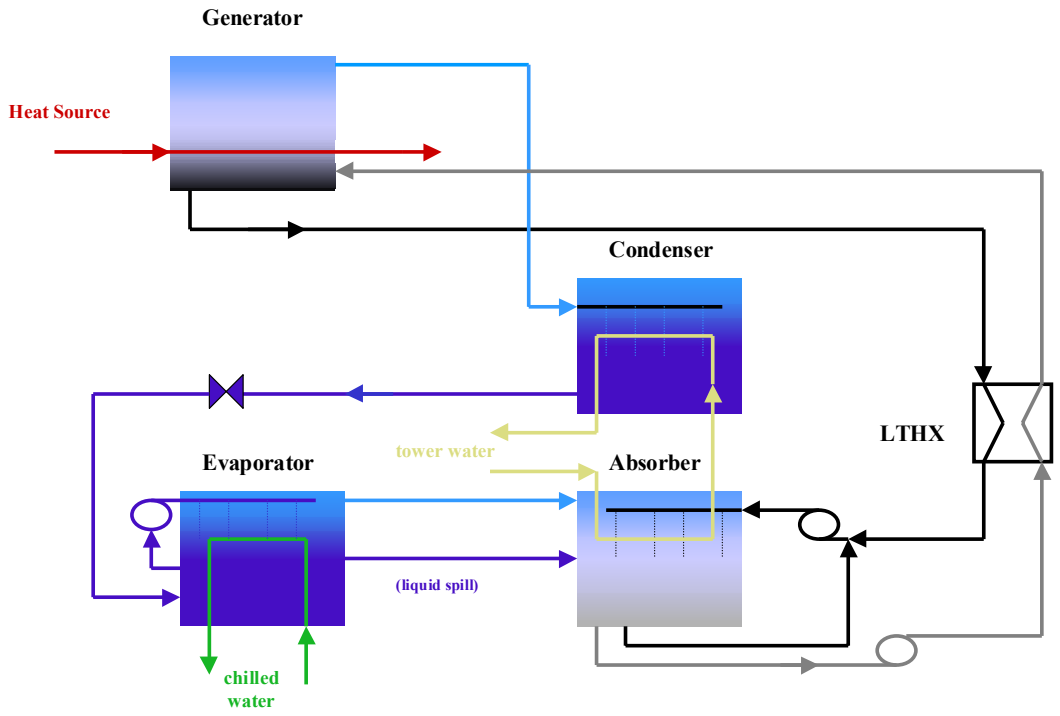

Figure 1-2. Schematic of the single-effect absorption chiller.

The ability for absorption to work is determined by the type of fluids that are chosen. The LiBr-H_2O combination uses the property that LiBr has an affinity for water. That is the chemical potential is favorable for the absorption of water into LiBr. The water in an

absorption cycle acts as the refrigerant and thus is the vapor leaving the evaporator. In a vapor compression refrigeration cycle, the water vapor would be compressed, but with absorption the water vapor is absorbed into the LiBr-H_2O solution and thus a liquid is pumped instead of a vapor. The pumping of a liquid requires less energy than the compression of a vapor. Absorption uses heat instead of electrical power to provide a cooling effect. The high pressure LiBr solution is then sent to the generator to recover the water that was absorbed. Figure 1-2 is a schematic of the components but Figure 1-3 is a realistic picture of the absorption process.

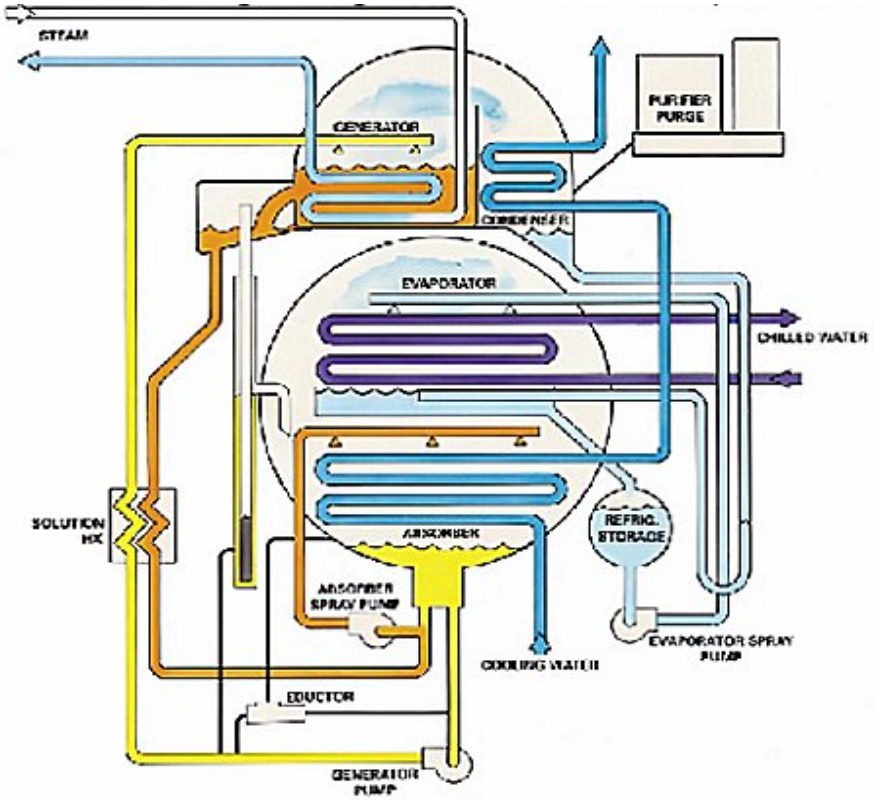

Figure 1-3. Single-effect absorption chiller (US chiller Manufacturer, 2000).

Figure 1-3 shows a cross-section of a single-effect absorption chiller. The chiller is split into two regions the generator-condenser at the top and the absorber-evaporator in the bottom. The sprays are used to ensure compete wetting of the tubes for better heat transfer. There is also a purge system that removes non-condensable gases from the system, which inhibit absorption of the water vapor. The solution heat exchanger on the bottom left in Figure 1-3 is used to reduce the heat input at the generator.

1.3 History of large tonnage absorption units

The following summary on the history of large tonnage [>100 tons] absorption units is taken from (Plzak, 1996).

Before the 1970's fuel oil and natural gas were inexpensive and readily available. Electricity was also inexpensive and thus efficiency was not a concern when operating a chiller. During this time an equal number of absorption and electric centrifugal chiller were sold.

In the 1970's, a steady increase in energy costs caused the chiller industry to examine the efficiency of their units. The double-effect unit was developed to increase the COP [Q_{cool}/Q_{in}], and thus their share in the market place using high-pressure steam increased. The oil embargo increased the price of fossil fuels more dramatically then electric energy prices and thus overnight killed the domestic absorption market. The absorption market has never recovered to its pre 1973 levels.

The 1980's saw flat or decreasing natural gas prices and a steady increase in electrical rates. This resulted in the growth of the newly developed single and double effect direct-fired absorption unit in the mid to late 1980's. A direct-fired unit is one is which natural gas is combusted in the generator instead of using the gas to create steam or hot water. The growth was also a result of the gas and electric utility initiatives, which supported programs for gas cooling in the summer, to keep the supply of natural gas constant throughout the year. The phase out of CFC based refrigerants used in electric centrifugal chillers also helped boost the direct-fired market.

The current single effect market is small but stable and is used in applications where low-grade heat is available. The applications are chemical and manufacturing processes, small co-generation systems, and buildings with existing low-pressure boilers. The current market for the single effect is about 50% of the total absorption market.

1.4 Where are commercial absorption units found?

The most common applications for absorption units are in situations with high electrical cost or a heat source of low pressure steam or hot water that is free. The types of co-generation applications are

- District heating and cooling networks
- Industry / Facilities with waste heat
- Schools / Hospitals

The single-effect is applicable in areas with sources of low-grade heat and low water costs (IEA, 1999). The single-effect unit can be competitive with an electric chiller where electric prices are high or the chiller operates a large portion of the year (IEA, 1999). The reason for the advantage of longer operation time is because the operating cost is much less for the absorption chiller and thus this could make up for the higher capital investment. Another aspect of absorption is that twice as much water is needed for the cooling tower and thus low water cost is also an important factor when deciding on absorption (IEA, 1999).

There is a need to develop systems for applications with temperatures in the range of 140-176^{o}F (60-80 C) (Lamp and Ziegler, 1996). The most viable alternative to cool with these temperatures is to use the half–effect cycle.

1.5 Who makes Absorption units?

Table 1-1 lists some of the companies that make absorption units and the characteristics of these units.

Table 1-1. Types of Absorption Units on the Market*

	TRANE	YORK	CARRIER	YAZAKI	SANYO
Capacity (Tons)	100-1500	100-1500	108-608	10	100-1500
Heat Source					
Hot Water	200-270°F	210°F	250°F	167-212°F	94°F
Steam	14 psig	15 psig	15 psig		11.4 psig (8kg/cm2-G)
Consumption					9.7lb/hr-Ton
Natural Gas					11905 Btu/hr-Ton
Chilled Water	40-50 °F	45°F	55°F No cooling Tower 40-55°F	48°F	41-54°F

*All data in the table is based on company website information.

CHAPTER 2

REVIEW OF PUBLISHED WORK ON LOW TEMPERATURE HEAT SOURCE APPLICATIONS

2.1 Overview

The purpose of this chapter is to review the published research done on the single effect absorption unit using a low temperature heat source. Lamp and Ziegler (1996) summarize the idea of using low temperature heat as follows.

> "Since the minimum driving temperature is determined by the boundary conditions of the evaporator, condenser, and absorber, the only way to lower the driving temperature is to increase the heat exchanger area. The above conclusion results in general to an economical question rather than a technical question for achieving lower driving temperatures."

There are many published papers on the single effect unit but it is the focus of this chapter to review low temperature applications with a single-effect lithium bromide absorption unit. For example there are single effect units with different working fluids [Water-NH_3] and there

are also solid absorption units. Chapter 2 also provides a published review of the half-effect lithium bromide cycle.

2.2 Low temperature heat source applications using the single-effect absorption unit

Lamp and Ziegler (1996) point out that it would be naive to obtain low firing temperatures by only increasing the size of the generator. They use the following example,
By doubling the generator area, 0.3 tons [1 kw] of cooling can be obtained with 174^{o}F [79 C] hot water. By increasing the size of all heat exchangers by the same total area, 0.3 tons of cooling can be obtained with 172^{o}F [77.6 C] hot water.

The above example demonstrates the importance of not only looking at the generator when designing an absorption unit to run off of a low temperature heat source. It is important to optimize the distribution of heat exchanger area.

A single-effect lithium bromide absorption chiller computer model was validated with experimental data (Homma et al., 1994). The capacity of the absorption chiller is 30 Tons (105.5 kW) and is driven by waste heat in the form of hot water from a gas engine. The absorption model consists of four main components [absorber, generator, evaporator, and condenser]. The model of each component is based on a log–mean temperature difference, energy balance, mass balance, salt balance, and an overall heat transfer coefficient. The form of the overall heat transfer coefficient is

$$UA = UA_o \left(\frac{F}{F_o} \right)^P \qquad [2\text{-}1]$$

where UA is the overall heat transfer coefficient [Btu/hr-F]
F is the volume flow rate of hot water [gpm]
P is a number determined from experiment
$_o$ subscript o means rated value.

The temperature drop across the generator is from 190-181^{o}F (88-83 C) and the evaporator is from 55-46^{o}F (13-8 C). The COP range predicted from the model is around 0.6-0.7. Major conclusions of the paper are.

- The COP and cooling capacity increase with an increase in the hot water inlet temperature over a range of 176-201^{o}F [80 – 94 C], thus having the exhaust gas of the engine being as high as possible is the best design to achieve higher capacities.
- The hot water flow rate can be used to control the generation of unutilized refrigerant by controlling the COP or keeping the COP constant by changing the cooling capacity.
- Decreasing the cooling water inlet temperature can increase the COP and cooling capacity.

If the hot water inlet temperature is decreased, the capacity of the single-effect unit will also decrease. With the addition of a compressor between the absorber and the evaporator the same capacity can be gained with a lower generator temperature (Thornbloom and Nimmo, 1994). Thornbloom and Nimmo (1994) demonstrated this effect on a 1 ton chiller. In order to achieve 1 ton of cooling with the conventional system, the hot water temperature needs to be at 200^{o}F (93.3 C) but with the compressor it can be lowered to 175^{o}F (79.4 C). The COP for both cycles is 0.77 [200^{o}F hot water] and 0.79 [Compressor]. Without the compressor the capacity is reduced to 0.23 tons and a COP of 0.63 with 175^{o}F hot water. A disadvantage of this cycle is the addition of the compressor to compress water vapor. For this example the

extra work was 0.15 hp [117 W], but for larger systems this parasitic load might not be an advantage to reducing operating costs.

A small scale experimental single-effect lithium bromide absorption chiller was used for an experiment in the Hot Springs of Sivas, Turkey (Kececiler,et al.,1999). A computer model was developed based on the experimental data to determine the performance of an absorption chiller. The availability of the geothermal heat source is too low to be used effectively in generating electricity but the hot water source can be used to air condition at 40-50^{o}F (4-10 C) (Kececiler,et al., 1999).

The results from the computer model for the optimum COP are given below.

Heat Source:		
Hot water:	140^{o}F (60 C)	
	7925 gpm	(500 l/s)
	99208 lb_m /hr	(12.5 kg/s)
COP	0.56	
Capacity	64 Tons	(225.5 kW)
Concentration	48% Generator	
	44% Absorber	
Chilled Water	36-37^{o}F	(2-3 C)
Cooling Water	85-96^{o}F	(30-35 C)

The only way Kececiler et al., (1999) were able to utilize such a low temperature heat source is because of the extremely high warm water flow rate. For example, 100 tons with a temperature drop of 10^{o}F would require a volumetric flow rate of approximately 300 gpm.

A parametric study on the input parameters shows an increase in COP for an increase in generator or evaporator temperatures and a decrease in COP for an increase in absorber cooling water temperature (Kececiler et al., 1999).

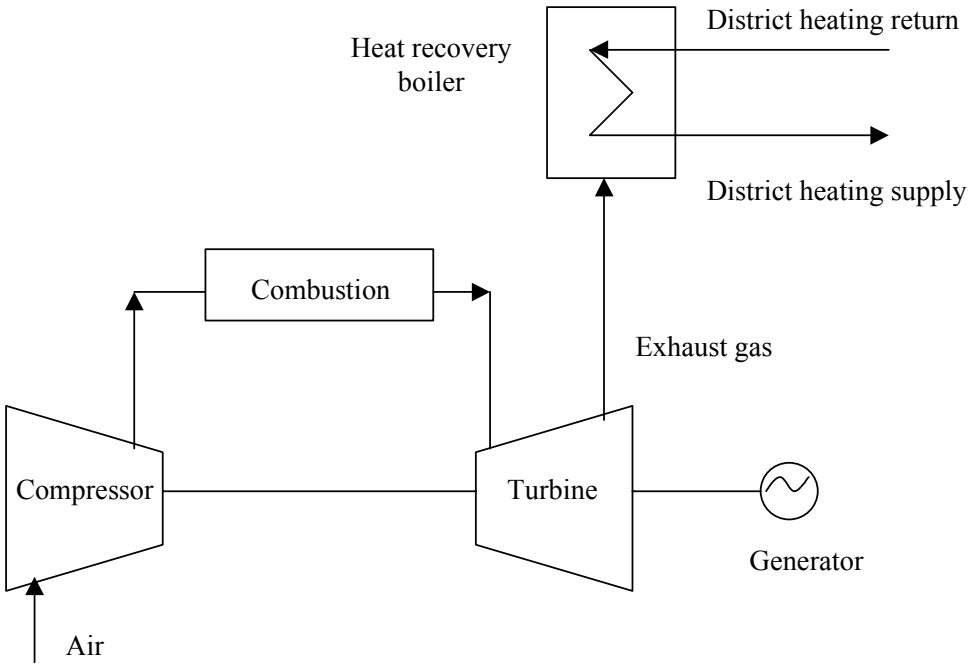

Figure 2-1. Simple CHP using a gas turbine (Meloche et al., 1996)

Bruno et al, (1996) and Meloche et al, (1996) discuss the integration of an absorption chiller in a combined heat and power plant [CHP]. Figure 2-1 is a schematic of a simple combustion turbine CHP. The district heating supply can then be used to run an absorption chiller when the heat supply is greater than the demand.

Other types of CHP systems are a reciprocating cycle or a steam turbine cycle. The electricity produced can be used to run an electric chiller to meet the cooling load and

electrical load or the heat supply can be used with an absorption chiller to meet the cooling load and hot water load. Bruno et al. (1996) examines the absorption unit as a steam consumer, where the steam flow rate is a function of the inlet air flow to the gas turbine, ambient air conditions, and refrigeration load. For Bruno et al. (1996) part of the cooling load is the result of cooling the gas turbine inlet air temperature to 60^{o}F [15 C], for a maximum efficiency. Bruno et al., (1996) concludes that the absorption chiller is economically viable with the gas turbine when the chiller is used to the cool the inlet air to the turbine to increase generator capacity and also cover additional refrigeration needs.

Meloche et al., (1996) assumes a heat supply recovery from the heat recovery boiler at 212^{o}F [100 C] and the heat return back to the boiler at 167^{o}F [75 C]. The gas turbine has an electrical efficiency of 35%, heat efficiency of 53%, and 12% losses. Meloche et al., (1996) examine running the gas turbine at an input of 100 units of fuel and determines the maximum cooling using a compression chiller and an absorption unit.

The calculation is based on maximum chilled water production from all the available energy, which is also a reason for the electricity to chillers to be large for the absorption chiller. The absorption chillers are being supplemented with electrical chillers from the excess electrical output. The net heating output in Table 2-1 is the amount of energy that was not useful enough to drive a heat driven chiller (Meloche et al., 1996).

Table 2-1. Comparison of different systems with a gas turbine CHP (Meloche et al., 1996)

Max Cooling	Electric Drive	1-Stage HW	1-Stage Steam	2-Stage Steam
Fuel Input	100.00	100.00	100.00	100.00
Electricity production	34.63	34.63	34.63	34.63
Thermal to chillers	0.00	51.28	50.10	48.49
Electricity to Chillers	29.85	28.14	28.25	27.77
Electricity to auxiliary	4.78	6.50	6.38	6.86
Net electricity	0.00	0.00	0.00	0.00
Net cooling	175.14	202.97	199.07	221.10
Net heating	53.71	2.42	3.61	5.22

The electricity to auxiliary row in Table 2-1 takes into account energy needed to operate a cooling tower fan and pumps for the cooling and chilled water. For a gas turbine CHP the 2-stage double-effect absorption chiller provides the largest amount of cooling, but the electric chiller is more efficient in terms of total energy output (Meloche et al., 1996). The major conclusions of the paper by (Meloche et al., 1996) are:

- There is no difference in the economics for using a heat driven chiller compared to a compression chiller for a new CHP facility.
- The difference in cooling cost between the different chillers was minimal because of the high cost of the CHP plant and there is a small difference in efficiencies when integrated with cogeneration in cooling mode.

The papers by Meloche et al., (1996) and Bruno et al., (1996) seem to reach different conclusions of integrating absorption chillers with a CHP but the systems they analyzed are different. Where Meloche is maximizing cooling output and Bruno is increasing the

efficiency of the gas turbine by cooling the inlet compressor air temperature. It is impossible to conclude from these two papers if absorption is competitive with electric chillers in CHP plants, because it is based on cooling, heating, electrical load, and ambient conditions.

2.3 Half-effect absorption unit

The half-effect absorption unit can be found in applications where the heat source temperature is too low to be used to fire a single-effect unit (Herold, et al., 1996). The advantage of the half-effect cycle is that the heat-input temperature can be less than the single-effect for the same evaporator and heat rejection temperature. The disadvantage of the half-effect cycle compared to the single-effect is the COP of the half-effect cycle is approximately half of the single-effect, which translates that for a given capacity the heat rejection of the half-effect cycle is larger. A half-effect cycle [50 tons [175 kW]] was built and tested in a laboratory funded by the DOE that confirms the above conclusions from Herold, et al., (1996).

Schweigler et. al (1996) describe a single-effect, half-effect combination unit [SE/HE]. A single-effect machine can operate at 176^{o}F (80 C), but in district heating networks the summer temperature for hot water is in the range from 158-176^{o}F (70-80 C). Thus a combination SE/HE will allow use in district heating networks. Two advantages of the SE/HE chiller are a reduction in heat exchanger area and it allows for a temperature glide in the generator of 54^{o}F (30 C).

The SE/HE chiller operates with a COP around 0.55 to 0.6 with driving heat supply / return temperature of 194 /140^{o}F (90/60 C) (Schweigler et al., 1996). The operation of the SE/HE chiller is driven by the available heat source temperature and flow rate. If the heat source temperature is above 176^{o}F (80 C) then the SE/HE acts as a SE unit with a COP of 0.7. Any temperatures below this the SE/HE acts as a combination SE-HE or pure HE, with the lower bound on the COP being 0.35 (Schweigler et al., 1996).

The control of the SE/HE at part load conditions can be met by decreasing the hot water flow rate or temperature. An important conclusion is that part load control by temperature reduces the COP, but controlling part loadwith mass flow rate, the COP slightly increases until 20% part load.(Schweigler et al., 1999). Part load below 20% the SE/HE operates as a half effect cycle and thus the COP drops to around 0.35-0.4.

Figure 2-2 displays the single-effect / half-effect combination. In Figure 2-2 the evaporator (E0), absorber (A0), condenser (C2), and generator (G21) are for the SE subcycle and the E0, A0, C2, G1, and G22 are for the HE cycle. Even though it looks like the SE/HE has three generators there is only two, where the G2 generator is able to act like two by how the flow is arranged.

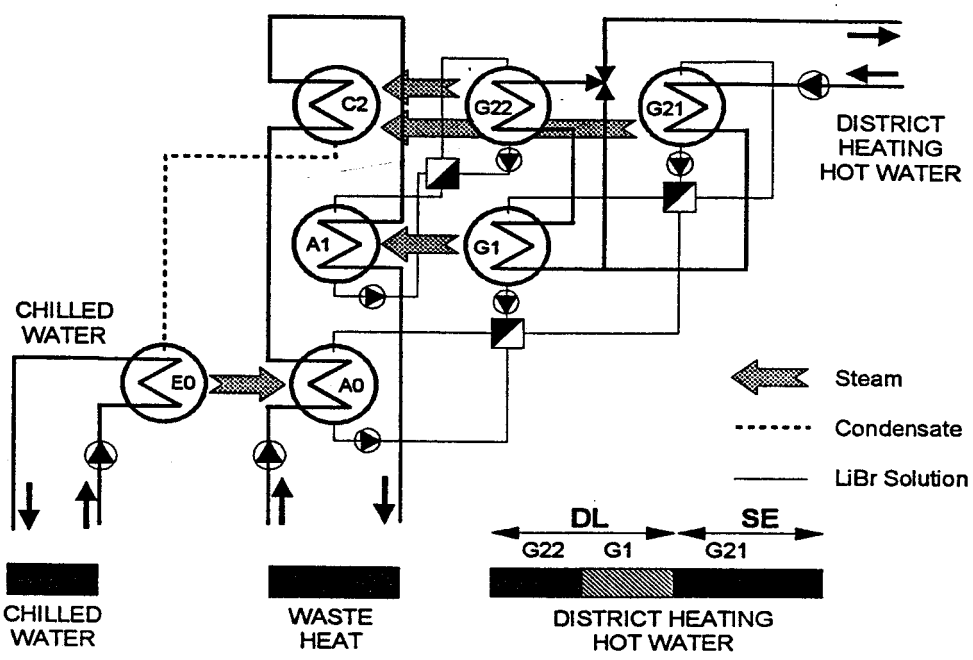

Figure 2-2. Flow chart of the SE/HE chiller (Schweigler et al., 1999).

The increase in COP at part load is gained by reducing the fraction of heat to the HE generators [G22, G1] more than the SE generator [G21] (Schweigler et al., 1999). This process is done by splitting the flow after it leaves the G21 generator and thus only a portion of the mass flow rate enters into G1 and G22 (Schweigler et al., 1999). This process can also control the temperature returning to the district-heating network. Mixing the flow from the G22 generator with the by-pass flow can maintain the desired return design point temperature, which is usually around 140^{o}F (60 C) (Schweigler et al., 1999).

Three pilot plant designs were implemented that have the SE/HE design. The Berlin and Düsseldorf pilot plants were designed for use in a district heating network and the other is used for co-generation in the Munich airport. Table 2-2 summarizes the operating parameters and size of the units.

Table 2-2. Summary of pilot plant designs (Schweigler et al., 1999).

	District Heating		Co-Generation
Installation	Technical University, Berlin	Power Plant Lausward, Düsseldorf	München Airport
Manufacturer	Entropie GmbH, Erding,Germany	GEA Luftkühler GmbH, Herne,Germany	Entropie GmbH, Erding,Germany
Design Point			
Driving Heat ^{o}F (C)	203/150 (95/65)	185/140 (85/60)	203/140 (95/60)
Cooling Water ^{o}F (C)		81/95 (27/35)	
Chilled Water ^{o}F (C)		54/43 (12/6)	
Cooling Capacity Tons (kW)	114 (400)	85 (300)	710 (2500)
COP	0.62	0.58	0.65
Dimensions ft LxWxH (m)	14.7x6.9x6.9 (4.5x2.1x2.1)	18x6.9x9.8 (5.5x2.1x3)	19.7x9.8x16.4 (6x3x5)
Weight tons (metric tons)	14.3 (13)	16.5 (15)	55.1 (50)

An important aspect of the SE/HE design is that the generators used in the SE/HE unit are falling film generators with multi-pass arrangement to ensure good heat transfer and large temperature glides. The units are also designed high and narrow in a rectangular profile to avoid the unfavorable large solution flow rates (Schweigler et al., 1999).

The main conclusions from the pilot plant test are (Schweigler et al., 1999).

- Operating expenses matched those with the theoretical performance predictions.
- COP increased during part load conditions while the temperature glide in the hot water remained constant.
- An increase in cooling capacity was achieved per unit of hot water mass flow compared with a standard single effect unit

Ma et al., (1996) examined a 100 ton (350 kW) half-effect absorption chiller driven by low temperature waste heat from a combined heat and power (CHP) plant in Beijing, China. The halfeffect chiller is able to operate at a hot water temperature of 187^{o}F (86 C) to produce 49^{o}F (9 C) chilled water using 87^{o}F (32 C) cooling water at a COP of 0.4(Ma et al., 1996). A single-effect chiller can not produce the specified chilled water with the given heat source temperature so a half-effect device must be used.

Erickson D. (1995) describes a half-effect cycle using (NH_3-H_2O), which is referred to as the vapor exchange cycle. The main advantage of this cycle over the LiBr-H2O unit, is that the evaporator temperature can go below 32^{o}F [0 C] because ammonia is the working fluid in the evaporator. The state of Alaska, the Alaska Science and Technology Foundation, and Alaska Energy Authority [AEA], helped fund the project. The capital cost for the 10 ton unit is about 7,000 $/ton but with 0.21 $/kWh the higher capital cost is worth the initial investment to reduce operating cost. The COP for half-effect cycle is about 0.306, which was determined from measuring the heat input and ice making output. The heat source comes from the jacket and exhaust of a diesel generator.

2.4 Summary

From examining the published literature the single-effect unit finds applications in co-generation, geothermal energy, and combined heating a cooling plants. The best method for designing single-effect units too operate on a low temperature heat source is to optimize the heat exchanger area of all components.

The half-effect unit can operate using a lower temperature heat source compared to the single-effect, but this ability comes at a cost, which is a lower cooling COP. No published literature was found that provides a detailed study of the complete system of absorption unit and cooling tower.

CHAPTER 3

SINGLE-EFFECT ABSORPTION MODEL DEVELOPMENT

3.1 Overview

Figure 3-1 is a schematic of the flow arrangement for a single-effect absorption unit. The main components of the absorption unit are; generator, condenser, evaporator, absorber, and low temperature heat exchanger [LTHX]. The brine or LiBr-H_2O solution is pumped from the absorber to the generator where the water is boiled off. The heat source is passed in a counter-flow arrangement through the generator to boil off water vapor from the LiBr-H_2O solution. The pressure of the system is about 1 psia at the generator and 0.1 psia at the absorber. This low pressure or vacuum system allows water to be used as a refrigerant.

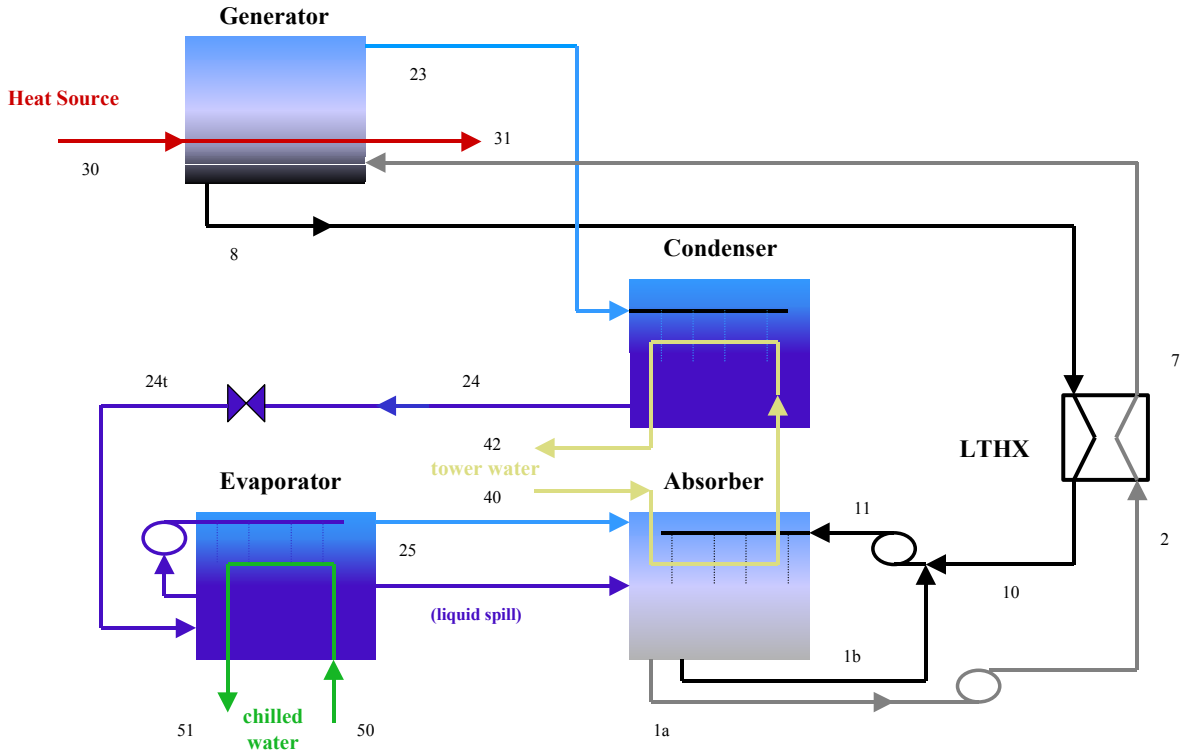

Figure 3-1. Schematic of the Single Effect Absorption Unit.

A cooling water loop is needed to condense the water vapor boiled off from the generator and to aid in the absorption of water vapor back into the LiBr-H_2O solution. This cooling water is passed first through the absorber and then the condenser. The evaporator takes in low-pressure cold water and produces a cooling effect by evaporating the water and passing it to the absorber.

A critical point in the system is the solution leaving the LTHX. The solution consists of a concentrated solution in LiBr at the lowest temperature in the cycle and thus a process called crystallization can occur.. Crystallization is the formation of salt crystals due to a low temperature high LiBr-H_2O solution. Crystallization must be avoided because the formation of a wet solid (slush) in the piping network over time could form a solid and block the flow

(Herold et al., 1996). Crystallization can be avoided by adding heat to the system in that area or diluting the solution with water from the evaporator (Herold et al., 1996)

A recirculation pump is used for the evaporator and absorber to ensure complete wetting of the tubes. The numbers in Figure 3-1 represent the states points used in the computer model. For example, T30 is the temperature of the entering hot water.

3.2 Model Input Parameters

3.2.1 Generator

Steam

T30	Temperature of Steam [F]
P30	Pressure of Steam [F]
H_ig	Inside heat transfer coefficient [Btu/hr-ft^2-F]
Tube#	Total Number of Tubes
NCG	Number of Tubes in column
D_g	Inner and Outer Diameter of Tubes [in]
Le_g	Length of Tubes [ft]

Hot Water

T30	Temperature of Water [F]
Vol30	Volume flow rate of Hot Water [gpm]
Tube#	Total Number of Tubes
NCG	Number of Tubes in column
D_g	Inner and Outer Diameter of Tubes [in]
Le_g	Length of Tubes [ft]

3.2.2 Condenser

UA_cond	[Btu/hr-F]
Or	
Tube#	Number of Tubes
D_tube	Inner and Outer Diameter of Tubes [in]
Le_tube	Length of Tubes [ft]
m41	Mass Flow Rate of Cooling Water [lbm/hr]

3.2.3 Evaporator

UA_evap	[Btu/hr-F]
Or	
Tube#	Number of Tubes
D_tube	Inner and Outer Diameter of Tubes [in]
L_tube	Length of Tubes [ft]

NCE	Number of Tubes in a column
m50	Mass Flow Rate of Chilled Water [lbm/hr]
T51	Temperature of Delivered Chilled Water [F]
Spill	Percent of liquid that is spilled directly to absorber [%]

3.2.4 Absorber

T40	Temperature of Entering Cooling Water [F]
m40	Mass Flow Rate of Cooling Water [lbm/hr]

Tube#	Number of Tubes
D_tube	Inner and Outer Diameter of Tubes [in]
L_tube	Length of Tubes [ft]
NCA	Number of Tubes in a column

3.2.5 Low-Temperature Heat Exchanger

η_lthx	Effectiveness of Low-Temperature Heat Exchanger

3.3 Assumptions

3.3.1 Overall

- Steady-state.
- The pressure in the evaporator is equal to the absorber and likewise for the generator and condenser.
- No pressure drop or heat transfer in the piping network.
- All components are modeled as shell and tube heat exchangers. The log mean temperature difference is used in the generator/absorber and effectiveness-NTU method for condenser/evaporator.
- The throttling device isoenthalpic.
- The solution pump is adiabatic.

3.3.2 Generator

- Equilibrium condition at the outlet of the generator point [8].
- No carry over of salt into the refrigerant.
- The steam leaves as saturated liquid.
- The outlet temperature of the refrigerant is the average of the equilibrium entering temperature and the outlet temperature. T[23]=(T7p+T[8])/2

3.3.3 Condenser

- The outlet of the condenser is saturated liquid at the generator pressure.

3.3.4 Evaporator

- The outlet of the evaporator is saturated vapor.
- A 4% spill of liquid from the evaporator goes directly to the absorber without evaporating.

3.3.5 Absorber

- The outlet absorber solution is sub-cooled.
- The absorber spray solution is an empirical function of capacity and inlet cooling temperature.

3.4 Model development for steam fired absorption unit

3.4.1 Overall

The four components (absorber, generator, condenser, and evaporator) are modeled based on energy balances for the internal and external streams, a heat transfer rate equation between the streams, salt balances, and mass balances. The overall heat transfer coefficient [UA] is determined from empirical relationships for the inside and outside heat transfer coefficient. The properties of enthalpy, pressure, temperature, concentration are determined from property relations. The mass and salt balance for the generator is of the form, where the numbers are based on Figure 3-1.

$$\dot{m}_7 = \dot{m}_{23} + \dot{m}_8 \qquad [\ 3\text{-}1\ ]$$

$$\dot{m}_7 x_7 = \dot{m}_8 x_8 \qquad [\ 3\text{-}2\ ]$$

The mass and salt concentration leaving the absorber is set equal to the mass entering the generator. The high and low pressures are determined from the saturated pressure of the water vapor (Electrical Research Association, 1967 Steam Tables).

3.4.2 Generator

Energy balances on the internal solution and heat source in the generator are

$$\dot{m}_7 h_7 + Q_g = \dot{m}_{23} h_{23} + \dot{m}_8 h_8 \qquad [\ 3\text{-}3\ ]$$

$$\dot{m}_{30} h_{30} - Q_g = \dot{m}_{30} h_{31} \qquad [\ 3\text{-}4\ ]$$

The heat transfer rate is calculated by

$$Q_g = UA_g LMTD_g \qquad [\ 3\text{-}5\ ]$$

where the LMTD is defined as

$$LMTD_g = \frac{T_8 - T_{7p}}{\ln\left(\dfrac{T_{7p} - T_{30sat}}{T_8 - T_{30sat}}\right)} \qquad [\ 3\text{-}6\ ]$$

where T_{7p} is the equilibrium temperature of the solution entering the generator at the generator pressure and solution salt concentration [F].
T_{30sat} is the saturation temperature of the steam at the given pressure [F].

Since the generator is steamed fired it does not matter if it is counter or parallel flow arrangement because the heat transfer is taking place at a constant steam saturation temperature.

The overall heat transfer coefficient is calculated using a resistance type equation.

$$UA_g = \frac{1}{\left(\frac{1}{h_{ig}A_{ig}} + \frac{1}{h_{og}A_{og}} + \frac{1}{R_g A_{ig}}\right)\frac{1}{Tube_g}} \qquad [\ 3\text{-}7\ ]$$

where h_{ig} is the inside heat transfer coefficient in the generator [Btu/hr-ft^2-F].
h_{og} is the outside heat transfer coefficient in the generator [Btu/hr-ft^2-F].
R_g is the resistance of the metal [Btu/hr-ft^2-F].
$Tube_g$ is the number of tubes in the generator.

The inside heat transfer coefficient for steam is assumed to be a constant at 1600 [Btu/hr-ft^2-F] (US Chiller Manufacturer, 2000). The outside heat transfer coefficient is based on an empirical relationship derived from data provided by a US chiller manufacturer for their single-effect unit. Figure 3-2 displays a graph of the relationship.

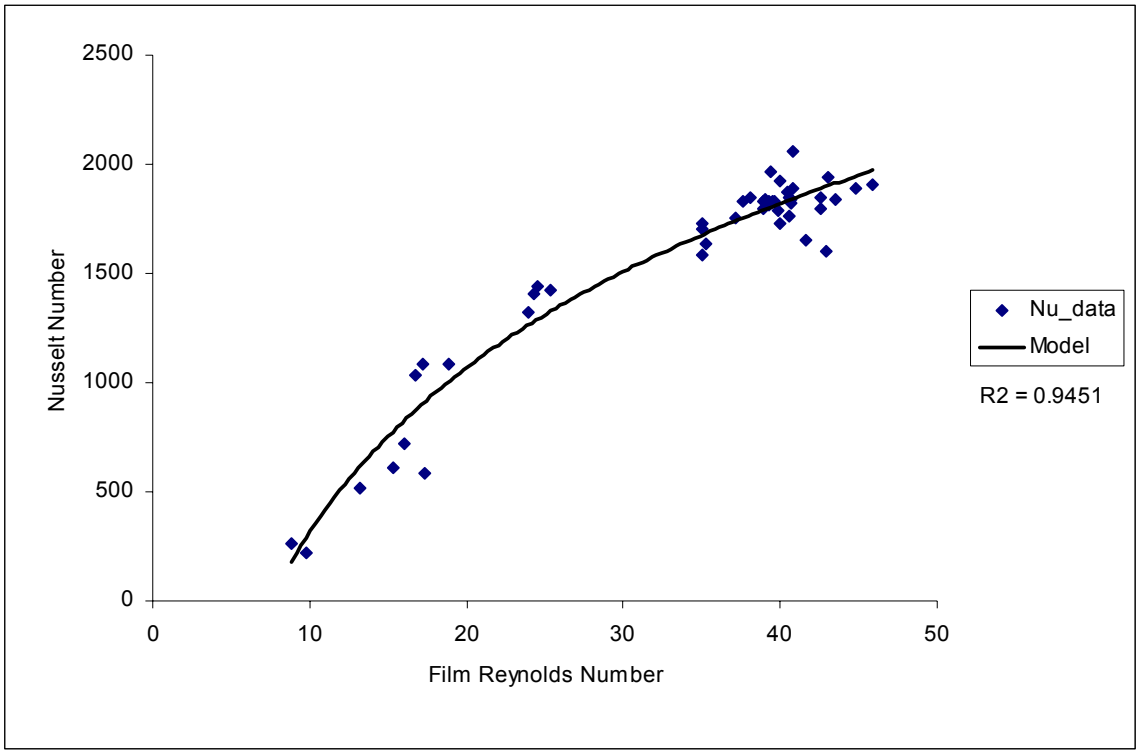

Figure 3-2. Empirical relationship between outside Nusselt number and film Reynolds number for the generator.

The data in Figure 3-2 are based on numerous experiments with different steam pressures / saturation temperatures and absorber inlet cooling water temperatures. A log fit was used to approximate the data with an R^2 of .95. Equation 3-8 is the log fit for the Nusselt number

$$Nu_g = 1087.3 \ln(\mathrm{Re}_{fg}) - 2189.4 \qquad [3\text{-}8]$$

where Re_{fg} is the film Reynolds number

$$\mathrm{Re}_{fg} = \frac{4\Gamma_g}{\mu_{fg}} \qquad [3\text{-}9]$$

where Γ_g is the film flow rate [lb_m/ft-hr]
μ_{fg} is the viscosity of the salt solution [lb_m/ft-hr]

The film flow rate is defined as

$$\Gamma_g = \frac{\dot{m}_7}{2le_{tube}NC} \qquad [3\text{-}10]$$

where NC is the number of tubes in a row.

The outside heat transfer coefficient is calculated from

$$h_{og} = \frac{Nu_g D_{og}}{k_{fg}} \qquad [3\text{-}11]$$

where k_f is the conductivity of the salt solution [Btu/hr-ft-F].
D_o is the outside diameter of the tubes [ft].

The model restricts the outside Nusselt number to be below 2000 so as not extrapolate past the data.

3.4.3 Absorber

Energy balances on the internal solution and the cooling water in the absorber are

$$\dot{m}_{11}h_{11} + \dot{m}_{25}h_{25} - Q_a = \dot{m}_{1a}h_{1a} + \dot{m}_{1b}h_{1b} \qquad [3\text{-}12]$$

$$\dot{m}_{40}h_{40} + Q_a = \dot{m}_{41}h_{41} \qquad [3\text{-}13]$$

The heat transfer rate is calculated by

$$Q_a = UA_a LMTD_a \qquad [3\text{-}14]$$

where LMTD is defined as

$$LMTD_a = \frac{(T_{11p} - T_{41}) - (T_1 - T_{40})}{\ln\left(\frac{T_{11p} - T_{41}}{T_1 - T_{40}}\right)} \qquad [3\text{-}15]$$

where T_{11p} is the equilibrium temperature of the salt solution at x_{11} concentration [F].

The LMTD is based on a counter flow heat exchanger arrangement.

The inside heat transfer coefficient is based on the Dittus-Boelter correlation (Incropera & DeWitt, 1996).

$$\frac{h_{ia} d_{ia}}{k_{wa}} = Nu_{ia} = .023 \,\mathrm{Re}_a^{.8} \,\mathrm{Pr}_a^{.4} \qquad [\ 3\text{-}16\ ]$$

where k_{wa} is the conductivity of the cooling water at an average inlet and outlet conditions [Btu/hr-ft-hr]
d_{ia} is the inner diameter of the pipe [ft].

The Gnielinski correlation would increase the accuracy of the inside heat transfer coefficienct but to be consistent with the data provided by the US chiller manufacturer the Dittus-Boelter correlation is used.

The outside heat transfer coefficient is also based on a empirical relationship of the form (Cosenza and Vliet, 1990)

$$\frac{h_{oa} d_{fa}}{k_{fa}} = Nu_{oa} = a(\mathrm{Re}_{fa})^b \qquad [\ 3\text{-}17\ ]$$

where k_f is the conductivity evaluated at a mean absorber temperature and concentration [Btu/hr-ft-hr]
d_{fa} is the average laminar film thickness around the tube bundle [ft]

$$d_{fa} = \left(\frac{3\mu_{fa}\Gamma_a}{\rho_{fa}^{\,2} g} \right)^{\frac{1}{3}} \qquad [\ 3\text{-}18\ ]$$

where μ_{fa} is the viscosity of the solution [lb_m/hr-ft].
Γ_a is the film flow rate per tube column per length of tube [lb_m/hr-ft].

The overall UA is calculated from

$$UA_a = \frac{1}{\left(\frac{1}{h_{ia}A_{ia}} + \frac{1}{h_{oa}A_{oa}} + \frac{1}{R_a A_{ia}}\right)\frac{1}{Tube_a}} \qquad [3\text{-}19]$$

Figure 3-3 demonstrates the correlation used by Nusselt number in equations 3-20 and 3-21. The symbols represent data points from the US chiller manufacturer and the numbers 85, and 65represent the inlet cooling temperature in ^{o}F to the absorber. Equation 3-20 represents the data for a cooling inlet temperature of 75 ^{o}F.

$$Nu_{85} = .0048\,\mathrm{Re}_{fa}^{1.6258} \qquad [3\text{-}20]$$

$$Nu_{65} = .0036\,\mathrm{Re}_{fa}^{1.6428} \qquad [3\text{-}21]$$

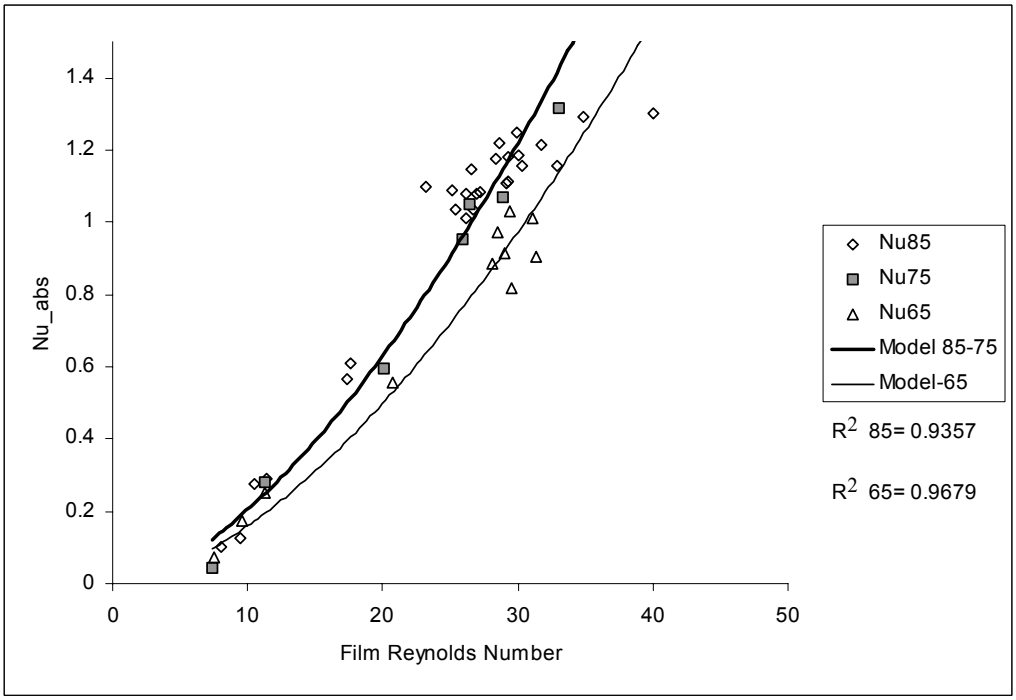

Figure 3-3. Nusselt number as a function film Reynolds number.

An important condition depicted in Figure 3-3 is the decrease in the Nusselt number for a decrease in absorber inlet cooling temperature. The most likely reason for this result is that

the mass flow rate decreases with a decrease in inlet cooling water. The absorption model prevents extrapolation beyond the data in Figure 3-3. The upper limit on the film Reynolds number is 31, which was derived from taking an average of film Reynolds numbers in the data set. This upper limit will show itself in chapter 8 when examining the effect on capacity by changing the internal solution flow rate.

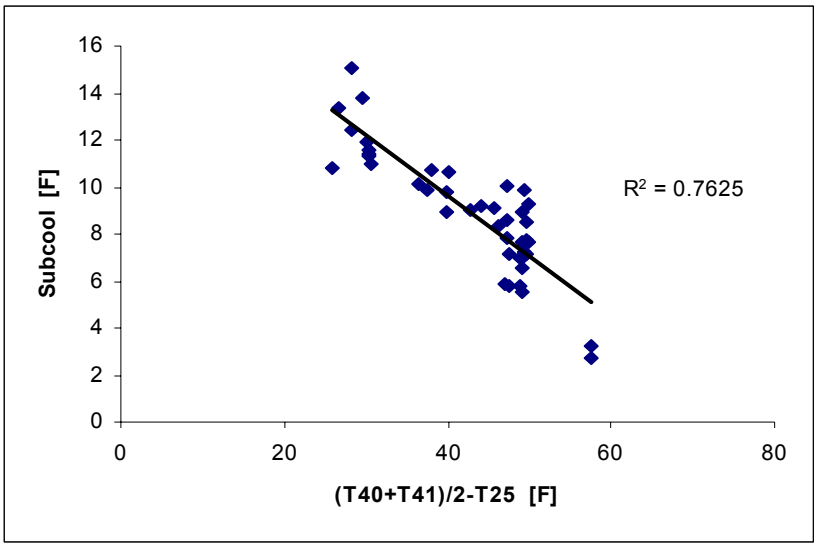

Figure 3-4. Sub-cooling as a function of evaporator and absorber inlet cooling temperature.

Sub-cooling takes into account the fact that if the equilibrium concentration leaving the absorber was calculated from the leaving temperature, the concentration would be to low. Figure 3-4 shows the trend of sub-cooling in the data and equation 3-22 is the empirical relationship derived from the data (US chiller manufacturer, 2000).

$$Subcool = -.2569\left(\frac{T_{40}+T_{41}}{2} - T_{25}\right) + 19.904 \qquad [\ 3\text{-}22\ ]$$

The linear fit has a low R^2 value, but the exact value of sub-cooling is not important. More important than the value is the trend of sub-cooling to acquire a rough estimate. The value of sub-cooling is used when solving for the concentration at the exiting solution of the absorber.

$$x_1 = xeq(T_1 + Subcool, T_{25}) \qquad [\ 3\text{-}23\ ]$$

where xeq is a function from ASHRAE Fundamentals (1989), based on LiBr properties.

3.4.4 Condenser

Energy balances on the internal solution and the cooling water in the condenser are

$$\dot{m}_{23} h_{23} - Q_c = \dot{m}_{24} h_{24} \qquad [\ 3\text{-}24\ ]$$

$$\dot{m}_{41} h_{41} + Q_c = \dot{m}_{42} h_{42} \qquad [\ 3\text{-}25\ ]$$

The effectiveness or ratio of heat transfer rate to maximum heat transfer rate is calculated by

$$\varepsilon_c = \frac{T_{42} - T_{41}}{T_{24} - T_{41}} \qquad [\ 3\text{-}26\ ]$$

where effectiveness is defined by Incropera & DeWitt, (1996).

$$\varepsilon_c = 1 - e^{-Ntu_c} \qquad [\ 3\text{-}27\ ]$$

Equation 3-27 is for all types of heat exchangers [concentric tube, shell and tube, and cross flow with multiple passes] that go through a phase change. The Ntu is defined by

$$Ntu_c = \frac{UA_c}{C_{\min}} \qquad [\ 3\text{-}28\ ]$$

where C_{min} is the mass flow rate of the cooling water times the heat capacity [Btu/hr-F].

The C_{min} is based on the cooling water because the capacity is infinite for a substance that goes through a phase change. The inside heat transfer coefficient is based on the Gnielinski correlation (Incropera & DeWitt, 1996).

$$h_{ic} = \frac{Nu_{ic} k_{wc}}{d_{ic}} = \frac{k_{wc}}{d_{ic}} \frac{(f/8)(\mathrm{Re}_c - 1000)\,\mathrm{Pr}}{1 + 12.7(f/8)^{\frac{1}{2}}(\mathrm{Pr}_{ic}^{2/3} - 1)} \qquad [\ 3\text{-}29\ ]$$

The Gnielinski correlation was used because it is claimed to have a higher level of accuracy over the Dittus-Boelter correlation (Incropera & DeWitt, 1996). The Gnielinski correlation is applicable over a wider range of Reynold and Prandtl numbers than the Dittus-Boelter equation. The outside heat transfer coefficient is based on correlation for laminar film condensation on horizontal tubes (Rohsenow, et.al. 1998).

$$h_{oc} = k_{lc}\left(\frac{\rho_{lc}(\rho_{lc} - \rho_{vc})g3600^2}{\mu_{lc}^2}\right)^{\frac{1}{3}} 1.51\,\mathrm{Re}_{fc}^{-1/3} \qquad [\ 3\text{-}30\ ]$$

where h_{oc} is the average outside heat transfer for an entire column in a tube bundle [Btu/hr-ft^2-F].
Re_{fc} is the film Reynolds number in a tube bundle.

The published correlation under predicts the outside heat transfer coefficient and thus a factor of 2.5 is used in equation 3-31. The factor of 2.5 was determined from calibration with data from a US chiller manufacturer.

$$h_{oc} = 2.5k_{lc}\left(\frac{\rho_{lc}(\rho_{lc} - \rho_{vc})g3600^2}{\mu_{lc}^2}\right)^{\frac{1}{3}} 1.51\,\mathrm{Re}_{fc}^{-1/3} \qquad [\ 3\text{-}31\ ]$$

The most likely reason for the under prediction is that the correlation is for laminar flow and with a film Reynolds number on the order of 100, there could be wavy effects that equation 3-30 does not take into account, which would increase the heat transfer coefficient.

The overall UA for the condenser is based on

$$UA_c = \frac{1}{\left(\frac{1}{h_{ic}A_{ic}} + \frac{1}{h_{oc}A_{oc}} + \frac{1}{R_c A_{ic}}\right)\frac{1}{Tube_c}} \qquad [\ 3\text{-}32\ ]$$

3.4.5 Evaporator

Energy balances on the internal solution and the chilled water in the evaporator are

$$\dot{m}_{24t}h_{24t} + Q_e = \dot{m}_{25l}h_{25l} + \dot{m}_{25v}h_{25v} \qquad [\ 3\text{-}33\ ]$$

$$\dot{m}_{50}h_{50} - Q_e = \dot{m}_{51}h_{51} \qquad [\ 3\text{-}34\ ]$$

The l and v represent the liquid and vapor that are spilled into the absorber. The idea of the liquid spill is that cold water that could be used to take in heat by evaporating is spilled over into the absorber and thus the machine has lost some cooling ability. Spill can occur because the evaporator is on top of the absorber [refer to Figure 1-3]. The fraction of m_{25l} and m_{25v} is calculated by

$$m_{25l} = m_{25}Spill \qquad [\ 3\text{-}35\ ]$$

$$m_{25v} = m_{25}(1 - Spill) \qquad [\ 3\text{-}36\ ]$$

where the spill fraction is usually around 3-5%.

The effectiveness or ratio of heat transfer rate to maximum heat transfer rate is calculated by

$$\varepsilon_e = \frac{T_{51} - T_{50}}{T_{25} - T_{50}} \qquad [\ 3\text{-}37\ ]$$

where effectiveness is defined by Incropera & DeWitt, (1996).

$$\varepsilon_e = 1 - e^{-Ntu_e} \qquad [3\text{-}38]$$

The Ntu is defined by the UA

$$Ntu_e = \frac{UA_e}{C_{\min}} \qquad [3\text{-}39]$$

where C_{min} is the mass flow rate of the chilled water times the heat capacity [Btu/hr-F].

The inside heat transfer coefficient is obtained from a correlation provided by a tubing manufacturer for double cut tubes. The double cut tubes represent fins on the inside and outside.

$$Nu_{ie} = b_o \, \mathrm{Re}_{De}^{b_1} \, \mathrm{Pr}_{ie}^{n} \qquad [3\text{-}40]$$

The constants b_o, b_1, and n are fitted parameters provided by the tubing manufacturer.

$$h_{ie} = \frac{Nu_{ie} D_{ie}}{k_{we}} \qquad [3\text{-}41]$$

The outside heat transfer coefficient is based on laminar evaporating films (Rohsenow, et.al. 1998).

$$h_{oe} = 1.1006 \, \mathrm{Re}_{fe}^{-1/3} \left(\frac{\rho_{le}^2 g 3600^2 k_{le}^3}{\mu_{le}^2} \right)^{\frac{1}{3}} \qquad [3\text{-}42]$$

Re_{fe} <20-30

The published correlation under predicts the outside heat transfer coefficient based on experimental data and thus a factor of 2.75 is used in equation 3-42. The factor of 2.75 was determined from calibration with data from a US chiller manufacturer.

$$h_{oe} = 2.75 * 1.1006 \, \mathrm{Re}_{fe}^{-1/3} \left(\frac{\rho_{le}^2 g 3600^2 k_{le}^3}{\mu_{le}^2} \right)^{\frac{1}{3}} \qquad [3\text{-}43]$$

The constant factor of 2.75 in equation 3-43 causes the heat transfer coefficient to be under predicted at full load and over predicted at part load. One possible reason why equation 3-42 under predicts is that the Reynolds number is calculated from the refrigerant flow rate but since the evaporator is using recirculation, the flow rate is higher, thus a larger Reynolds number. A larger Reynolds number could cause turbulence or a wavy region, which increases the heat transfer. The tubes are finned on the outside so the factor 2.75 could be thought of as increasing the surface area due to calculating the outside area based on smooth tube geometry. No data were available for fin pitch or height. Since the evaporator is using re-circulation the UA for the evaporator should be a constant, and thus the data demonstrates a relatively constant UA for full and part load conditions.

The UA for the evaporator is determined by

$$UA_e = \frac{1}{\left(\frac{1}{h_{ie} A_{ie}} + \frac{1}{h_{oe} A_{oe}} + \frac{1}{R_e A_{ie}} \right) \frac{1}{Tube_e}} \qquad [3\text{-}44]$$

3.5 Control Strategy

In order to model a single-effect absorption unit it is important to have a control strategy. Since the current design employs recirculation for the absorber, two control strategies are needed. The reason for these control strategies is so the computer model can predict what the internal solution and re-circulation flow rate should be for a given capacity and temperature

margin. The T_{margin} is the temperature difference between the low temperature concentrated solution leaving the LTHX and the crystallization point at that concentration

$$T_{margin} = T_{10,LTHX} - T_{crystillization} \qquad [3\text{-}45]$$

The capacity of the unit determines what the leaving flow rate out of the absorber should be [m1a] and the temperature margin regulates what needs to be re-circulated from the absorber [m1b].

Figure 3-5 shows a plot of relationship between capacity and absorber solution flow rate. The numbers 85, 75, and 65 represent the inlet cooling water temperature in ^{o}F. The data points in Figure 3-5 represent calculated data from a US chiller manufacturer. Recall m1a is the solution flow rate leaving the absorber and entering the generator.

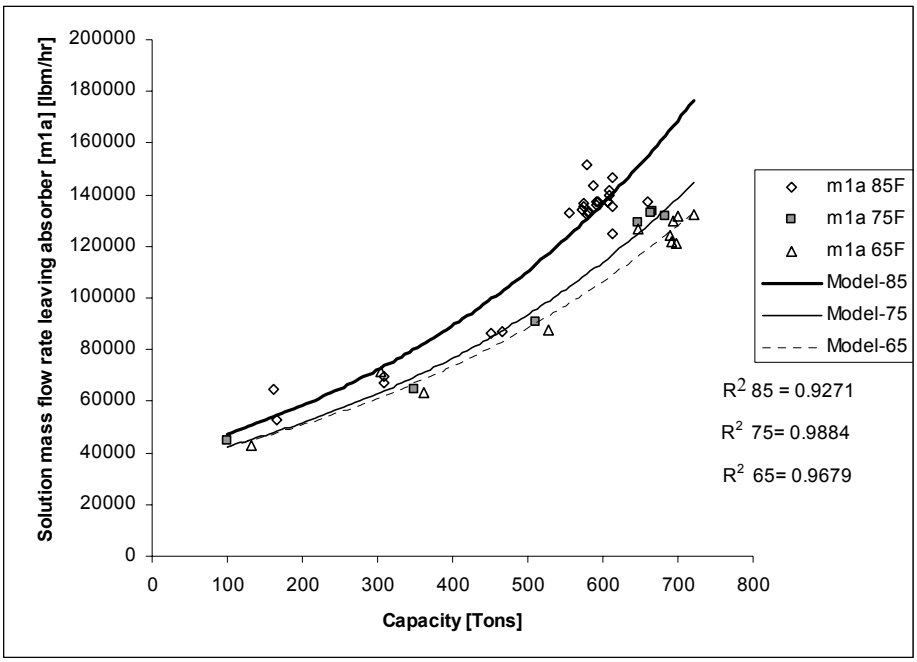

Figure 3-5. Absorber outlet solution flow rate as a function of capacity and temperature.

The three exponential relationships for the internal solution flow rate were chosen based on a high R^2 value and reproducibility of the data. The following equations are:

$$m1a_{85} = 38155e^{.0021Capacity} \quad [3\text{-}46]$$

$$m1a_{75} = 34788e^{.002Capacity} \quad [3\text{-}47]$$

$$m1a_{65} = 35137e^{.0018Capacity} \quad [3\text{-}48]$$

The absorption model limits the mass flow rates above a specified capacity based on what the inlet cooling water temperature is. TABLE 3-1 specifies the limits of equations 3-46, 47, and 48. Also note in Figure 3-5 the dependence on the absorber inlet cooling temperature. The reason for the temperature dependence is that the lower inlet cooling absorber temperature is able to remove heat more effectively and thus a lower solution flow rate is needed to obtain the same capacity.

The advantage of this control strategy is that the input [capacity] is a parameter that is usually known and measured with high accuracy.

Table 3-1. Limits on outlet absorber solution flow rate [m1a].

	85°F	75°F	65°F
Capacity [Tons]	620	680	700
m1a [lbm/hr]	140,000	135,000	125,000

The limits were found by taking an average of the m1a data at full load for each of the inlet cooling temperatures.

3.6 Calibration

The calibration phase consisted of supplying the model with the absorber to generator flow rate and recirculation flow rate in the absorber. The model then calculated the T_{margin}, capacity, temperatures, concentration, etc. One argument that was made was to calibrate the model with concentration instead of mass flow rates; the reason being is that concentration was actually measured where as the mass flow rates were calculated by a data reduction of the measured parameters. The main reason against this technique is that a small change in concentration results in a large change in mass flow rates. Thus by forcing the concentration, one has the potential to produce large errors in flow rates. If the mass flow rate is forced the potential to produce errors in concentration is low.

The next step was to implement both control strategies, [T_{margin} and the empirical relationships from Figure 3-5]. The model then predicted performance based on the two control strategies and the above model development equations. If the predicted values followed the trend of the data [mass flow, concentration, temperature] and were within ± 5-10%, then the calibration was done. Part load conditions required the T_{margin} to be slightly adjusted from the control set point to fit the measured data of concentration and mass flow rate.

The numerical values for the outside heat transfer coefficients for the condenser and evaporator were also determined once the proper control strategy was fixed. Figures 3-6 to 3-

18 show the relationship between measured data and model predictions for capacity, COP, UA, concentration, and mass flow rates. In each of the graphs a 45^{o}degree line is used to shows deviations from the model and data set.

One important clarification is that when the term data is used for capacity, COP, UA's and flow rates it really means calculated values from a chiller manufacturer, the only measured data are concentration and temperature. The manufacture has provided a proprietary analyses program to estimate values of capacity, COP, UA's, and flow rates based on the measured temperatures and concentration. It is these estimates to which the model developed in this thesis is compared

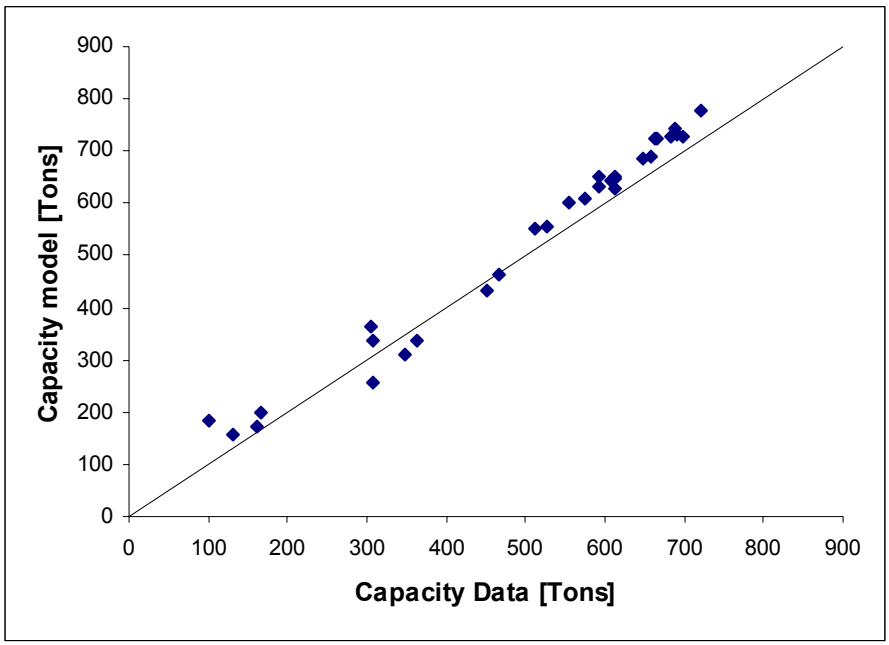

Figure 3-6. Comparison between model and data for capacity

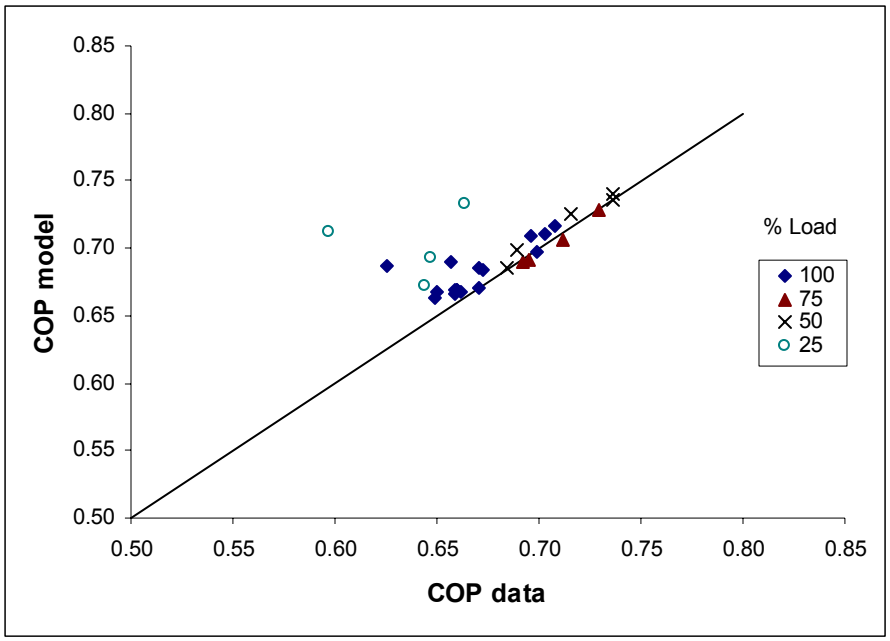

Figure 3-7. Comparison between model and data for COP.

The capacity predictions are in good agreement but the COP shows the model is not able to predict COP at 25% of full load. The main reason for this is that the model was able to predict the COP at 25 % full load, but it also predicted negative re-circulation rates. When a lower limit of zero was placed on the re-circulation flow rate the COP estimates at 25% of full load are over-predicted. The data set given by the US chiller manufacturer also contained negative re-circulation rates.

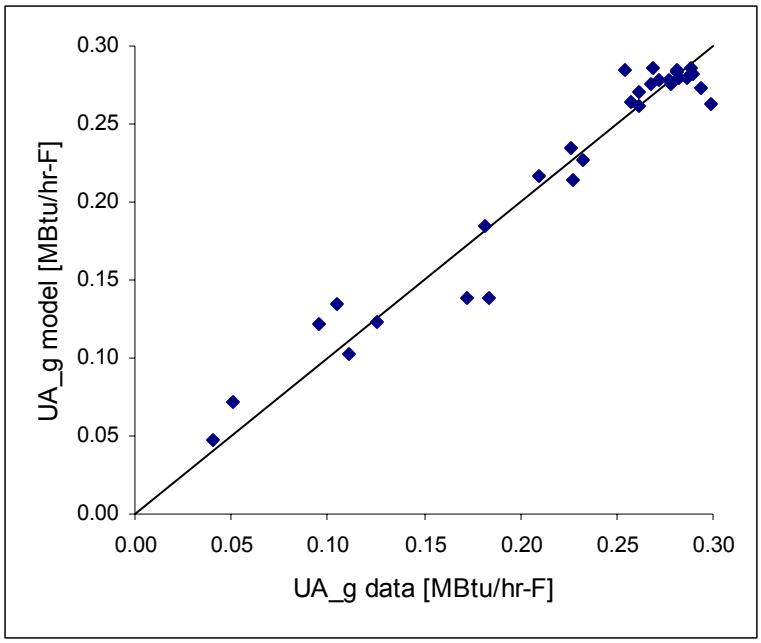

Figure 3-8. Comparison between model and data for UA generator.

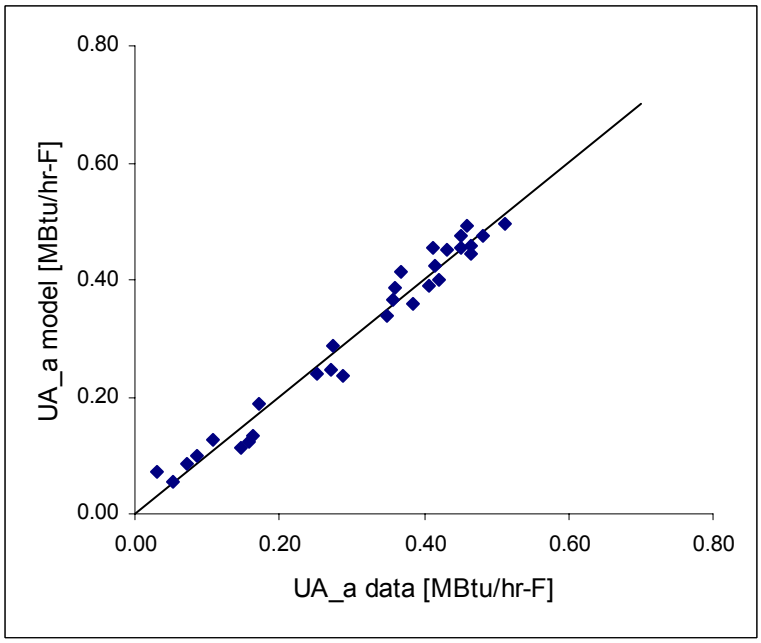

Figure 3-9. Comparison between model and data for UA absorber

The model predictions for the UA of the absorber and generator are in good agreement but the condenser and evaporator, show considerable scatter of data.

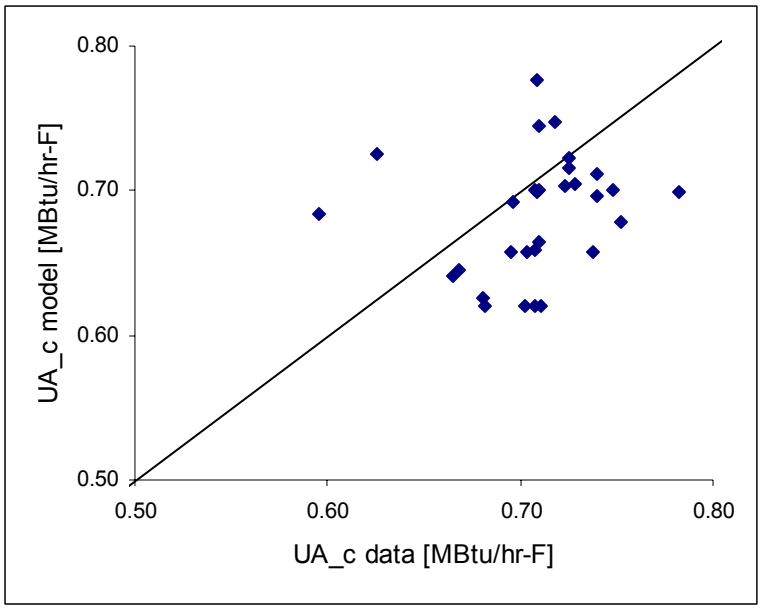

Figure 3-10. Comparison between model and data for UA condenser.

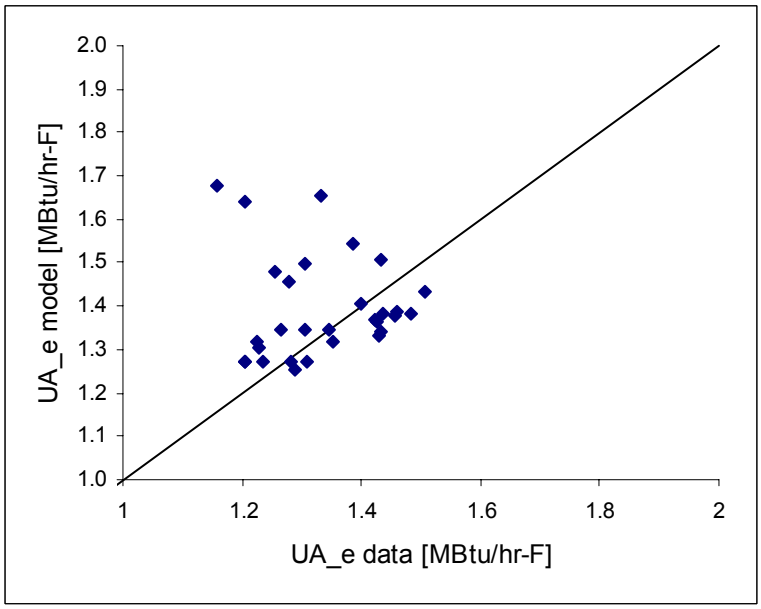

Figure 3-11. Comparison between model and data for UA evaporator.

As will be shown later, the UA of the condenser and evaporator do not matter because each component is oversized and a ±10-15 % error will not effect the system performance significantly.

The concentration and mass flow rate graphs demonstrates the models' ability to predict performance.

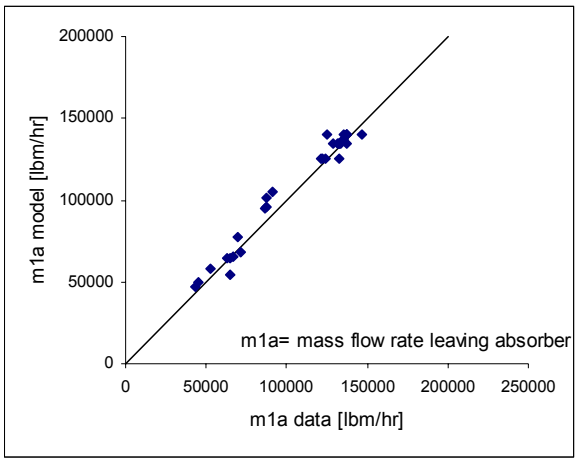

Figure 3-12. Comparison between model and data for mass flow rate leaving the absorber.

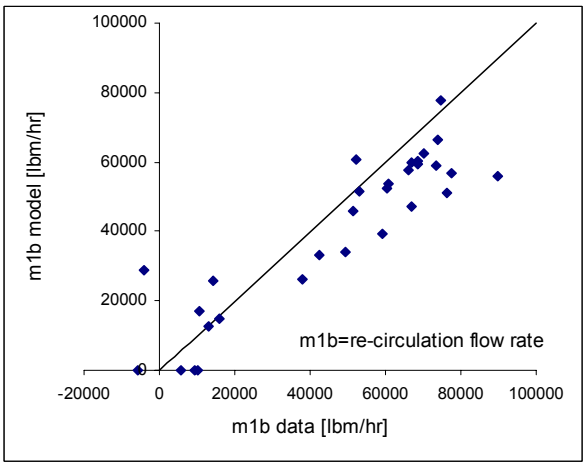

Figure 3-13. Comparison between model and data for re-circulation flow rate.

In Figure 3-13 some of the data shows a negative re-circulation flow rate but the model re-circulation flow rate was limited to positive values and thus over predicts since it can not go below zero. These negative re-circulation flow rates are the cause for the higher COP at some part load conditions. Notice that even though there is a large error in re-circulation it still does not have a large effect on capacity. Figure 3-12 shows good agreement with data. Figure 3-14 and Figure 3-15 demonstrates good agreement with the data.

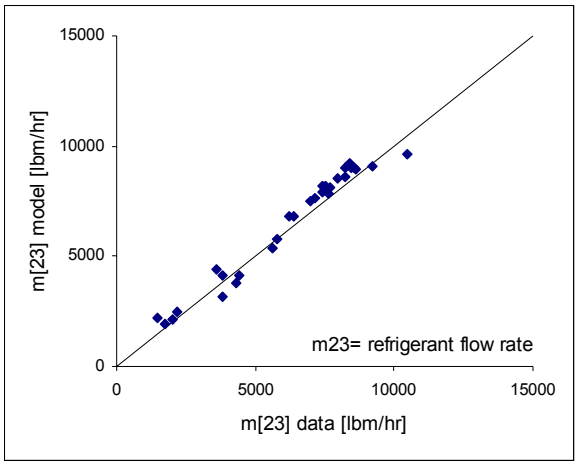

Figure 3-14. Comparison between model and data for refrigerant flow rate.

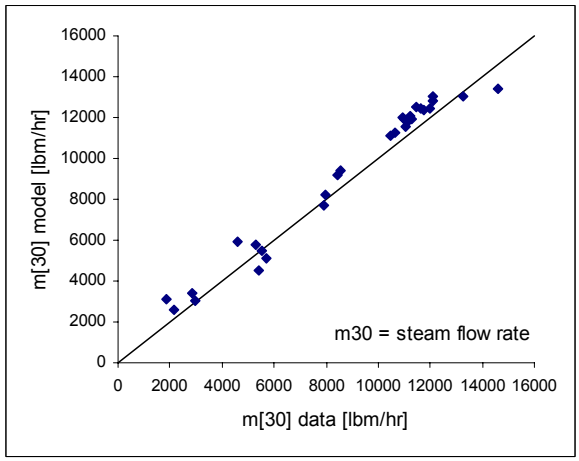

Figure 3-15. Comparison between model and data for steam flow rate.

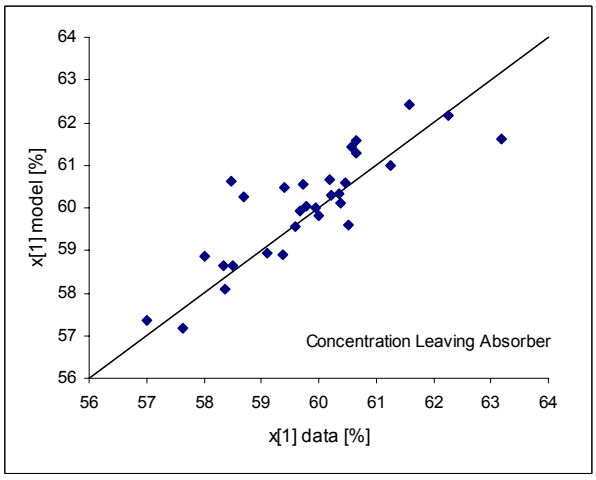

Figure 3-16. Comparison between model and data for concentration leaving absorber.

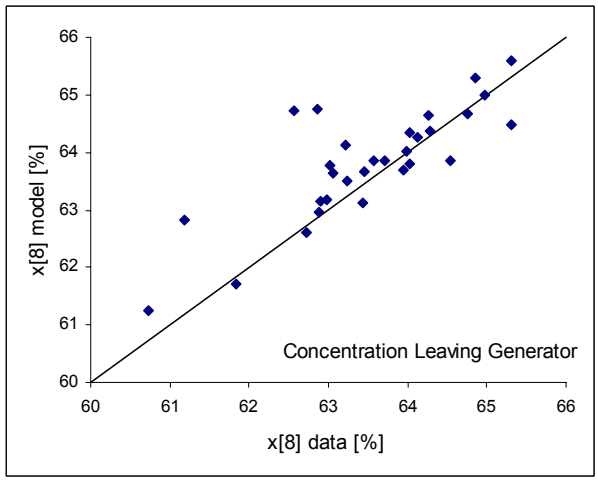

Figure 3-17. Comparison between model and data for concentration leaving generator.

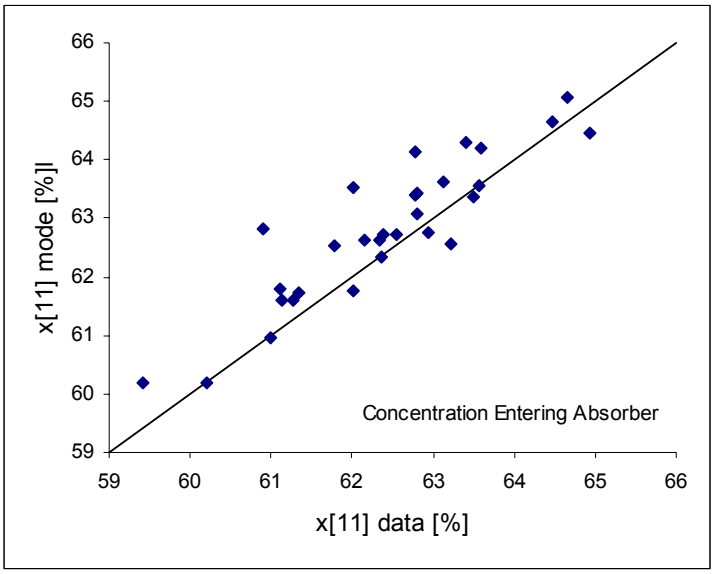

Figure 3-18. Comparison between model and data for concentration entering absorber.

Figure 3-16 - Figure 3-18 compares the concentration at the generator and absorber. The graphs show small differences between model and data.

The symbols in Figure 3-19 and Figure 3-20 represent the data and the lines are the absorption model, T_{51} is outlet temperature of the chilled water. Figure 3-19 compares the model predictions of capacity for various inlet absorber cooling water temperatures as a function of part load.

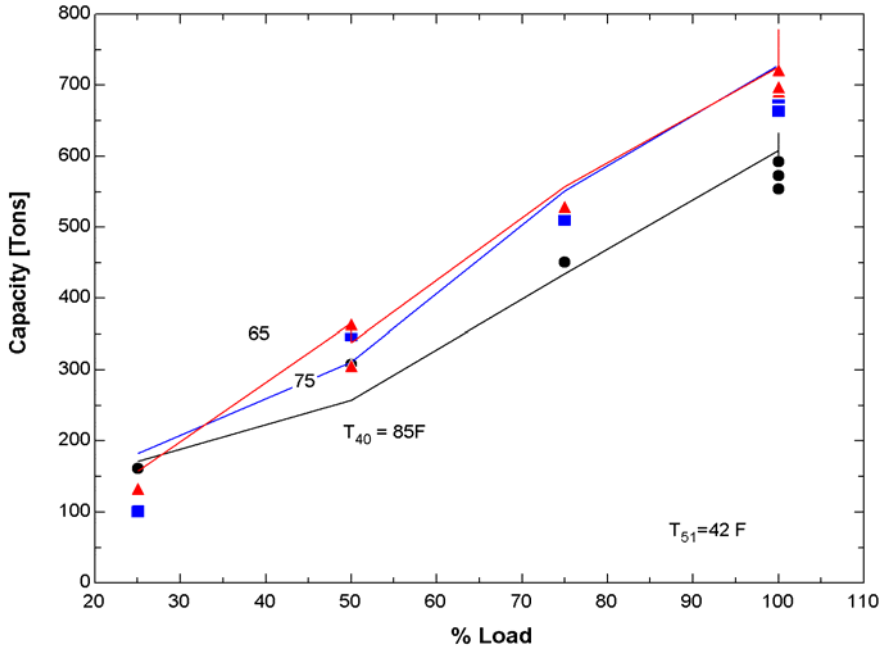

Figure 3-19. Capacity as a function of load for different inlet absorber cooling temperatures.

The above graph shows that the model is able to follow the trend of the data. Two important characteristics of this plot that will be seen later is the linear relationship of capacity with load and the increase in capacity as the cooling water is decreased for a given load.

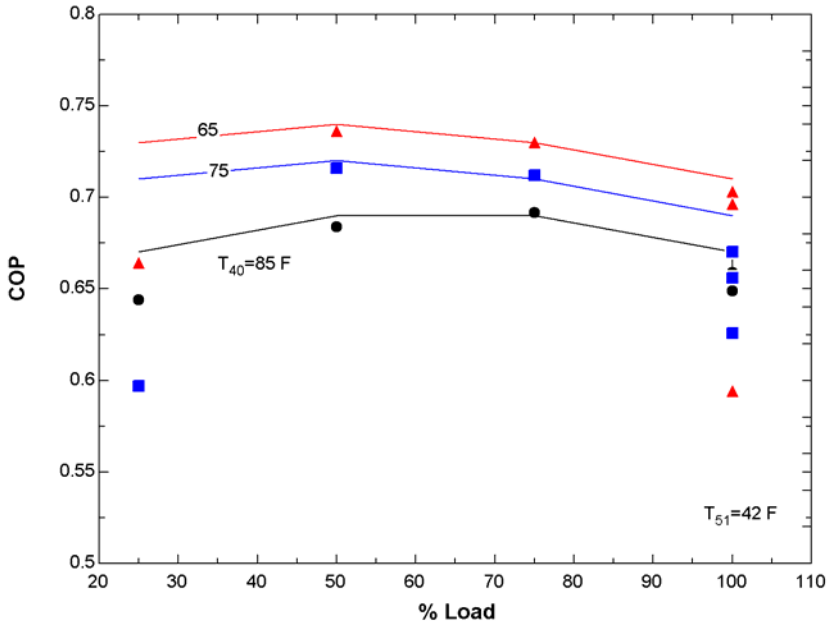

Figure 3-20. COP as a function of load for different inlet absorber cooling temperature.

Even though Figure 3-20 is an expanded scale, there is a distinct deviation from data at 25 % part load condition. There are small differences at 100% due to 1 or 2 data points but for the most part the model is able to predict the data for a wide range of part load conditions. Again the trend of the COP for part load conditions is very important and will be seen in future chapters. COP is almost liner with load because as the cooling capacity is decreased so is the heat source.

3.7 Model Development: Hot Water Fired Generator

The hot water fired generator is a counter flow 2-pass shell and tube heat exchanger. The overall heat transfer coefficient [UA] is calculated from an inside and outside heat transfer coefficient. The inside coefficient is a standard empirical relationship for water and the outside coefficient is based on a paper by Wang, et al. (1999) for a falling film generator.

3.7.1 Difference between steam fired and hot water fired generator

The main difference between the two generators is that a steam fired generator "pulls in" the amount of steam needed for a capacity by condensation and thus the mass flow rate of the steam is not an input to the model. Instead of specifying the steam flow rate, an assumption is used that the steam leaving the generator is saturated water and thus the model calculates the steam flow rate. For the hot water system the mass flow rate is an input and the leaving water temperature is determined from the model.

Another main difference between the absorption system with hot water and steam is that the recirculation flow to the absorber is set to zero and thus the control strategy for temperature margin is no longer needed. The recirculation was removed because future designs will incorporate an absorber that will be taller and narrower than the current design. A taller design will ensure that the tubes are fully wetted.

3.7.2 Inside Heat Transfer Coefficient

The Gnielinski correlation is used for the generator inside heat transfer coefficient (Incropera & DeWitt, 1996).

$$\frac{h_{ig} d_{ig}}{k_{wg}} = Nu_{ig} = \frac{(f/8)(Re_{Dg} - 1000)\, Pr_{ig}}{1 + 12.7\left(f/8\right)^{\frac{1}{2}} (Pr_{ig}^{\,2/3} - 1)} \qquad [3\text{-}49]$$

where $h_{i,g}$ is the inside heat transfer coefficient [Btu/hr-ft^2-F]
d_{ig} is the inner pipe diameter [ft]
k_{wg} is the conductivity of the water [Btu/hr-ft-F]
Re_{Dg} is the Reynolds number for pipe flow.
Pr_{ig} is the Prandtl number
Nu_{ig} is the Nusselt number
f is empirical relationship for smooth tubes based on the Moody diagram[Incropera & DeWitt, 1996].

$$f = (.79 \ln Re_{Dg} - 1.64)^{-2} \qquad [3\text{-}50]$$

3.7.3 Outside Heat Transfer Coefficient

The outside generator heat transfer coefficient h_{og} was developed by integrating three graphs from (Wang et al., 1999). The three graphs are falling film outside heat transfer coefficient

versus spraying density and pressure, and leaving concentration as a function of spraying density for a falling film generator using hot water. The spraying density [φ] is the mass of brine solution per unit length of tube and time. Figure 3-21 and Figure 3-22 displays the relationship of the outside heat transfer coefficient and exiting concentration as a function of pressure and spraying density. Figure 3-23 displays the change in outside heat transfer coefficient as a function of spraying density for smooth and finned tubes.

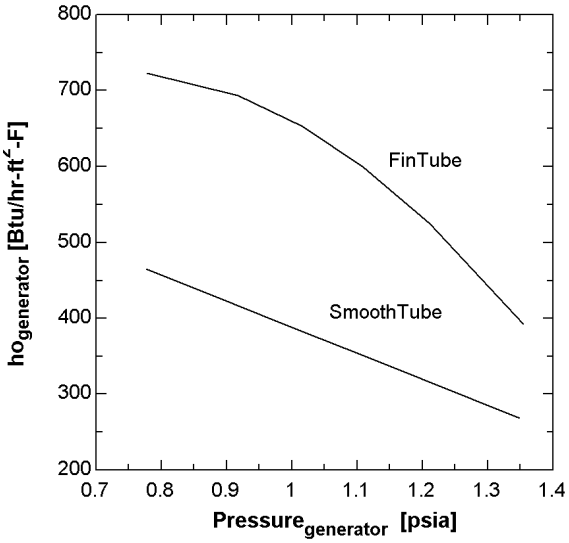

Figure 3-21. Change in outside heat transfer coefficient as a function of generator equilibrium pressure (Wang et al., 1999).

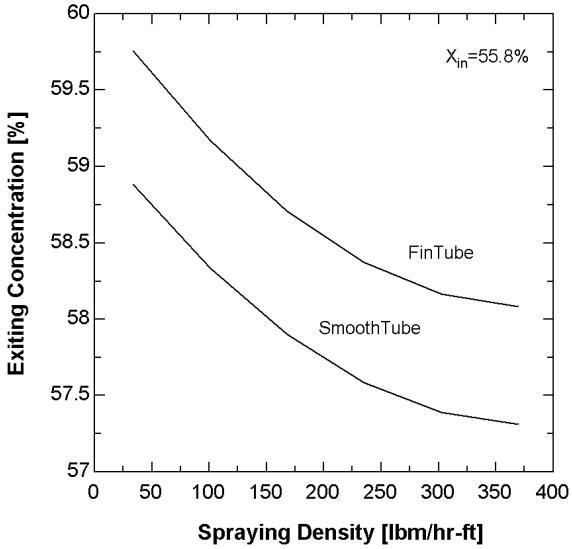

Figure 3-22. Change in exiting concentration as a function of spraying density (Wang et al., 1999).

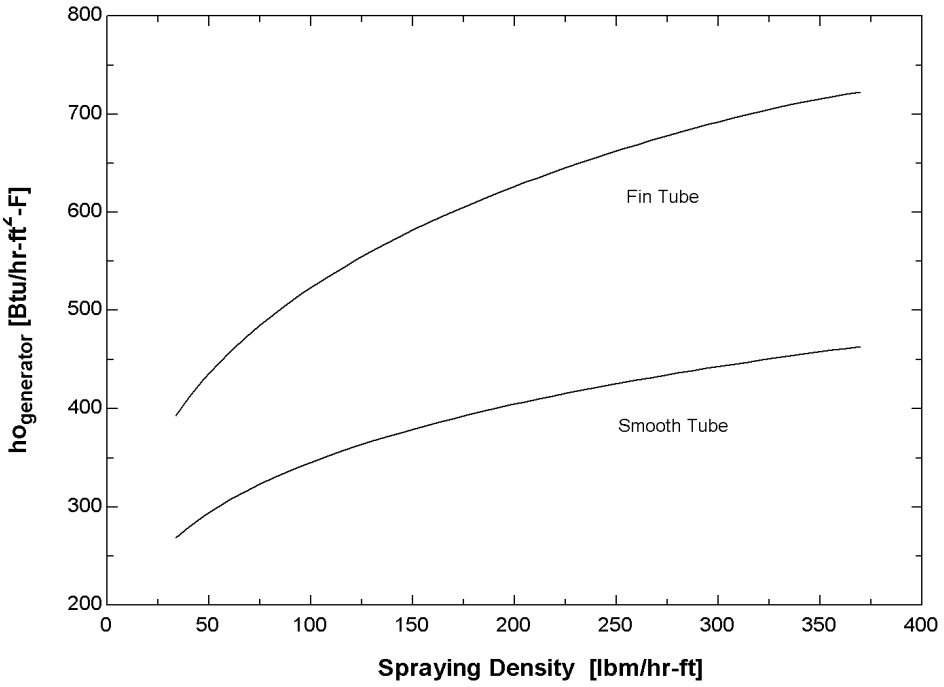

Figure 3-23. Change in outside heat transfer coefficient as a function of generator spraying density Wang et al., (1999).

The following is a summary of the experimental set-up and parameters (Wang et al., 1999)

It is an open cycle system
The generator consists of eight rows of horizontal tubes
The tubes are approximately .4 m / 1 ft in length and 16mm / .6 inch inner diameter.
The inlet LiBr solution is between 55-56.7 %.
The hot water at the inlet is between 80-96 ^{o}C / 176-204 ^{o}F
The spraying density range was 85-510 [kg/hr-m] / 33-370 [lbm/hr-ft]

The geometry of the finned tube is a fin height of 1.4 mm / 0.055 in , fin width of 0.3 mm / 0.012 in, and the distance between fins is 1.4 mm / .055 in. This is approximately 15 fins per inch.

The spraying density was specified, which allowed the determination of the leaving concentration and outside heat transfer coefficient using the empirical relationships derived from Figure 3-21 and Figure 3-22. The subscripts ft and st represent finned tube and smooth tube.

$$x_{o,ft} = 60 - .011\varphi + 1.4e^{-5}\varphi^2 \qquad [3\text{-}51]$$

$$x_{o,st} = 60 - 9.9e^{-3}\varphi + 1.3e^{-5}\varphi^2 \qquad [3\text{-}52]$$

where $x_{out,ft}$ is the exiting concentration for finned tube[%]
φ is the spraying density [lbm/hr-ft]

The following sets of equations are derived from Figure 3-23. The subscript o represents outside and g represents generator.

$$h_{og,ft} = 160\varphi^{.26} \qquad [3\text{-}53]$$

$$h_{og,st} = 120\varphi^{.23} \qquad [3\text{-}54]$$

With h_{og} known the generator pressure can then be determined from the empirical relationship derived from Figure 3-21.

$$h_{og,ft} = 415 + 970P_{g,ft} - 727P_{g,ft}^2 \qquad [3\text{-}55]$$

$$h_{og,st} = 731 - 342P_{g,st} \qquad [3\text{-}56]$$

where P_g is the equilibrium pressure in the generator [psia].

With the pressure known, the temperature of the entering and exiting solution can be determined from property relations and thus an average viscosity can also be determined from property relations. The main objective of determining the average viscosity is to relate the outside heat transfer coefficient to a film Reynolds number.

$$\mathrm{Re}_{fg} = \frac{4\Gamma_g}{\mu_{fg}} \qquad [\ 3\text{-}57\ ]$$

where Γ_g is the film flow rate $\Gamma_g = \dfrac{\dot{m}_7}{2Le_{tube}NC_g}$ [lbm/hr-ft]

Le_{tube} is the length of generator tubes [ft].
NC_g is the number of tube columns.
$\dot{m}_7$ is the mass flow rate of the weak solution entering the generator[lbm/hr].

The main difference between film flow rate and spraying density is the film flow rate is the spraying density divided by two, because the flow is equally split between the tubes.

Figure 3-24 shows the outside heat transfer coefficient as a function of the film Reynolds number.

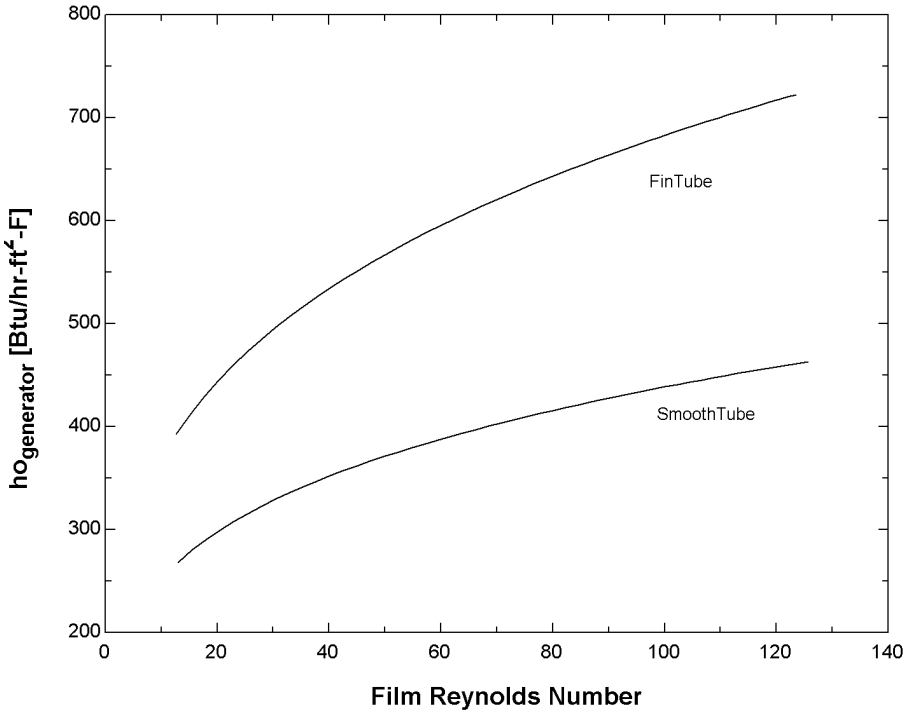

Figure 3-24. Outside heat transfer coefficient as a function of Reynolds number.

Equations 3-58 and 3-59 are the film Reynolds correlations. The power series was used because it has the best R^2 value of the forms investigated and is the common relationship used by the industry.

$$ho_{g,st} = 145\,\mathrm{Re}_{fg}^{.24} \qquad [3\text{-}58]$$

$$ho_{g,ft} = 199\,\mathrm{Re}_{fg}^{.27} \qquad [3\text{-}59]$$

The film Reynolds correlation is then compared with empirical relationships for multi-component mixtures and turbulent falling films from Rohsenow et al., (1998). Figure 3-25 illustrates the large difference between the correlations of Wang and Rohsenow. The Rohsenow correlation for multi-component mixtures was developed for an ethylene glycol / water mixture, which might explain why there is a difference. The turbulent correlation takes into account wave properties of the falling film but it is based on a single component solution.

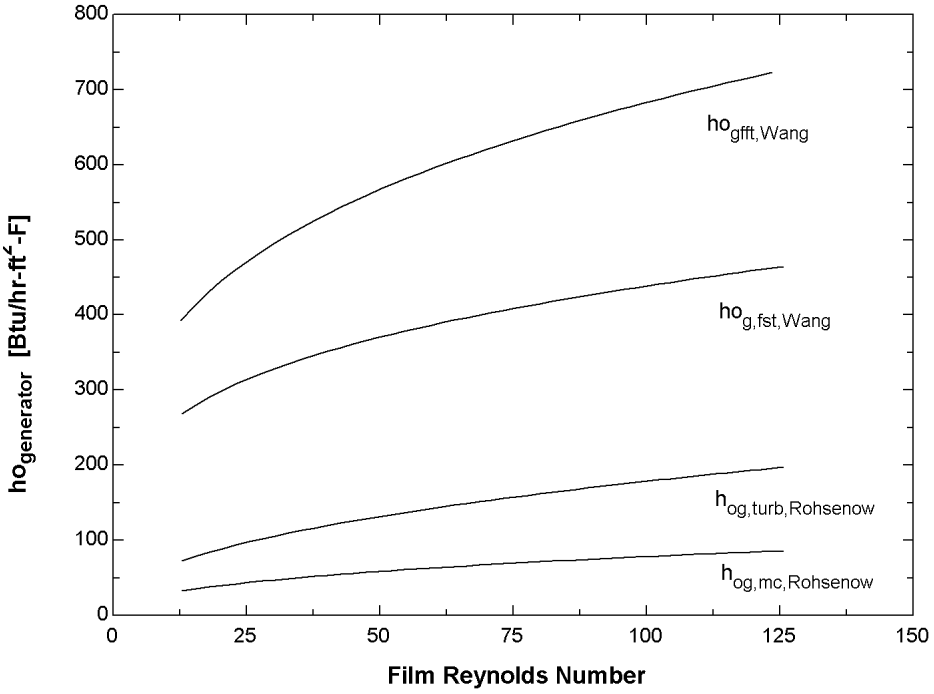

Figure 3-25. Comparison between outside heat transfer coefficient for different correlations.

The Wang heat transfer coefficient is an average value across the entire length of tube. It should also be noted that this correlation will be used for a tube bank that is larger than 8 columns and 1 row, which means the correlation does not take into the account the effect of heat transfer as the falling film proceeds down the tube column.

CHAPTER 4

MODEL DEVELOPMENT OF HALF EFFECT CYCLE

4.1 Overview

Figure 4-1 is a schematic of the half-effect cycle. The major difference between the single and half effect cycle is the addition of a second generator and absorber. This addition allows for an extra operating pressure at the low concentration [LC] absorber and low temperature [LT] generator.

The principle of the half effect cycle is that it has two lifts. The term lift is used to represent a concentration difference between the generator and absorber. This concentration difference is what drives or gives the potential for mass to flow into the absorber. With the single effect there is only one lift and thus as the hot water temperature is decreased the difference between the two concentrations decreases. The two lifts enable the half-effect cycle to operate at lower firing generator temperatures.

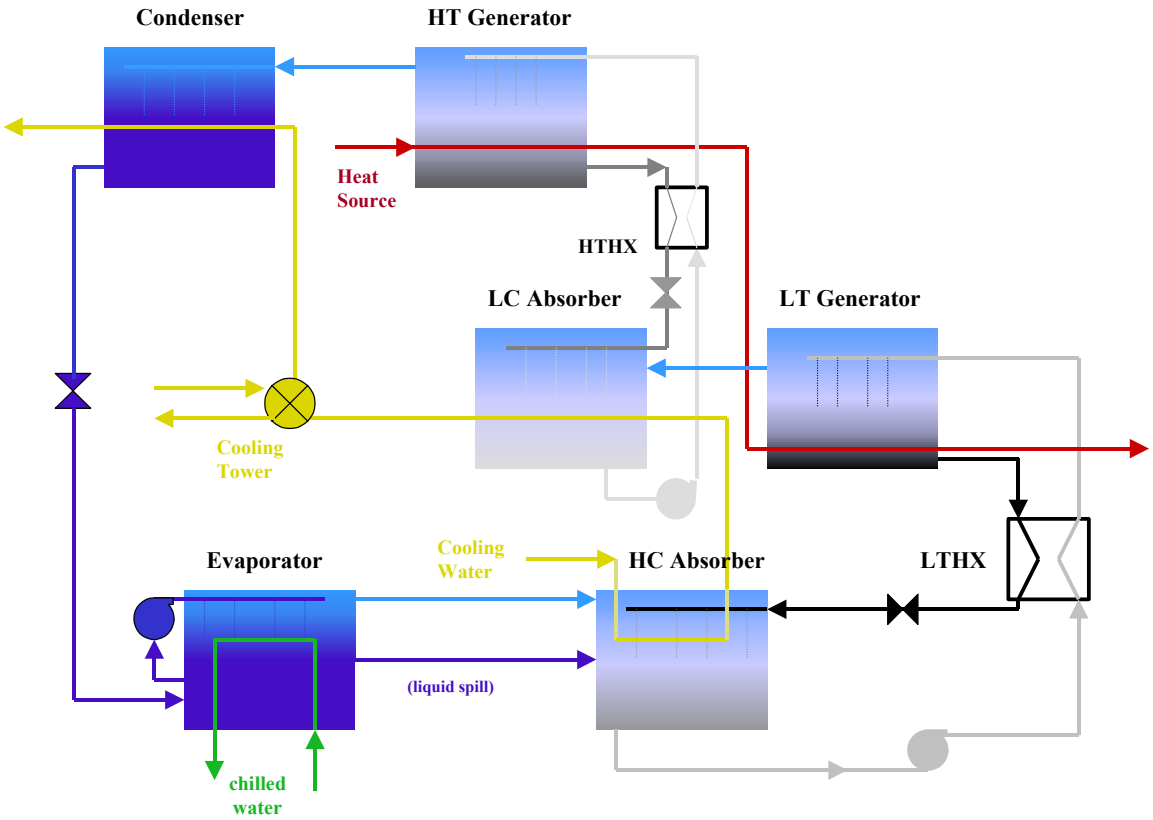

Figure 4-1. Schematic of the half-effect cycle.

The disadvantage of the half-effect cycle is that the COP is approximately half that of the single-effect and thus more thermal energy is required to produce a specified cooling capacity. Consequently higher rates of heat rejection are required for a specified capacity. The higher heat rejection necessitates a larger cooling tower, which translates to higher operating cost and a larger capital investment. The advantage is that the half-effect cycle can operate with the same capacity using lower firing temperatures and thus the heat source has the potential of being free.

Figure 4-2 represents a Dühring plot of the half effect cycle with the corresponding components. The sloped lines represent constant concentration of LiBr in water. The y-axis is

the equilibrium temperature of the water vapor being absorbed or boiled off and the x-axis is the equilibrium temperature of the LiBr-H_2O solution.

The absorption process on the Dühring plot shows a process at constant refrigerant temperature and concentration. The process at constant refrigerant temperature occurs in the absorber and generator. The constant concentration lines describe the processes occurring when the solution is passing through the heat exchanger.

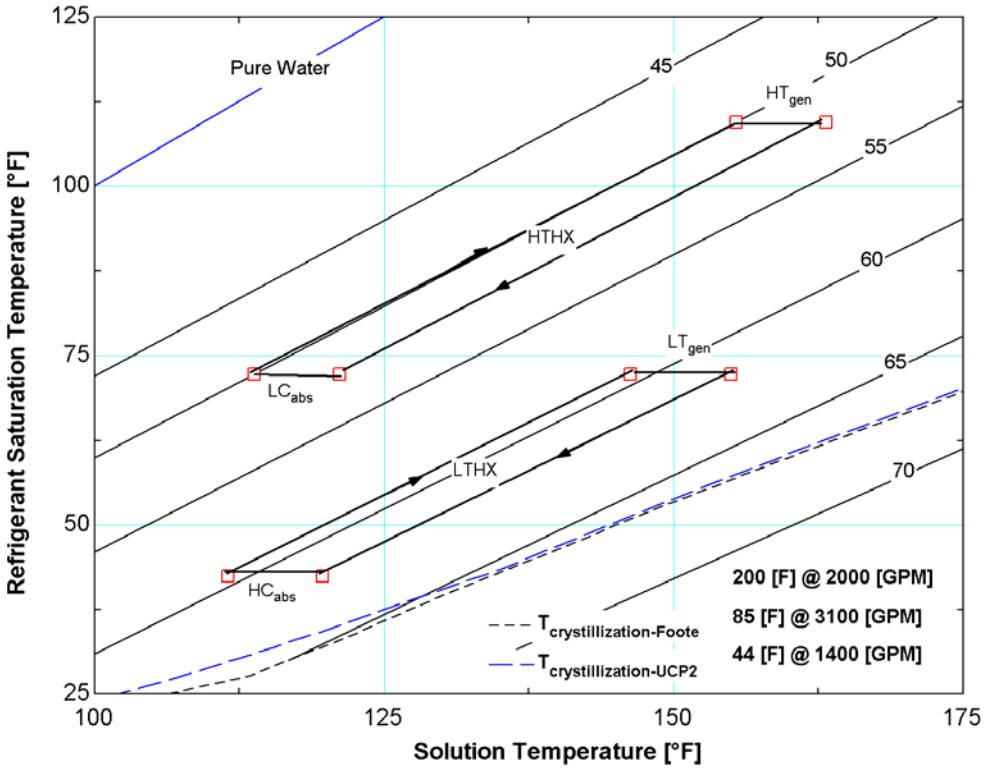

Figure 4-2. Dühring plot of the half-effect cycle.

The important distinction between the single and half-effect cycle can be seen in Figure 4-3, for the single-effect there are two paths of constant refrigerant temperature where the half-effect has three.

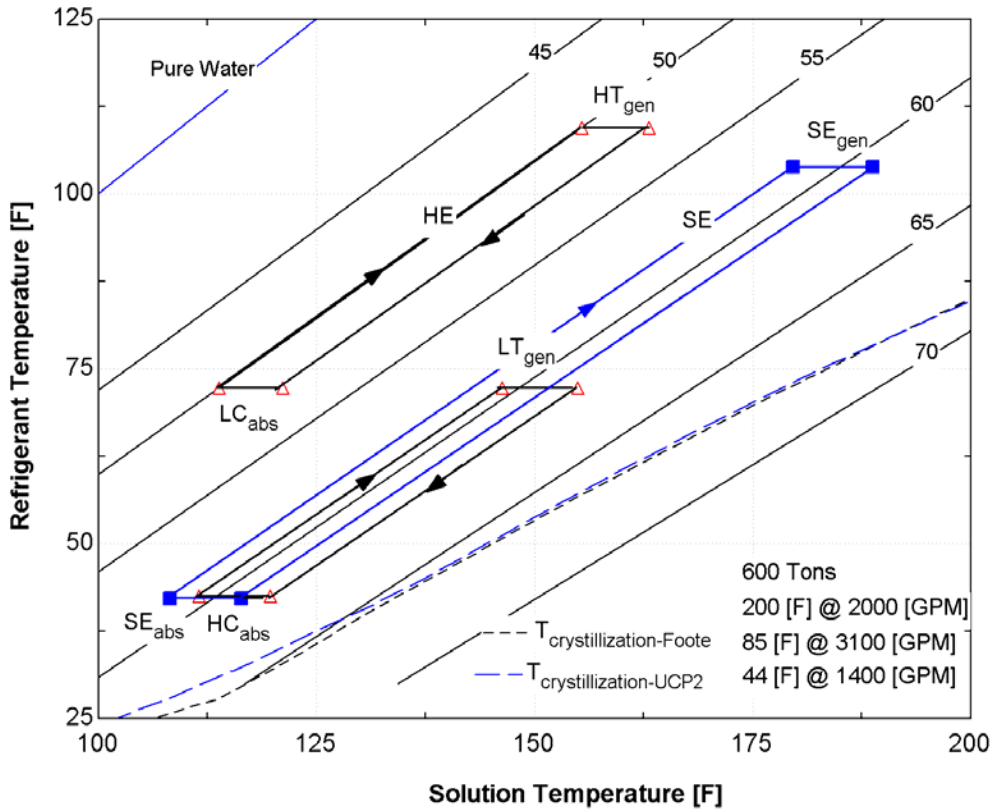

Figure 4-3. Dühring plot comparison between the half-effect and single-effect cycle.

This difference allows the half-effect cycle to produce a larger overall concentration difference compared with the single-effect. The greater the separation between the concentration lines the greater the lift and thus the ability to generate cooling. Since both plots are at 600 tons, the greater concentration separation allows the half-effect cycle to have the sum of the UA for all components to be less than the single-effect, which also means less tube area. The ability for the half-effect cycle to operate using a lower temperature heat source can be seen in Figure 4-3 by comparing the solution temperature. The HT_{gen} solution temperature is less than the single-effect generator solution temperature because the concentration is less even though the pressure or refrigerant temperature is slightly greater. Also the LT_{gen} solution temperature is less than the single-effect because the pressure or

refrigerant temperature is less even though the concentration is the same. By having a lower generator solution temperature enables the half-effect to operate with lower inlet hot water temperatures.

4.2 Inputs

The same inputs are required for each component as for the single-effect model. The main difference between the half-effect and single-effect model is that an additional mass and salt balance is required. The following is a complete list of the inputs for the half-effect cycle.

4.2.1 HTGenerator

T30	Temperature of hot water [F]
Vol30	Flow rate of hot water [gpm]
Tube#	Total Number of Tubes
NCG_ht	Number of Tubes in column
D_g	Inner and Outer Diameter of Tubes [in]
Le_g	Length of Tubes [ft]

4.2.2 LTGenerator

Vol_{31}	Flow rate of hot water [gpm]
Tube#	Total Number of Tubes
NCG_lt	Number of Tubes in column
D_g	Inner and Outer Diameter of Tubes [in]
Le_g	Length of Tubes [ft]

Signal_hs	Control variable to determine if temperature entering is leaving HT generator temperature or if a defined temperature. '0' split flow and '1' series flow

4.2.3 Condenser

Tube#	Number of Tubes
D_tube	Inner and Outer Diameter of Tubes [in]
Le_tube	Length of Tubes [ft]

Signal	Control variable used to determine if cooling water flow rate and temperature is equal to absorber flow rate and leaving LC absorber '0' closed valve [specify temperature and flow rate] '1' open valve no input required

4.2.4 Evaporator

Tube#	Number of Tubes
D_tube	Inner and Outer Diameter of Tubes [in]
L_tube	Length of Tubes [ft]
NCE	Number of Tubes in a column
m50	Mass Flow Rate of Chilled Water [lbm/hr]
T51	Temperature of Delivered Chilled Water [F]

4.2.5 HC Absorber

T40	Temperature of Entering Cooling Water [F]
m40	Mass Flow Rate of Cooling Water [lbm/hr]
Tube#	Number of Tubes
D_tube	Inner and Outer Diameter of Tubes [in]
L_tube	Length of Tubes [ft]
NCA_hc	Number of Tubes in a column

4.2.6 LC Absorber

Tube#	Number of Tubes
D_tube	Inner and Outer Diameter of Tubes [in]
L_tube	Length of Tubes [ft]
NCA_lc	Number of Tubes in a column

4.2.7 High-Temperature Heat Exchanger

η_hthx	Effectiveness of High-Temperature Heat Exchanger

4.2.8 Low-Temperature Heat Exchanger

η_lthx Effectiveness of Low-Temperature Heat Exchanger

4.3 Assumptions

The same assumptions are applied to the half-effect cycle model as for the single-effect model (section 3.3) with the following differences

The sub-cooling and liquid spill in the single-effect model is not applied to the half-effect cycle. This gives a small advantage to the half-effect cycle, but since no data is available it would be unfair to penalize a cycle without knowing if sub-cooling or liquid spill would occur. If it turns out that the half-effect cycle is not economically viable in the ideal case then why go into the detail of sub-cooling and liquid spill.

The additional assumption is that the refrigerant flow rate leaving the low temperature generator is equal to the refrigerant flow rate leaving the high temperature generator. Since the model is steady state and does not allow for storage of mass, this assumption must be implemented to ensure mass conservation. Each of the components in the half-effect cycle are modeled using the same equations as described in section 3.4.

CHAPTER 5

COOLING TOWER

5.1 Overview

The cooling tower model is needed to predict parasitic fan power for different design and operating characteristics of the absorption chiller. As the cooling water flow rate is increased, the absorber has a higher overall heat transfer coefficient [UA_{abs}], but it comes at a cost because a larger cooling tower is needed. The cooling tower model is based on the analogy approach developed by Braun et al. (1989). A program called UPDATE 3.34, (Marley Cooling Tower Company, 1998) generated performance curves, which were used to compute the cooling tower overall heat transfer coefficient [UA_{tower}], needed for the analogy approach method. Figure 5-1 displays a schematic drawing of a cooling tower with the inputs and outputs used in the model.

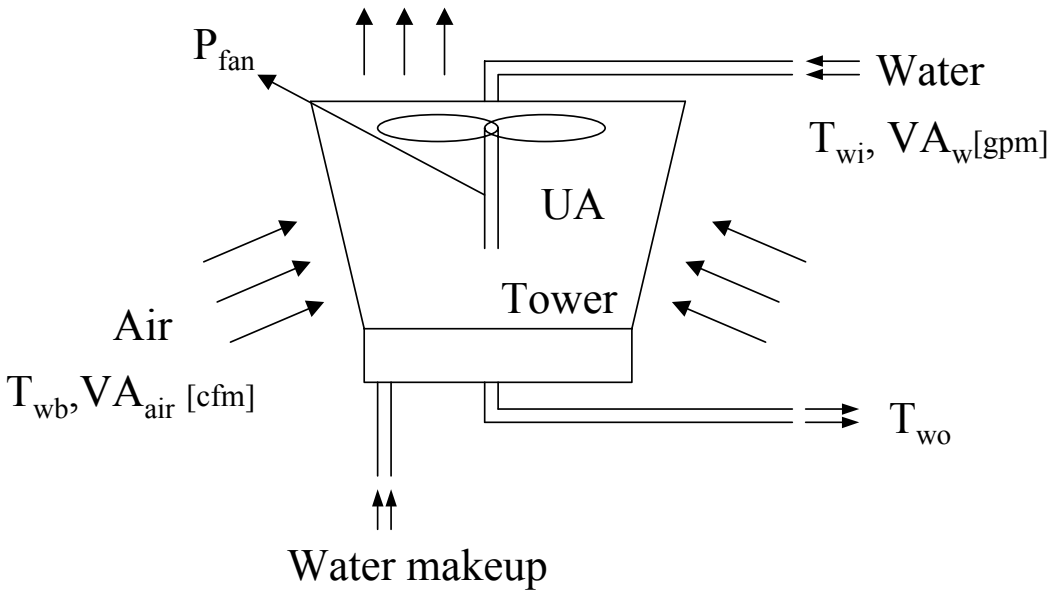

Figure 5-1. Schematic diagram of a cooling tower.

The inputs to the model

T_{wi}	Inlet water temperature [F]
VA_w	cooling water flow rate [gpm]
T_{wb}	Wet bulb temperature [F]
UA_{tower}	Tower UA [Btu/hr-F]
T_{wo} or P_{fan}	Outlet water temperature or Fan Power [F] or [hp]

The last input enables the model to either hold fan power constant and have the outlet water temperature vary with wet-bulb temperature or require a constant cooling water temperature and vary the fan power. The water makeup is an output of the model although it is physically an input to the cooling tower, due to the water loss into the air stream.

5.2 Analogy Approach

The analogy approach is based on the same principles as a sensible heat exchanger cooling coil. The following description is a condensed version from Braun et al. (1989). The mass and energy balance on the cooling tower is:

$$\dot{m}_{w,o} - \dot{m}_{w,i} = w_{a,o}\dot{m}_{a,o} - w_{a,i}\dot{m}_{w,i} \qquad [5\text{-}1]$$

$$C_w(\dot{m}_{w,o}T_{w,o} - \dot{m}_{w,i}T_{w,i}) = \dot{m}_a(h_{a,o} - h_{a,i}) \qquad [5\text{-}2]$$

where $\dot{m}$ is the water or airflow rate [lbm/hr]
w is the humidity ratio of the air [$lbm_w/lbm_{dry,a}$]
C_w is the specific heat of water [Btu/lbm-F]
h is the enthalpy [Btu/lbm]
T is temperature [F]
$_w$ represents water
$_a$ represents air
$_{i,o}$ represent in and out

The effective specific heat is the change in enthalpy with temperature along the saturation line. The effective specific heat can be used to rewrite the energy equation is terms of enthalpies.

$$C_s = \frac{h_{a,sat,i} - h_{a,sat,o}}{T_{w,i} - T_{w,o}} \qquad [5\text{-}3]$$

where $h_{a,sat}$ is the air saturation ethanlpy at the water inlet and outlet temperature.
C_s is the effective specific heat

Thus the equivalent capacitance rate is defined as

$$m^* = \frac{\dot{m}_a C_s}{\dot{m}_{w,i} C_w} \qquad [5\text{-}4]$$

The effectiveness is defined similar to a counter-flow heat exchanger except C^* is replaced with m^*.

$$\varepsilon = \frac{1 - e^{-Ntu(1-m^*)}}{1 - m^* e^{-Ntu(1-m^*)}} \qquad [5\text{-}5]$$

With an effectiveness relationship known the heat transfer is given by

$$q = \varepsilon \dot{m}_a (h_{a,sat,i} - h_{a,i}) \qquad [5\text{-}6]$$

The outlet air conditions are based on an air passing over a uniform wetted surface at a specified uniform temperature. The energy equation for this effective enthalpy is

$$h_{a,eff} = h_{a,i} + \frac{h_{a,o} - h_{a,i}}{1 - e^{-Ntu}} \qquad [5\text{-}7]$$

An outlet air humidity ratio is also determined by a similar approach

$$w_{a,o} = w_{s,eff} + (w_{a,i} - w_{s,eff}) e^{-Ntu} \qquad [5\text{-}8]$$

An energy balance on the air side yields

$$q = \dot{m}_a (h_{a,o} - h_{a,i}) \qquad [5\text{-}9]$$

All of the above equations are based on a general cooling tower design. The Ntu is determined from a UA, which is based on the characteristics of an actual cooling tower. The Ntu is defined as

$$Ntu = \frac{UA}{\dot{m}_a C_a} \qquad [5\text{-}10]$$

5.3 Fan Power

It is assumed that the fans obey the cubic power law and thus the power consumed as a function of air flow rate can be represented by

$$\dot{P}_{fan} = \sum_{i=1}^{N_{cell}} \gamma_i^3 \dot{P}_{fan,nom,i} \qquad [5\text{-}11]$$

where $\gamma = \dfrac{VA_{air}}{VA_{air,nom}}$

The nominal air flow and fan power is based on standard conditions of 78^{o}F wet bulb, 95/85 ^{o}F inlet and outlet water temperature, and 3 gpm/Ton.

The fan blade mechanical efficiency at part load conditions is given by the function [Koeppel, 1994]

$$\eta_{mech} = -1.3323E-15 + 2.8047\gamma - 2.756\gamma^2 + .90133\gamma^3 \qquad [5\text{-}12]$$

Koeppel (1994) suggest a curve fit for a pump motor/drive efficiency in the calculation of the fan motor efficiency of the form:

$$\eta_{motor} = -.00031247 + 2.1943\gamma - .49874\gamma^2 - 1.7454\gamma^3 + 1.0504\gamma^4 \qquad [5\text{-}13]$$

Thus the electrical power consumption is

$$\dot{P}_{elec} = \frac{\dot{P}_{fan}}{\eta_{motor}\eta_{elec}} \qquad [5\text{-}14\ ]$$

5.4 Overall Tower Heat Transfer Coefficient

The UA for a cooling tower was determined from performance curves provided by UPDATE 3.34 (Marley Cooling Tower Company, 1998). The performance curves are fan power [P_{fan}] versus wet bulb temperature for 3 different ranges. The range is defined as the temperature difference between the water entering and leaving the cooling tower. The three ranges are 8, 10 and 12^{o}F. The UA_{tower} was determined by inputting the fan power to the model and having the analogy approach calculate the UA_{tower} for that fan power at a given wet bulb temperature. Since the program only provides graphs, the fan power and wet bulb temperature values were read from the graph. The graphs provided by UPDATE 3.34 are presented as 'guaranteed' performance curves.

Figure 5-2 displays UA_{tower} as a function of airflow rate for a constant range and capacity. The airflow rate is used because there is not enough information available on the geometry to take a Reynolds number approach. The empirical linear relationship [UA_{tower} Model] developed from the performance data is used to determine the UA_{tower} for one type of cooling

tower. The empirical relationship was developed out of a need to determine the fan power for part load conditions. The relationship is of the form

$$UA_{tower} = \frac{mVol_a}{N_{cells}} + b \qquad [\ 5\text{-}15\ ]$$

where m and b are constants determined from the performance data [Btu-min/hr-F-ft^3] and [Btu/hr-F]
N_{cells} is the number of cells in the cooling tower
Vol_a is the air flow rate [cfm]

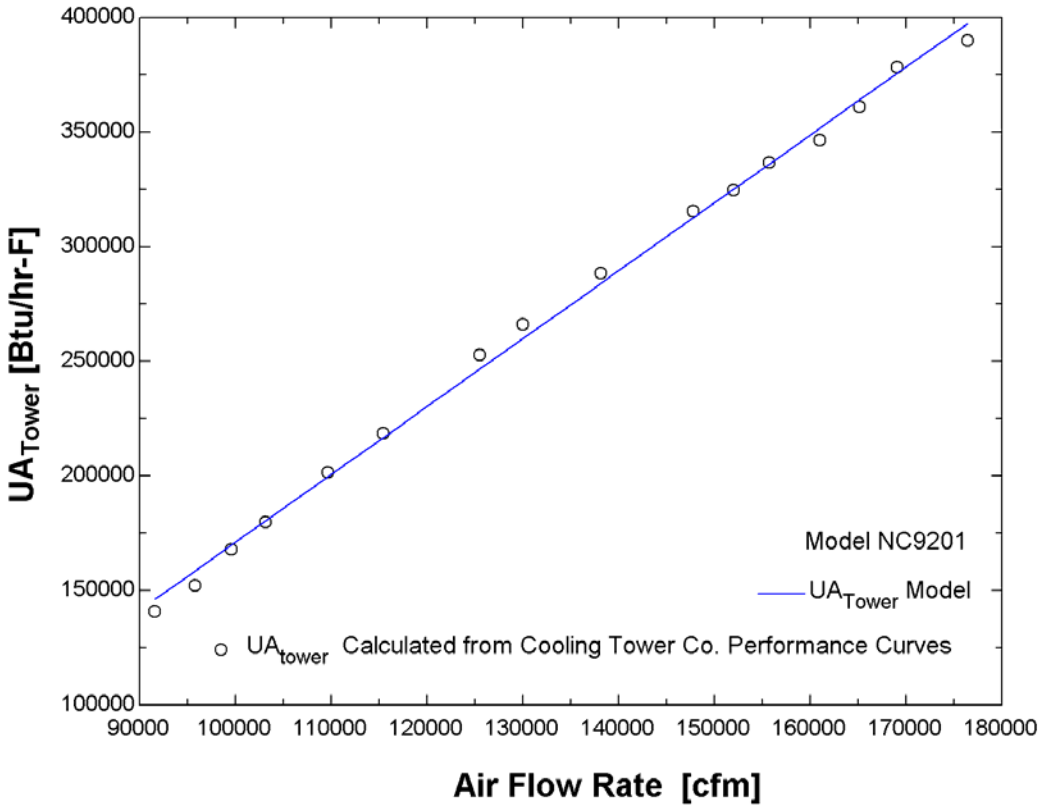

Figure 5-2. UA_{tower} versus air flow rate for 10 Range, T_{wo}=85°F , T_{wb}=78°F, VA_w=2000 [gpm]

The same type of liner relationship is used to determine the UA_{tower} for 4 other cooling towers. The different relationships are needed because as the cooling water flow rate is varied different cooling tower sizes are needed. For example choosing only one cooling tower and varying the flow rate would greatly under or over design the system. Table 5-1 list the different types of cooling towers used in the system model.

Table 5-1. Different types of cooling towers available

Model	VA_{air} [cfm] per cell	VA_w [gpm]	Cost Factor	cells	$FanPower_{max}$ [hp] per cell
NC9202	176400	4000	1.31	2	25
NCB222	190100	4000	1.00	2	40
NCB202	164300	3500	1.09	2	25
NCA202	163700	3000	1.13	2	25
NCC221	235400	2500	1.10	1	40
NC9201	176400	2000	1.31	1	25

The cost factor is the relative increase in price due to a larger cooling tower with less fan power. The importance of the cost factor is that there are cooling towers available that can meet the same load with different fan powers, thus the cost factor can be used to see if the lower operating cost compensates for the increase in heat transfer area which translates to a higher capital investment.

5.5 Calibration/Prediction

Figure 5-3 and Figure 5-4 demonstrate the ability of the analogy approach to predict fan power and outlet water temperature as a function of wet bulb temperature. The performance curve data is read off of graphs generated by UPDATE 3.34.

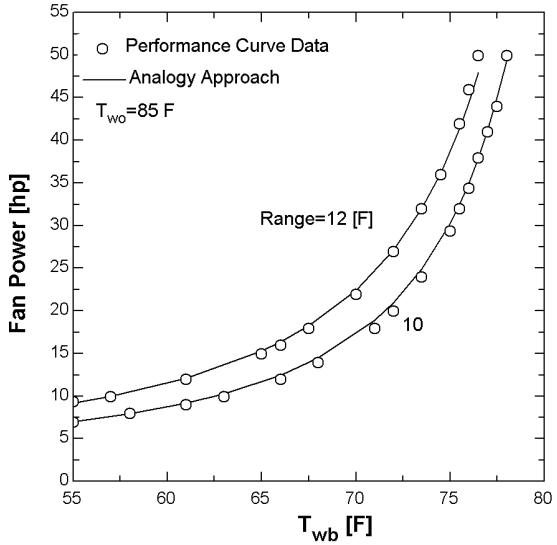

Figure 5-3. Fan Power versus wet bulb temperature [4000 gpm, NC9202]

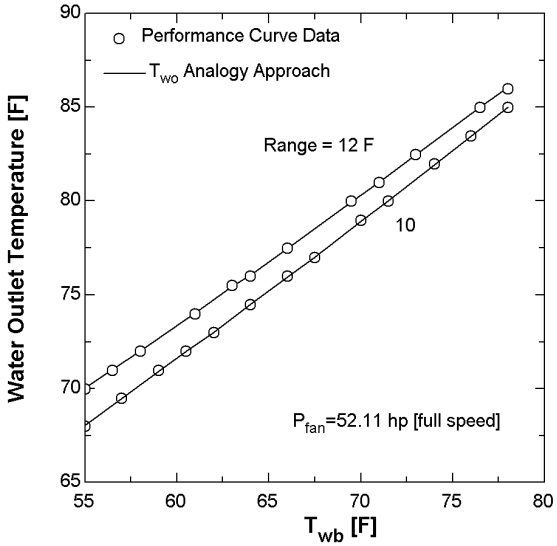

Figure 5-4. Water outlet temperature versus wet bulb temperature [4000 gpm, NC9202]

The model was calibrated for a temperature range of 10°F and is able to predict a 12°F temperature range with the same accuracy. The above graphs demonstrate the linear relationship of UA_{tower} as a function of airflow rate and the analogy approach are valid for modeling a cooling towers power consumption and outlet water temperature.

CHAPTER 6

ECONOMICS

6.1 Overview

Economics is the parameter that bridges the gap between a thermodynamic analysis and the power required to operate the unit. Thermodynamics indicates that the optimal system will have the highest overall heat transfer coefficient [UA]. However, in reality economics puts a limit on what the UA can be. For example, it is possible to increase the capacity by increasing the cooling water flow rate. However, an increase in cooling tower water requires a larger cooling tower and higher operating cost. The purpose of this section is to set up the assumptions and cost figures that will be used to optimize the absorption chiller system. Two different economic analyses are performed using the P_1, P_2 method (Beckman and Duffie, 1992). The first analysis determines the "best" design of absorption chiller and cooling tower system. The second analysis determines the cost of heat needed to make an absorption chiller competitive with an electric centrifugal chiller

6.2 Material / Installation Cost Assumptions

6.2.1 Absorption chiller

The material cost for the absorption chiller is primarily based on the number of tubes, shell area, and pumps. These three components have the greatest effect on dollars per ton of cooling capacity for a change in cooling water temperature, or heat source temperature, and flow rate. For example, a lower heat source temperature will require a larger UA in the generator to meet a fixed capacity. The purging system, salt solution, control system, piping, etc., are relatively minor costs and are not effected by a change in the heat exchanger design. A constant price of $20,000 will account for the above components.

The following cost parameters reflect the figures used to determine the capital cost of an absorption chiller (US chiller manufacturer, 2000). Table 6-1 lists the cost of each tube in the various components.

Table 6-1. Price Range for the tube cost of each component (US chiller manufacturer, 2000).

Component	Low [$/ft]	High [$/ft]
Absorber	0.35	0.55
Evaporator	0.8	1.0
Generator [Smooth]	0.4	0.6
Generator [Finned]	0.8	1.2
Condenser	0.5	0.7

Rather than taking into account how the shell geometry will change by increasing the number of tubes, it is assumed that the shell, tube sheet, tube supports, and solution distribution network of the generator-condenser are 75%, and those for the evaporator-absorber are 65% of the total cost of the tubes. A base case cost of tubes is used to calculate this cost, thus when the finned tubes are used instead of smooth, the cost of the shell does not increase with the cost of the tubes but rather with the number of tubes. The installation cost for the tubes is assumed to be $4 per tube. The installation takes into account the drilling and welding for each tube. The labor and overhead for the construction of the absorption unit is assumed to be 65% of the total material cost (US chiller manufacturer, 2000). The installation of the absorption unit itself is 25% of the total capital cost (RS Means Co. Inc., 1998).

6.2.2 Electric Centrifugal Chiller

RS Means Co. Inc., (1998) lists a cost for a water-cooled electric centrifugal chiller at 300 $/ton for 600 tons and an absorption unit cost of 475 $/ton for 600 tons, while the US chiller manufacturer (2000) quotes the latter price at 200 $/ton. To stay consistent with the manufacturer's data for an absorption units tube and shell cost, the capital cost for the manufacturer's electric chiller will be 150 $/ton. The installation cost is roughly 30% of the capital cost (RS Means Co. Inc., 1998).

6.2.3 Cooling Tower

RS Means Co. Inc., 1998 quotes the capital cost for the cooling tower at 62$/Ton for galvanized steel and 100 $/Ton for the stainless steel. Within this range, the capital cost of 70 $/Ton, quoted by Fairchild, (2000), is used. Since it is possible to have more than one cooling tower meet the demand with different fan power consumption, a cost factor adjustment is used. The cost factor takes into account the larger unit with smaller fan power. Refer to the chapter 5, Table 5-1 for the cost factors that are used for different cooling tower models. The installation cost for a cooling tower is 50% of the capital cost (Fairchild, 2000). The installation is based on piping, electrical connection, and foundation.

6.3 Operating Cost Assumptions

The operating cost for the absorption system consists of the cooling tower fan and pumps. The pumps include cooling water, heat source, evaporator, and internal brine solution leaving the absorber. It is important to take into account the pumps because by increasing the cooling or heat source flow rate, the absorption chiller capital cost will decrease while the operating cost will increase.

In analyzing the "best" absorption system, the heat source is assumed to be free, thus no cost for the heat is included. The model does not take into account any adverse effects on the equipment from where the heat source comes from. For example, if the cooling jacket of a diesel generator is used for the waste heat, it may change the performance of the diesel

generator necessitating more fuel to meet the electrical demand. The model does not take into account maintenance cost for the absorption or electric centrifugal chiller.

6.4 Life Cycle Cost Approach

The economic parameters are P_1, P_2, time period of investment, and electrical cost. Table 6-2 lists the numerical range for each one of these parameters. The following section demonstrates how P_1 and P_2 are determined.

Table 6-2. Range of numerical parameters.

P_1	P_2	Time Period	Electrical Cost
Time Period /2	0.8-1.2	10-20 years	.05-.2 $/kW

A life cycle cost analysis is performed on the absorption and electric centrifugal chillers. The life cycle cost combines present worth factors into two variables named P_1 and P_2. P_1 takes into account fuel inflation rate and discount rate. P_2 takes into account taxes, mortgage rates, maintenance, insurance, etc, for a fraction of the initial investment. The following life cycle cost equations are used for the analysis to determine the cost of heat. The subscripts used in the nomenclature are

ec is electric centrifugal chiller
ab is absorption chiller
sp is solution pump
ct is cooling tower
fan is the cooling tower fan

$$LCC_{ec} = P_1(\dot{P}_{ec} + \dot{P}_{ec,fan})C_e + P_2(1.3C_{ec} + 1.5C_{ec,ct}) \quad [6\text{-}1]$$

$$LCC_{ab} = P_1(\dot{P}_{ab,fan} + \dot{P}_{sp} + \dot{P}_{evap})C_e + P_1 Q_{hs} C_h + P_2(1.5C_{ab,ct} + 1.2C_{ab}) \quad [6\text{-}2]$$

where P_1 is the ratio of life cycle fuel cost savings to first year fuel cost [~ $N_e/2$]
P_2 is the life cycle expenditures because of the capital investment. [~ 0.8-1.2]
P is pumping or fan power [kW]
C_e is the cost of electricity [$/kW]
C_h is the cost of heat [$/Therm]
C is capital investment [$]
Q_{hs} is the heat source input [Therms]

The definition of P_1 is (Duffie and Beckman, 1991)

$$P_1 = (1 - C\bar{t})PWF(N_e, i_f, d) \quad [6\text{-}3]$$

where $\bar{t}$ is the effective income tax rate.
PWF is a present worth factor
N_e is the period of economic analysis [year]
i_f is the fuel inflation rate.
d is the discount rate.

Businesses are able to deduct fuel cost and the effective income tax rate is about 50%. If the effective interest rate equals the fuel inflation rate then P_1 is approximately equal to $N_e/2$. If the fuel inflation rate is less than the discount rate then P_1 is less than $N_e/2$.

The definition of P_2 is (Duffie and Beckman, 1991)

$$P_2 = D + (1-D)\frac{PWF(N_{\min,}0,d)}{PWF(N_L,0,d)} - \bar{t}(1-D)\left[PWF(N_{\min,}m,d)\left(m - \frac{1}{PWF(N_L,0,m)} \right) + \frac{PWF(N_{\min,}0,d)}{PWF(N_L,0,m)} \right] \qquad [6\text{-}4]$$

$$+M_s(1-\bar{t})PWF(N_e,i,d) + tV(1-\bar{t})PWF(N_e,i,d)$$

$$-\frac{C\bar{t}}{N_D}PWF(N'_{\min},0,d) - \frac{R_v}{(1+d)^{N_e}}(1-C\bar{t})$$

where D is the ratio of down payment
N_L is the term of the loan [years]
N_{min} is the year of mortgage payments min(N_L or N_e) [years]
m is the annual mortgage interest rate
M_s is the ratio of first year cost (maintenance, insurance) to initial investment
t is the property tax based on assessed value
V is the ratio of assessed valuation of the system in first year to the initial investment
N_D is the depreciation lifetime [years]
N'_{min} is the years which depreciation contributes min(N_D or N_e).
R_v is the ratio of the resale value.

If D is set to one and there is no maintenance cost, resale value, assessed valuation, or depreciation then P_2 is equal to 1. A value less than one for P_2 means there is depreciation, or a resale value or part of the initial investment is made through a loan. A value greater than one for P_2 means there are maintenance costs or property taxes.

If the heat source is free then a maximum capital investment for heat recovery is determined by solving

$$P_1 Q_{hs} C_h - P_2 C_{hr} = 0 \qquad [6\text{-}5]$$

where C_{HR} is the capital investment necessary for heat recovery [$]

The result of setting equations 6-1 and 6-2 equal to each other will determine the bread even cost of heat. The result from equations 6-1 and 6-2 is used in conjunction with equation 6-5, to calculate an equivalent heat recovery investment based on the breakeven cost of fuel. For example, the capital investment for heat recovery could be a heat exchanger for the exhaust of a diesel generator, gas turbine, or industrial stack gases.

CHAPTER 7

SINGLE-EFFECT ABSORPTION CHILLER SYSTEM OPERATION

7.1 Overview

The single-effect absorption chiller system encompasses the cooling tower, heat exchanger, pumps for cooling water and heat source, and the absorption chiller. Figure 7-1 is a schematic diagram of the absorption chiller system.

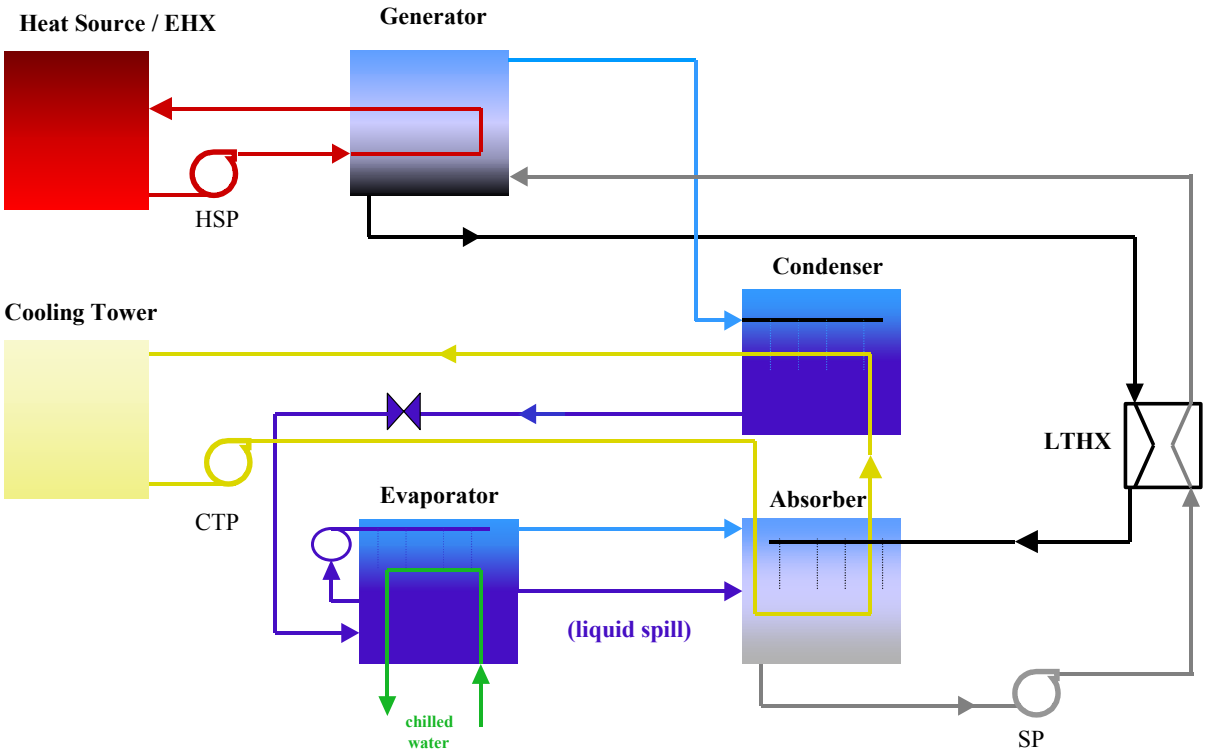

Figure 7-1. Single-Effect Absorption Chiller System.

7.2 Optimization of the absorption chiller system for a given heat source temperature

The first step in designing an absorption chiller using low temperature waste heat is to determine which component will have the largest change in capacity for an equivalent change in UA. Table 7-1 lists the base case for the single-effect absorption chiller

Table 7-1. Base case component size and internal solution flow rate [200 F @ 2000 gpm]

	Absorber	Condenser	Evaporator	Generator
Tubes	514	128	336	262
UA [Btu/hr-ft^2-F]	535304	877538	1.4e6	309516
Internal solution flow rate	230 [gpm]			

The design condition of 600 tons is based on the fact that the component sizes in Table 7-1 can obtain this capacity with 27 psia steam. The capacity for the base case at 200°F hot water is 418 tons, thus the component sizes must be changed to meet the design conditions.

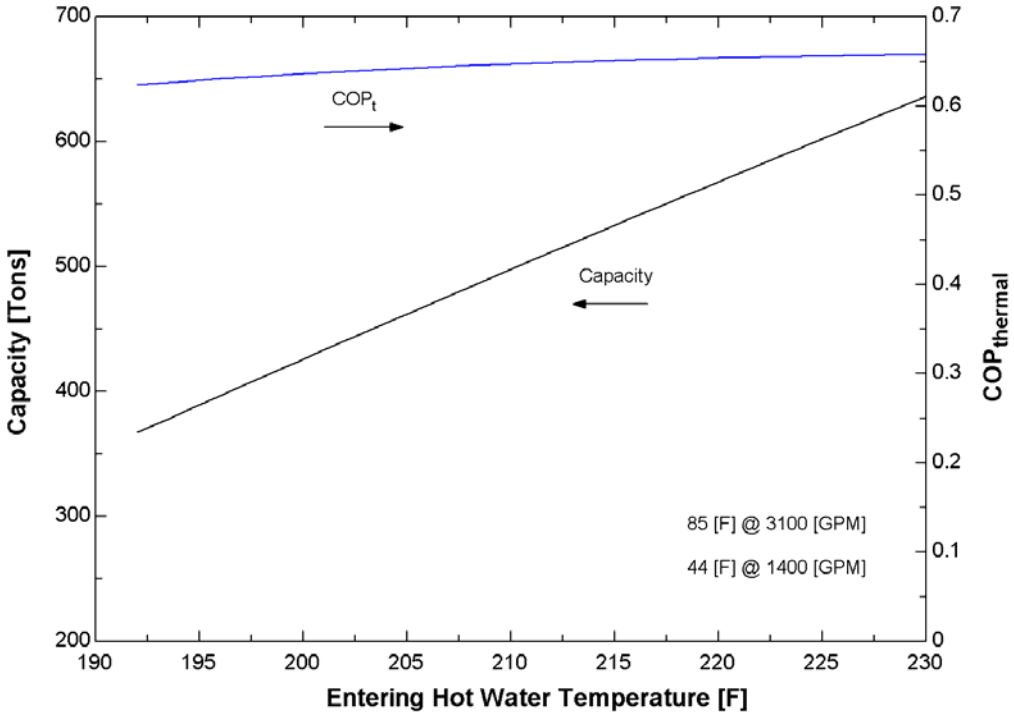

Figure 7-2. Base case Capacity and COP versus entering hot water temperature.

Figure 7-2 displays the need for design changes in the base case absorption unit because as the entering hot water temperature drops to 225 °F, the capacity falls below design conditions. The COP in is independent of the entering hot water temperature.

Figure 7-3 displays a plot of the factor change in each component and the corresponding change in capacity for the base case. Holding 3 out of the 4 component sizes constant while allowing capacity to change was the method used to produce Figure 7-3. The generator has

the steepest slope of the four at 1, therefore any investment should first be put into the generator.

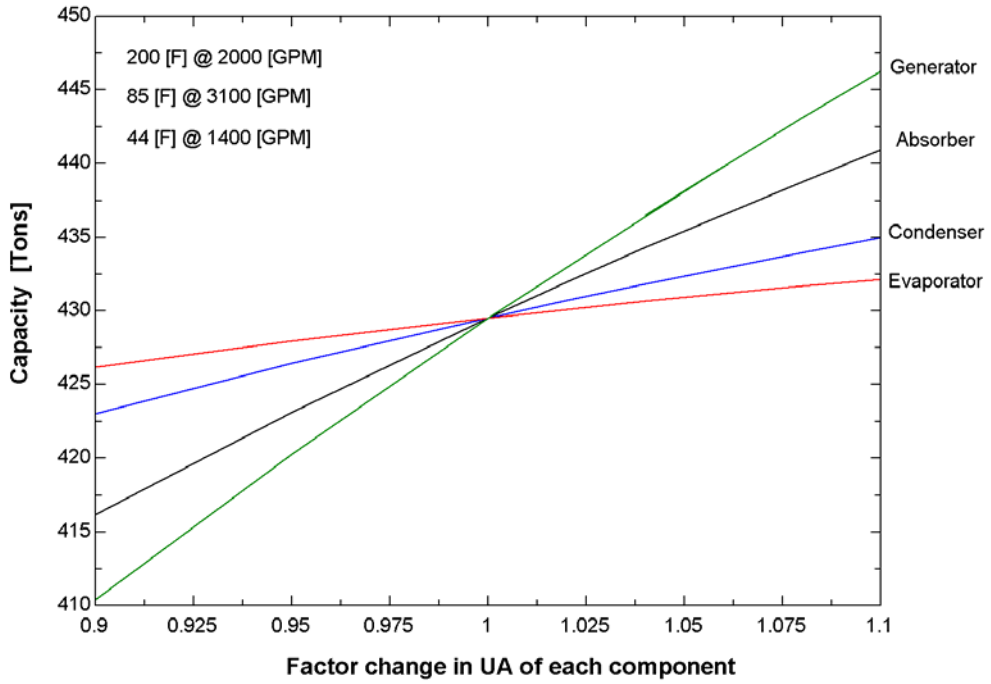

Figure 7-3. The effect of capital dollars per ton for a factor change in UA.

It is possible that an optimum could be found by changing the generator and absorber, however, for this analysis only one component at a time is changed. This method allows one to see the effect of each component separately rather than try to do all combinations simultaneously. Another result of Figure 7-3 is that the evaporator and condenser show the least increase in capacity for an increase in the UA.

The optimization of the absorption chiller system includes minimizing capital and operating cost for the cooling tower, pumps, and absorption chiller. The optimization uses equation 6-

2, with the exception of C_h being set to zero. The analysis involves finding the minimum value of LCC_{ab}. The flow rates are used as the decision variables because they have the largest effect on capital and operating cost. Figure 7-4, Figure 7-5, and Figure 7-6 show contour plots of the volume flow rate of heat source and cooling water with the life cycle cost [LCC_{ab}] as the contour variable for 200°F hot water, for various values of P_1. The capacity is held constant and the number of tubes in the generator changes to find the optimum generator size based on cooling water and heat source flow rate. The condenser, evaporator, and absorber are sized for the base case [Table 7-1]. The type of cooling tower also changes with regard to flow rate. For example, at 4000 gpm, a larger cooling tower is used compared to 3000 gpm.

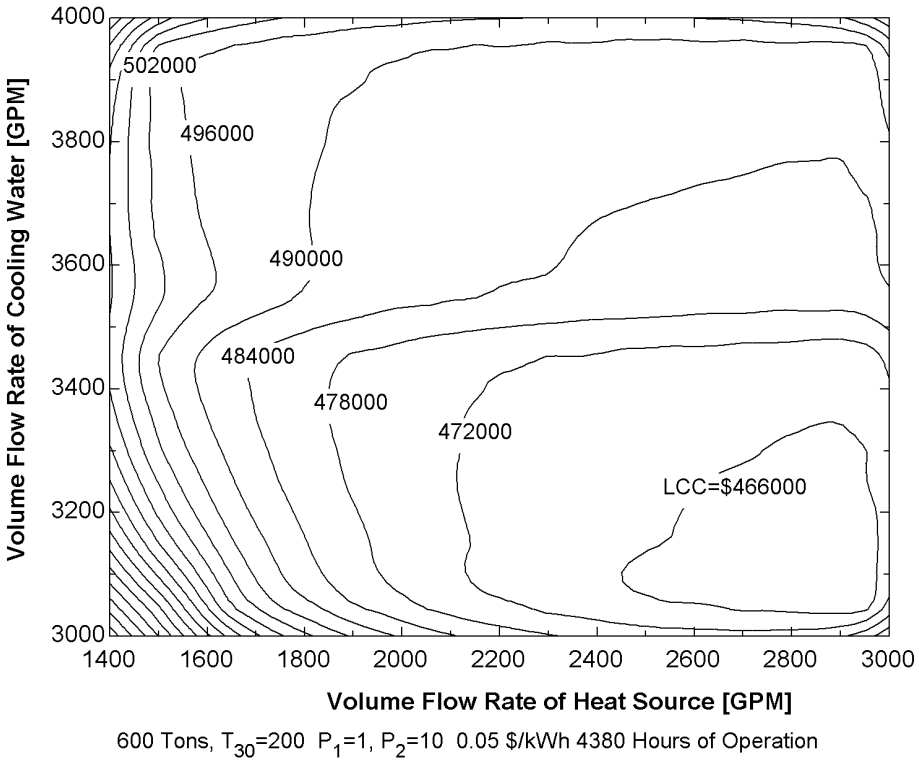

Figure 7-4. Contour plot of PV for 200 F entering hot water, P_1=1.0

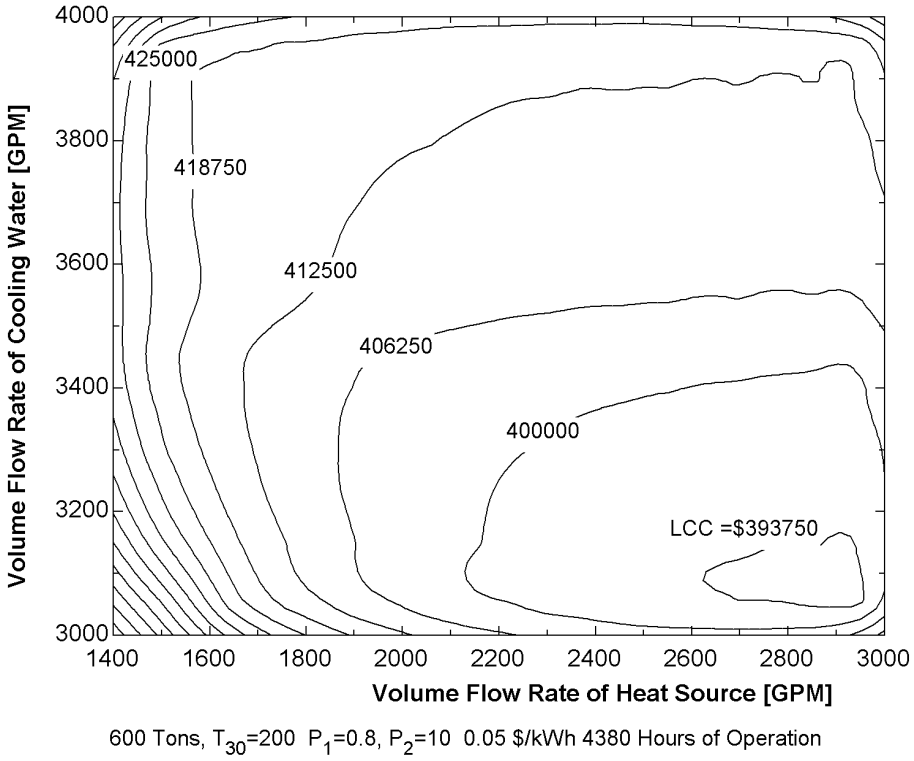

Figure 7-5. Contour plot of PV for 200 F entering hot water, P_1=0.8

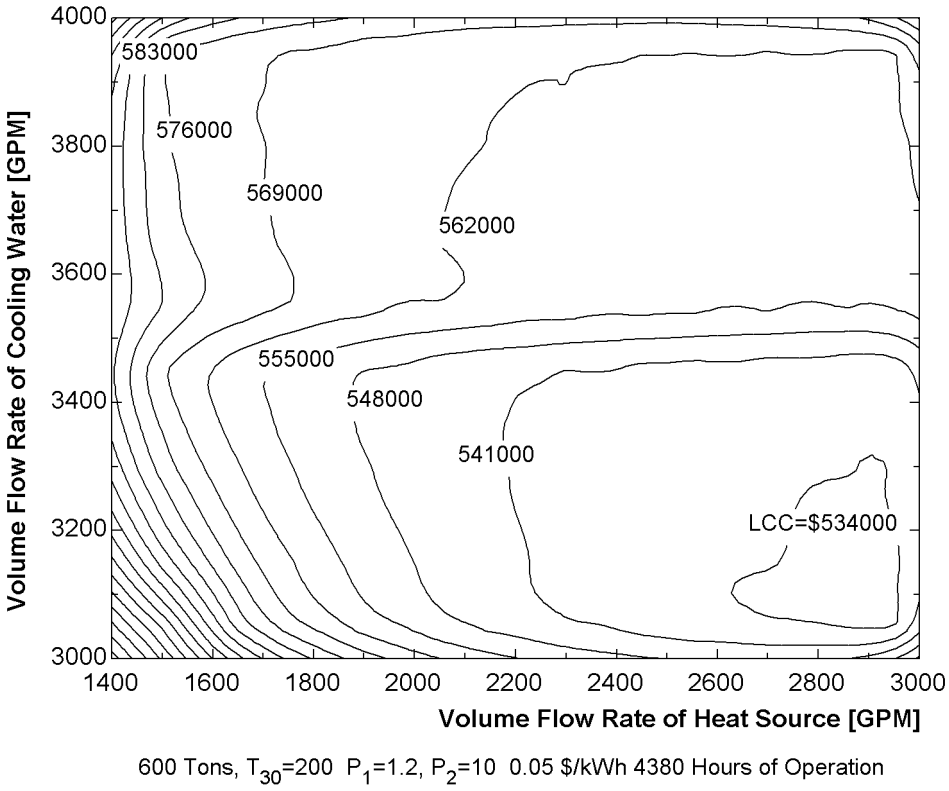

Figure 7-6. Contour plot of PV for 200 F entering hot water, P_1=1.2

Figure 7-4, Figure 7-5, and Figure 7-6 demonstrate that changing P_1 only changes the LCC and not the position of the optimum solution. The optimum solution is around 3100 gpm for the cooling water and 2600 gpm for the hot water flow rate.

The above graphs are based on an electrical cost of 0.05 $/kWh, thus Figure 7-7 and Figure 7-8 display the effect of an increase in electrical cost to 0.1 and 0.2 $/kWh.

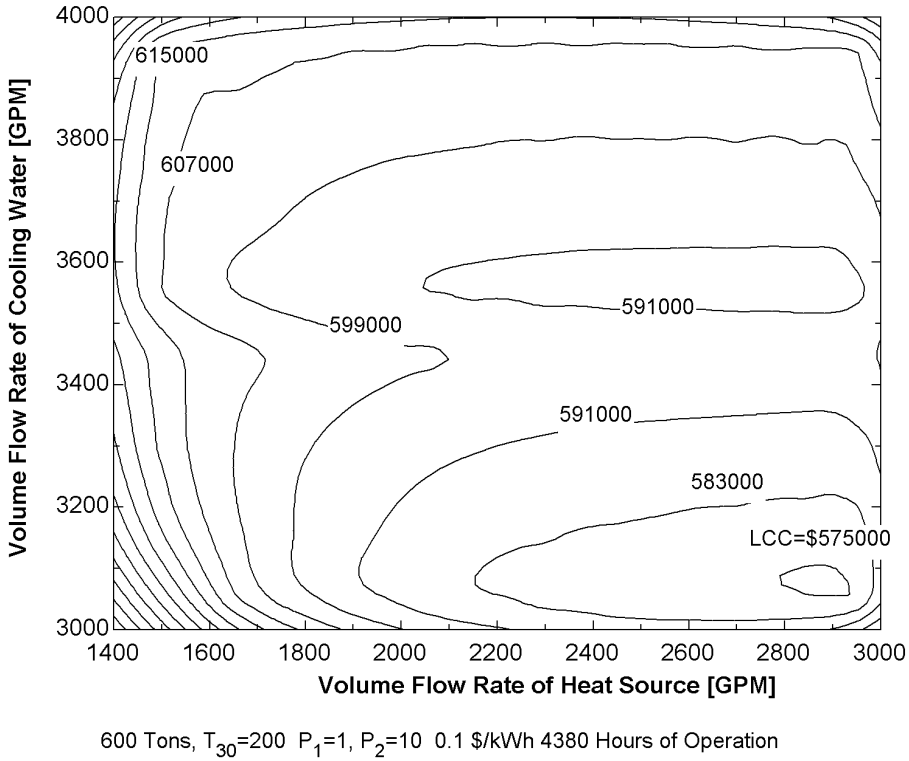

Figure 7-7. Contour plot of PV for 200 F entering hot water, 0.1 $/kWh electrical cost

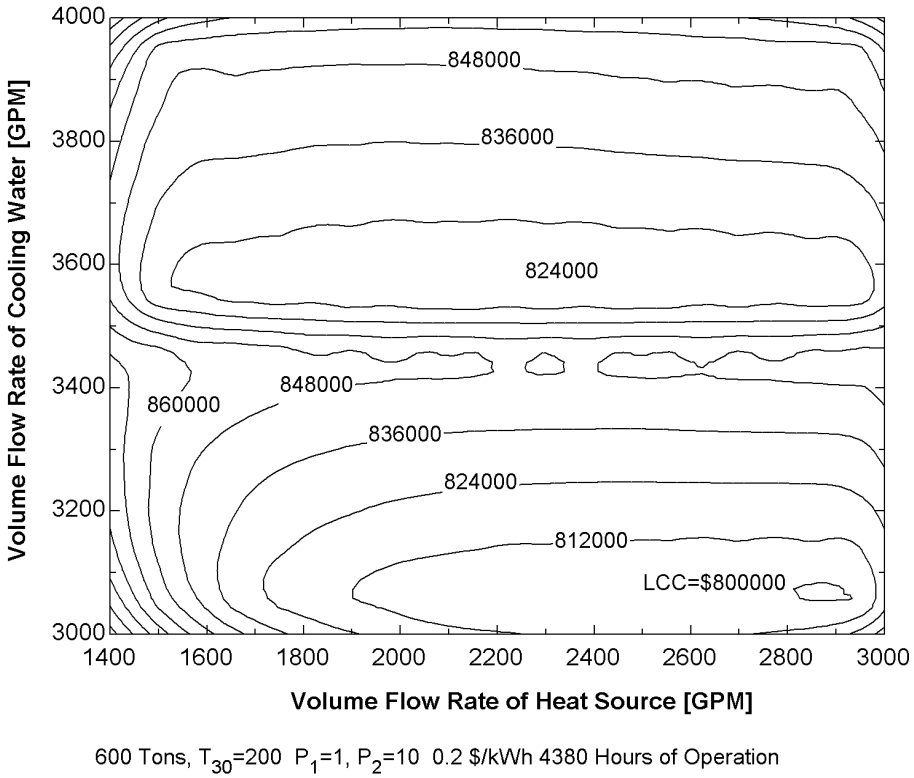

Figure 7-8. Contour plot of PV for 200 F entering hot water, 0.2 $/kWh electrical cost

One interesting result is that a local minimum occurs at a higher cooling water flow rate. The second minimum occurs because the cooling tower operating cost is the same for 3600 gpm and 3100 gpm. The difference is the capital cost of the cooling tower; Figure 7-7 and Figure 7-8 reveal the second minimum at 3600 gpm. Figure 7-4, Figure 7-5, and Figure 7-6 also show a second minimum, but the resolution is not small enough to show the minimum in the graphs. Figure 7-6 discloses a small sign of the second minimum due to the indention at 3600 gpm.

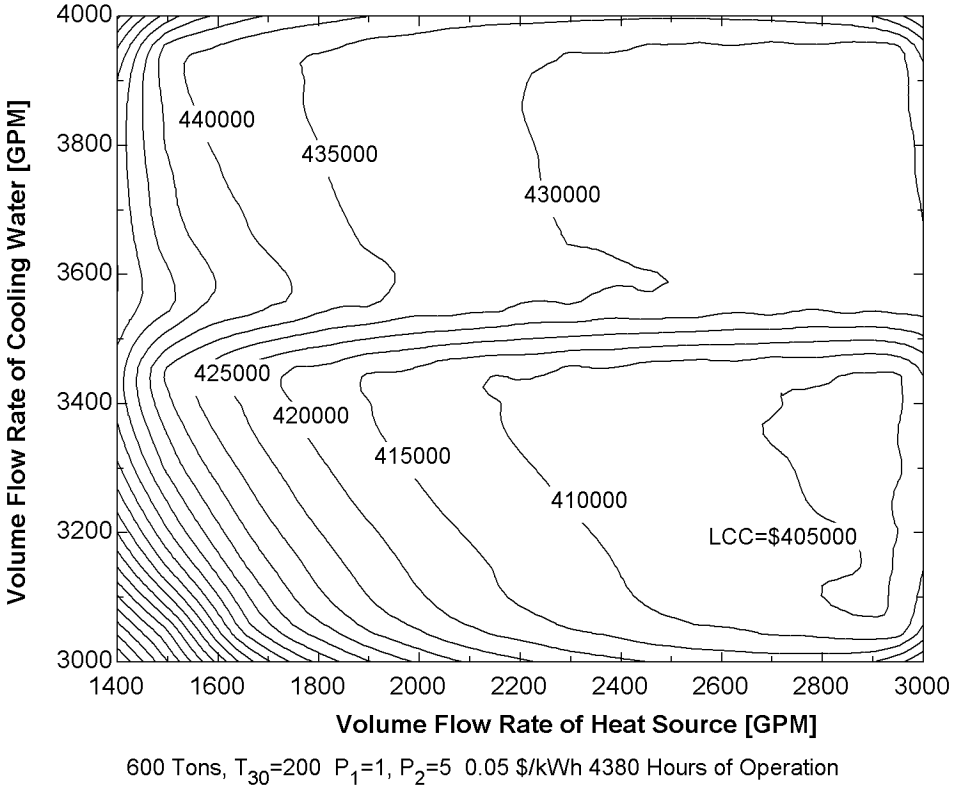

Figure 7-9. Contour plot of PV for 200 F entering hot water, P_2=5 or 10 year life cycle.

Figure 7-9 shows the contour plot when the life cycle is 10 years instead of 20, as in Figure 7-4. The optimum solution is near 3100 gpm for the cooling water and 2900 for the heat source flow rates.

With a change in P_1, P_2, the cost of electricity, and the life cycle time, the optimum solution flow rates for the absorption chiller system remained the same. The only change is in the value of the LCC_{ab}. The importance of the above parameters will be discussed when comparing this system to an electric centrifugal chiller.

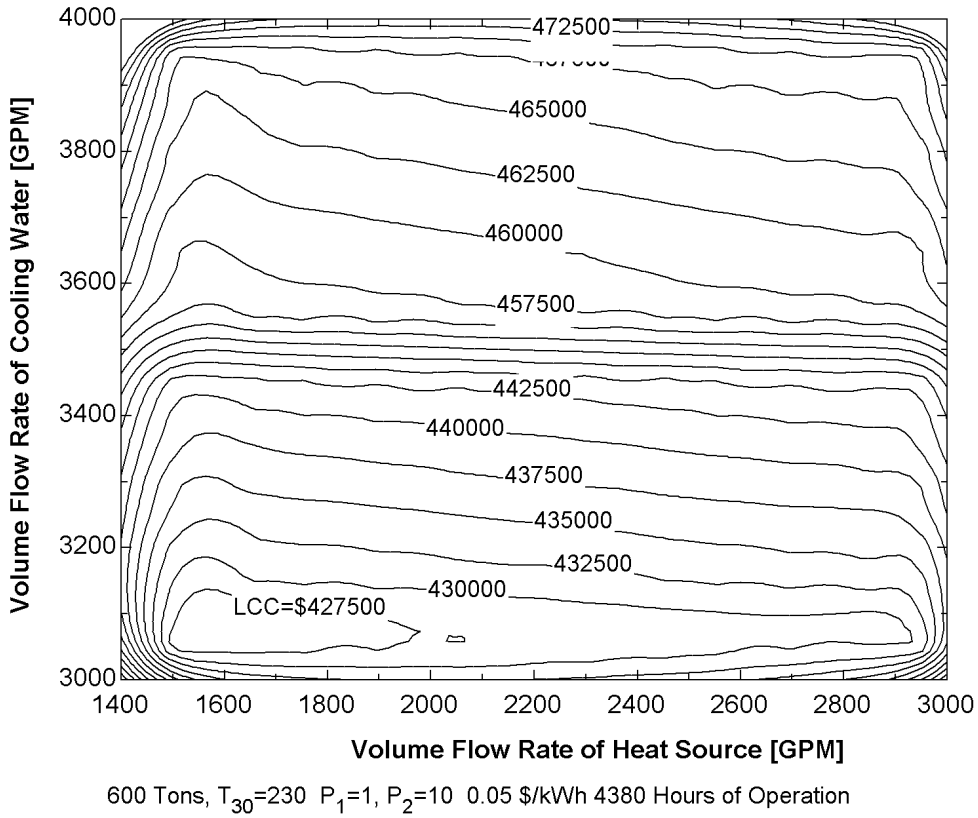

Figure 7-10. Contour plot of PV for 230°F entering hot water.

Figure 7-10 shows the effect on the contour plot by changing the inlet hot water temperature. The optimum solution for a higher inlet hot water temperature moves the flow rate from the right corner to the left. This result was expected because a higher temperature heat source requires less flow rate for the same capacity.

From Figure 7-4 to Figure 7-10 the optimum value for the cooling water flow rate is independent of the heat source temperature. The range of 4000 to 3000 gpm was chosen based on numerous runs to investigate possible solutions. Below 3000 gpm the capital cost is extremely high and anything above 4000 gpm is too large of a flow rate. Likewise, for a

lower heat source temperature a larger flow is advantageous because it reduces capital cost more than the extra operating cost for the larger pump.

7.3 Effect of heat source temperatures

Firing the absorption chiller at lower temperatures is possible but it comes at a cost. The lower temperatures require a larger unit, increasing the capital cost. Figure 7-11 and Figure 7-12 examines the effect of UA and capital dollars per ton.

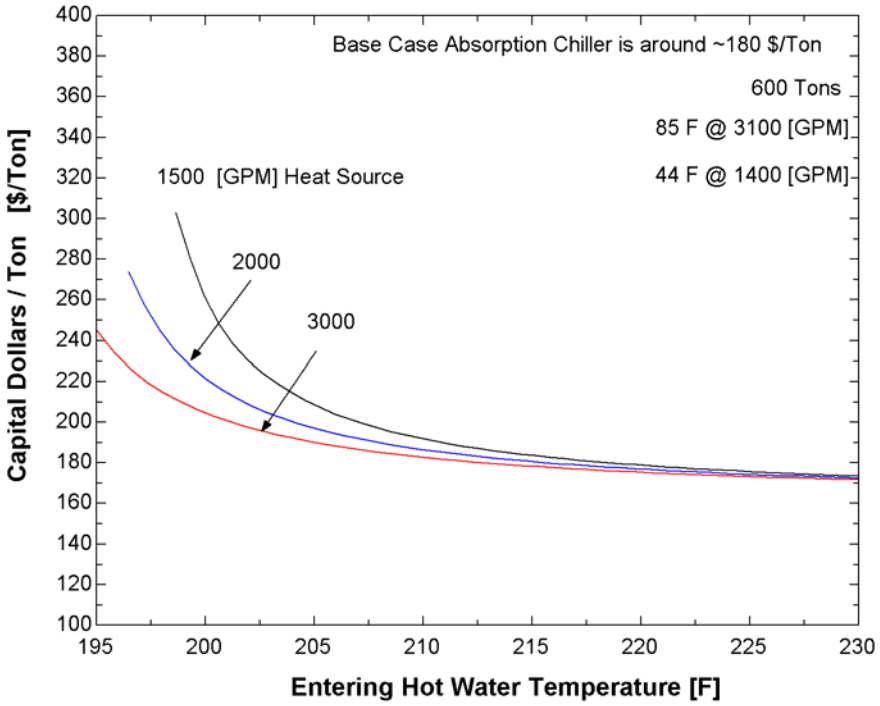

Figure 7-11. Capital dollars per ton as a function of entering hot water.

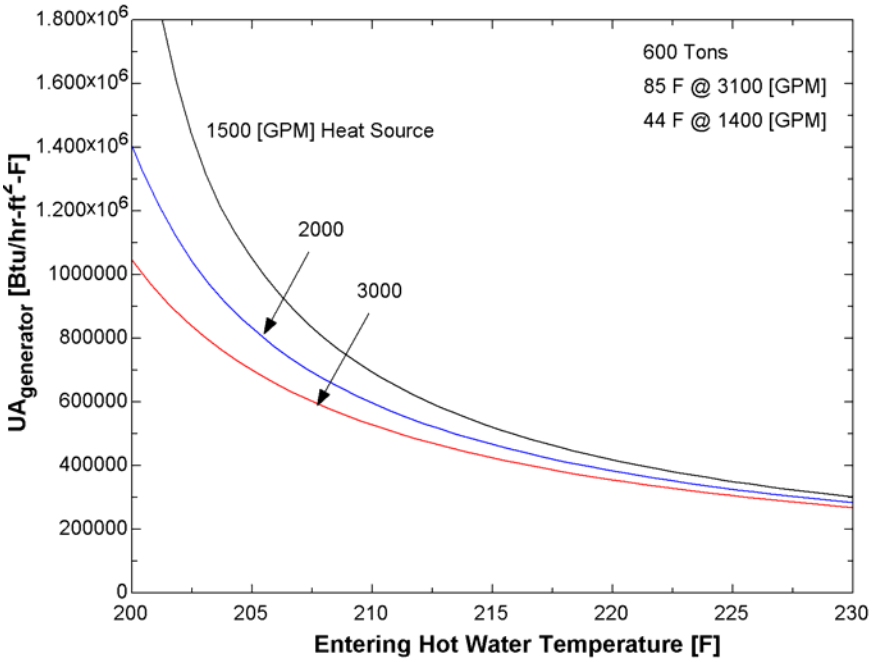

Figure 7-12. UA generator as a function of entering hot water.

The UA and dollars per ton reveal the same trends, however, it is important to look at both the cost and the UA. The dollars per ton is calculated by using empirical heat transfer coefficients and pricing assumptions based on material and labor costs [Refer to chapter 3 and chapter 6]. The UA is calculated by energy, mass balances, and property data, requiring fewer assumptions and making it less uncertain.

Figure 7-12 shows that at temperatures below 205°F, the chiller design starts to change rapidly to accommodate lower firing temperatures. At around 210°F the $UA_{generator}$ nearly doubles in size compared to the base case in Table 7-1. As the entering temperature is lowered the effect of hot water flow rate becomes more important in the design.

The capital dollars per ton is based on material, labor and overhead cost for the absorption chiller presented in 6.2. Figure 7-11 shows the same trends as Figure 7-12, but this can be used as a tool to compare with other first cost cycles and a standard parameter used by the refrigeration industry. At 200°F, a 33% increase from 1500 to 2000 gpm in heat source flow rate can reduce the capital cost by approximately 20% from 260 to 220 $/Ton, assuming one can acquire a heat source with a flow rate of 2000 gpm for a reasonable investment.

7.4 Sensitivity Analysis on UA of each component.

In order to meet the 600 tons at 200°F entering hot water the base case designed must be changed. Table 7-2 lists the absorption chiller design to meet the 600 tons of cooling.

Table 7-2. Component size and internal solution flow rate to meet 600 Tons [200°F @ 2000 gpm]

	Absorber	Condenser	Evaporator	Generator
Tubes	514	128	336	1730
UA [Btu/hr-ft^{2}F]	522470	853445	1.4e6	1.35E6
Internal solution flow rate	230 [gpm]			

Table 7-2 shows about a 650% increase in the number of generator tubes, compared to Table 7-1 to deliver 600 tons at 200°F entering hot water. In Table 7-2 only the generator size was changed, thus a sensitivity analysis on each component UA is needed to obtain a more effective design. The capacity is held constant and the number of generator tubes is changing as the absorber, evaporator, and condenser UA is increased and decreased.

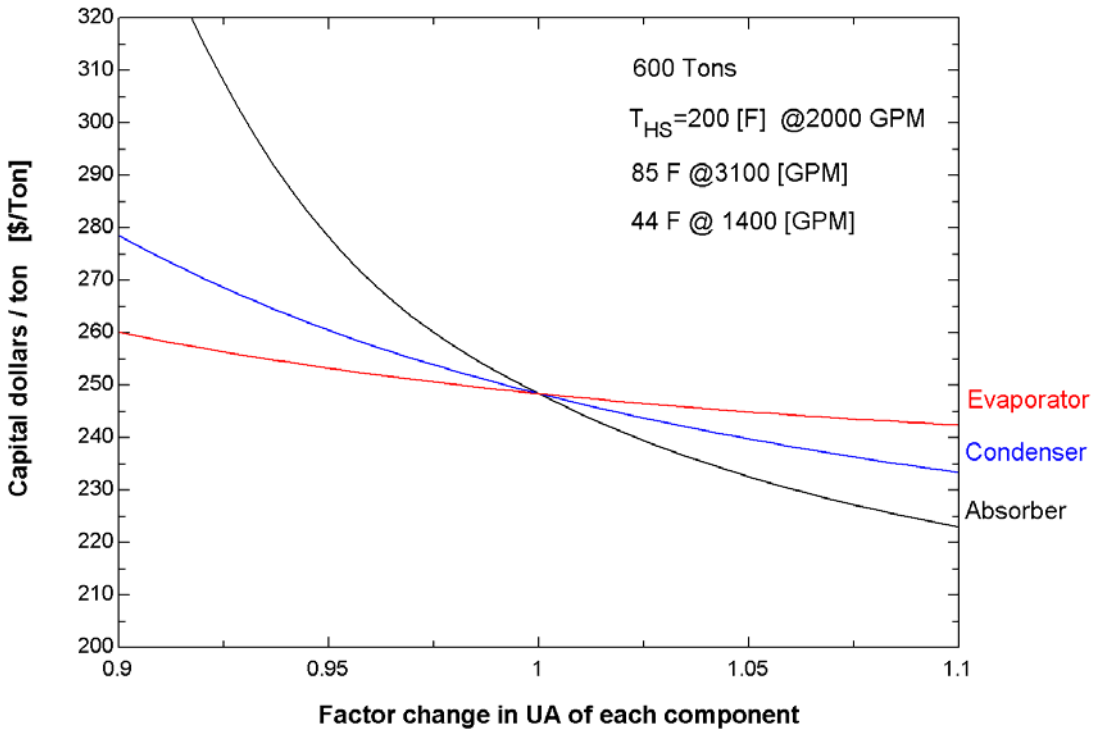

Figure 7-13. The effect of capital dollars per ton for a factor change in UA.

Figure 7-13 demonstrates that increasing the size of the absorber and correspondingly decreasing the size of the generator will have the largest effect on cost while maintaining a fixed capacity. Any investment made into improving the design of the low temperature hot water absorption chiller should be put into the absorber first. Table 7-3 shows that by increasing the number of tubes in the condenser, it will reduce the greatest amount of generator tubes. Since there are fewer tubes in the condenser, a 2% increase will result in an increase of 3 tubes for the condenser where as 10 for the absorber. The disadvantage is that the condenser tubes are more expensive than absorber tubes, making it more economical to increase the absorber tubes [see Table 6-1 for tube cost information].

Table 7-3. The effect of increasing the tubes in the absorber, condenser, and evaporator with the corresponding decrease in generator tubes.

%Change in UA	$Tube_a$	$Tube_g$	$Tube_c$	$Tube_g$	$Tube_e$	$Tube_g$
2%	+10	-150	+3	-74	+6	-40
4%	+20	-270	+5	-140	+14	-75
6%	+30	-370	+8	-200	+20	-108
8%	+40	-454	+10	-250	+27	-138
10%	+50	-526	+13	-300	+34	-165

Table 7-3 indicates that if 10 tubes are added to the absorber, 150 tubes can be taken out of the generator.

The low temperature heat exchanger was assumed to have 0.76 effectiveness for the above analysis. The effect on capacity and cost for increasing the effectiveness was investigated. The effectiveness of the brazed plate heat exchanger is increased by adding more brass plate. Figure 7-14 and Figure 7-15 compares the effect on capacity and unit cost for a change in the effectiveness of the solution heat exchanger.

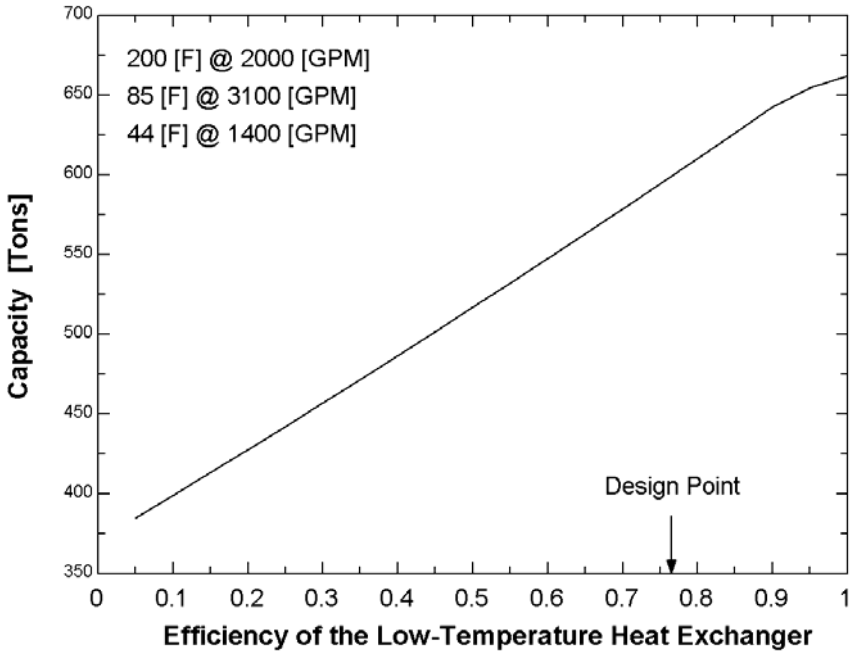

Figure 7-14. Capacity effect due to changing LTHX effectiveness.

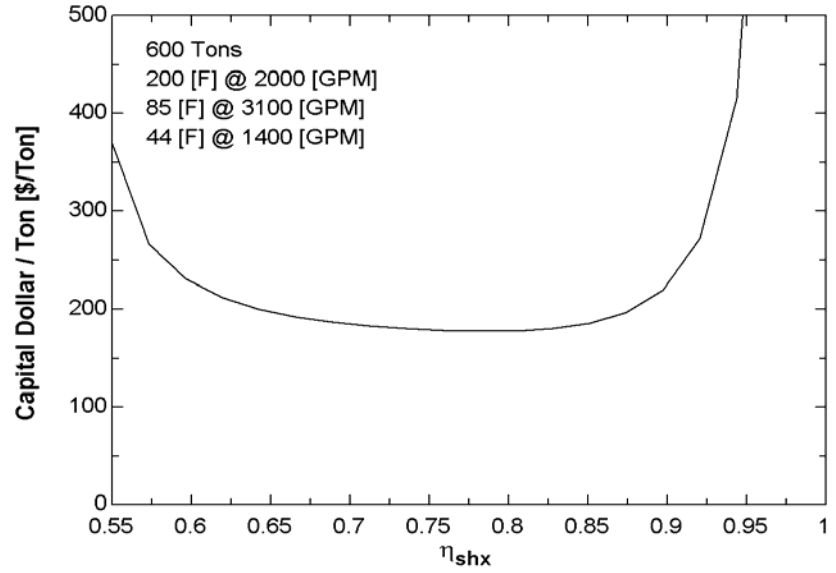

Figure 7-15. Capital dollars per ton due to changing LTHX effectiveness

Using an effectiveness of 0.8 increases the capacity by around 15 tons and at no extra cost since the generator can be made slightly smaller.

Another approach to decrease the number of generator tubes is to use finned tubes in place of smooth tubes. Figure 7-16 and Figure 7-17 displays the decrease in the number of tubes and the cost associated with making such a change.

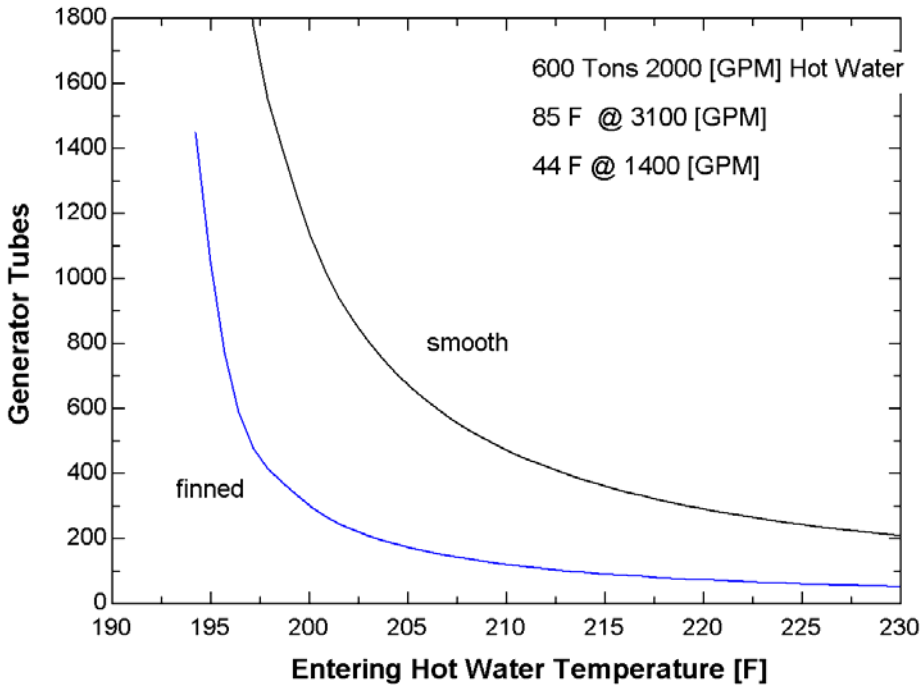

Figure 7-16. Comparison between finned and smooth tubes.

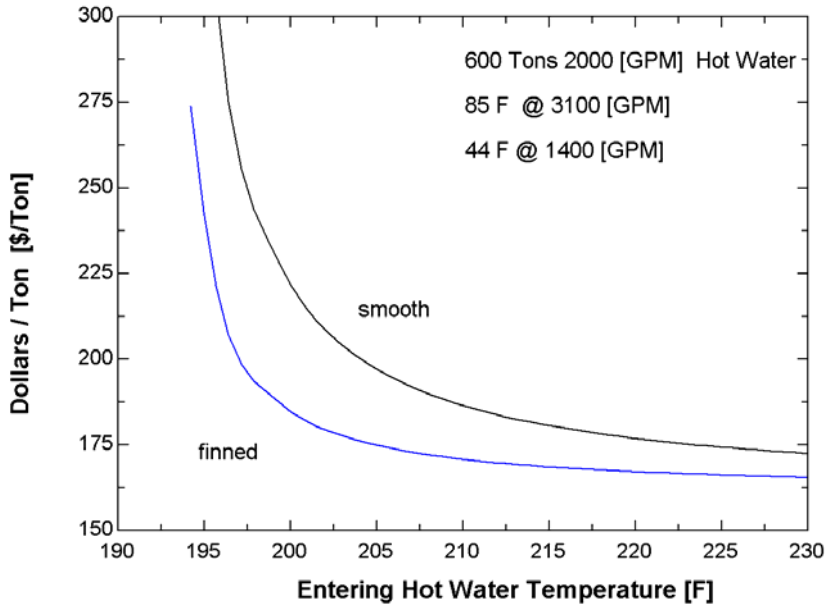

Figure 7-17. Cost Comparison between finned and smooth tubes.

Figure 7-16 shows that using finned tubes decreases the number of generator tubes. Based on the assumption that finned tubes cost twice as much as smooth tubes, the reduction in generator tubes is enough to compensate for the higher priced tubes. Figure 7-17 shows that the overall design price is much lower for the finned tubes, making it economically and thermodynamically advantageous to use finned tubes in a generator fired with low temperature hot water.

With falling film generators there is the potential for the exiting brine solution leaving the generator to be superheated. Figure 7-18 and Figure 7-19 displays a comparison between no superheat and a 3^{o}F superheat for smooth and finned tubes. Superheat is the condition where the exiting brine solution leaving the generator is at a higher temperature then the equilibrium

temperature for that concentration and pressure. Due to the loss of performance caused by superheat in the generator, there is an increase in the cost.

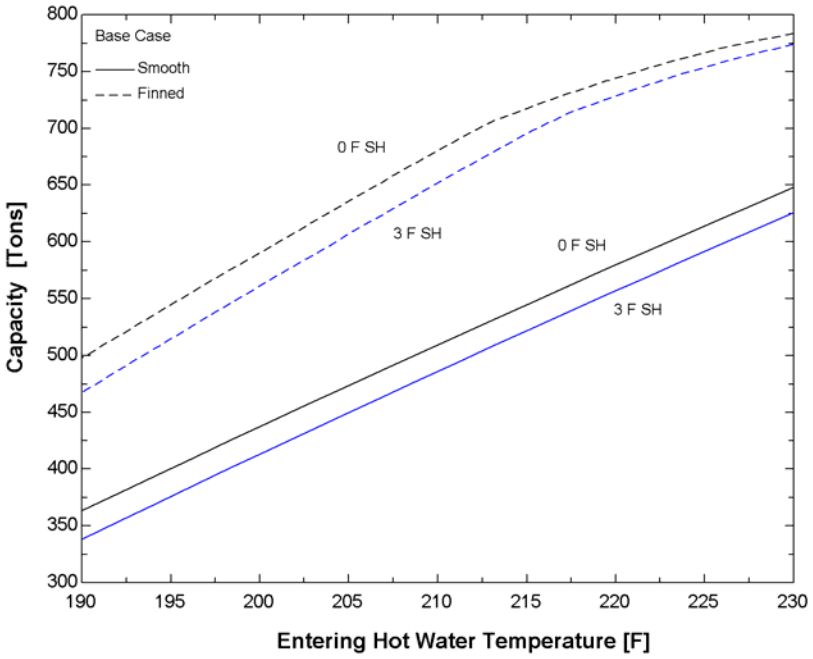

Figure 7-18. Capacity effect between finned and smooth tube with and without superheat.

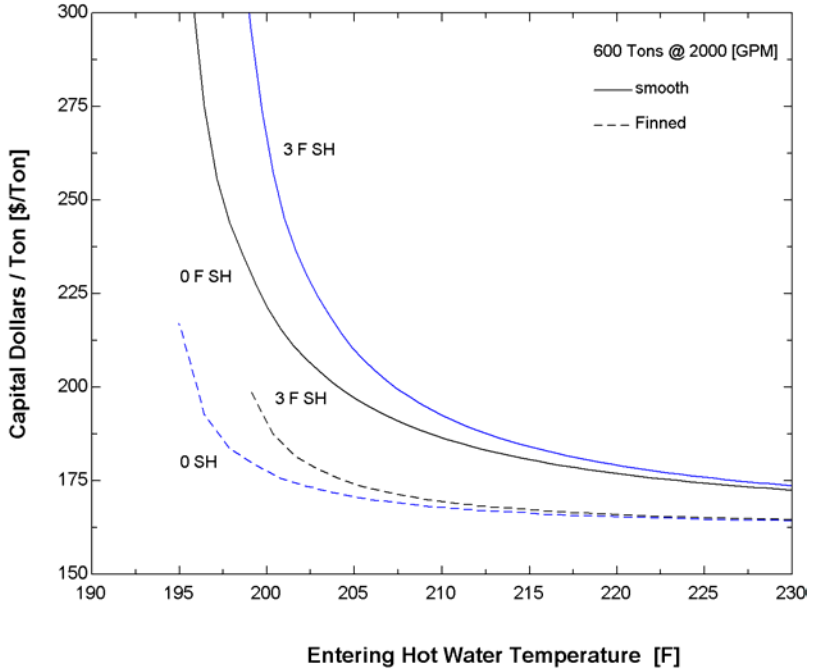

Figure 7-19. Capital dollars effect between finned and smooth tube with and without superheat.

The conclusion of Figure 7-18 and Figure 7-19 is that the finned tube generator is superior to the smooth tube with or without superheat.

Table 7-4 lists the final design parameters for a single-effect chiller using low temperature hot water. An 1133-tube count in the generator is still not a feasible design for the generator. The major changes in the final design are the increase in absorber tubes from 514 to 554 and the slight increase in effectiveness of the LTXH from 0.76 to 0.8.

Table 7-4. Lists the final design for the absorption chiller using low temperature waste heat [600 Tons, 200°F @ 2000 gpm, no superheat 0.8 LTHX effectiveness].

	Absorber	Condenser	Evaporator	Generator
Tubes	554	128	336	300 Finned 1133 Smooth
UA [Btu/hr-F]	558751	852738	1.35e6	993439
Internal solution flow rate	230 [gpm]			

Figure 7-20 compares the system and absorption chiller cost as a function of entering hot water temperature based on the final design. The cooling tower cost is based on 70 $/ton and thus an uncertainty of ±20 $/ton is examined in the system curve. The ±20 $/ton is used because it encompasses the cost range of a lower tower cost for galvanized steel and an upper cost for stainless steel.

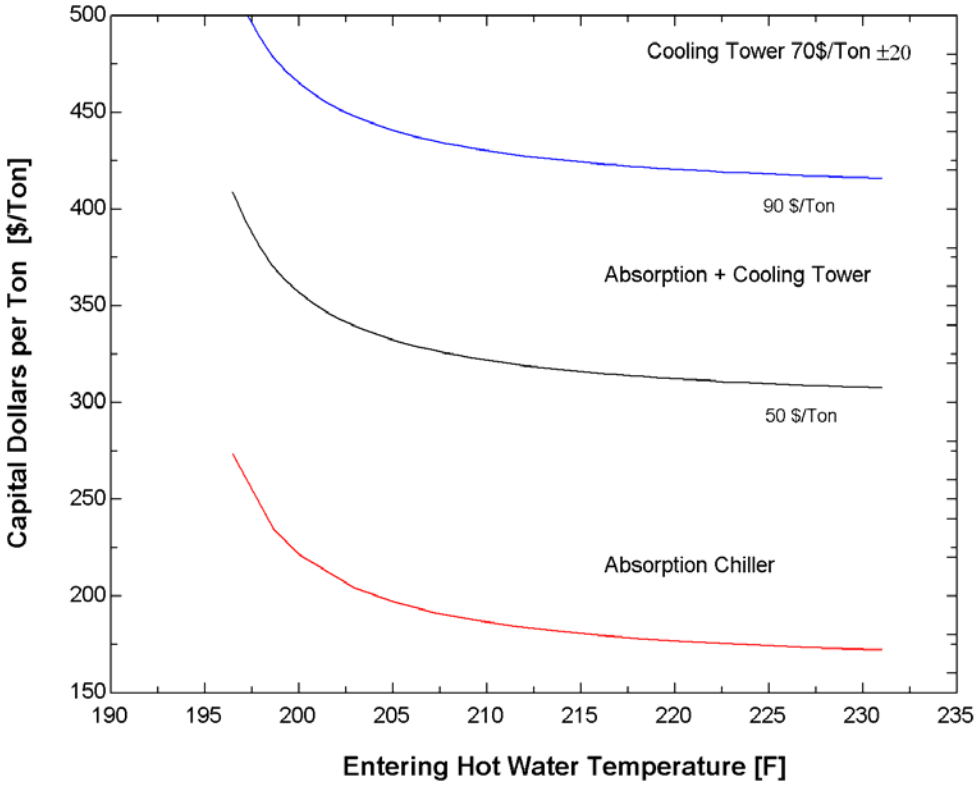

Figure 7-20. Capital dollars per ton comparison between single-effect absorption chiller and system.

At 200°F and 2000 gpm the absorption chiller and system cost is

222 $/ton	411 $/ton ± 54.2 $/ton	[smoothed tubes]
185 $/ton	374.2 $/ton ± 54.2 $/ton	[finned tubes]

The plus and minus is based on the cooling tower cost range. The important result is that the cost of the system has approximately doubled due to the cooling tower.

7.5 Sensitivity analysis on tube cost and generator outside heat transfer coefficient.

Since the dollars per ton is such an important parameter used by the industry it is important to perform a sensitivity analysis. Using the range of tube cost [0.10 $/ft] from the economics chapter, Figure 7-21 demonstrates the sensitivity of dollars per ton.

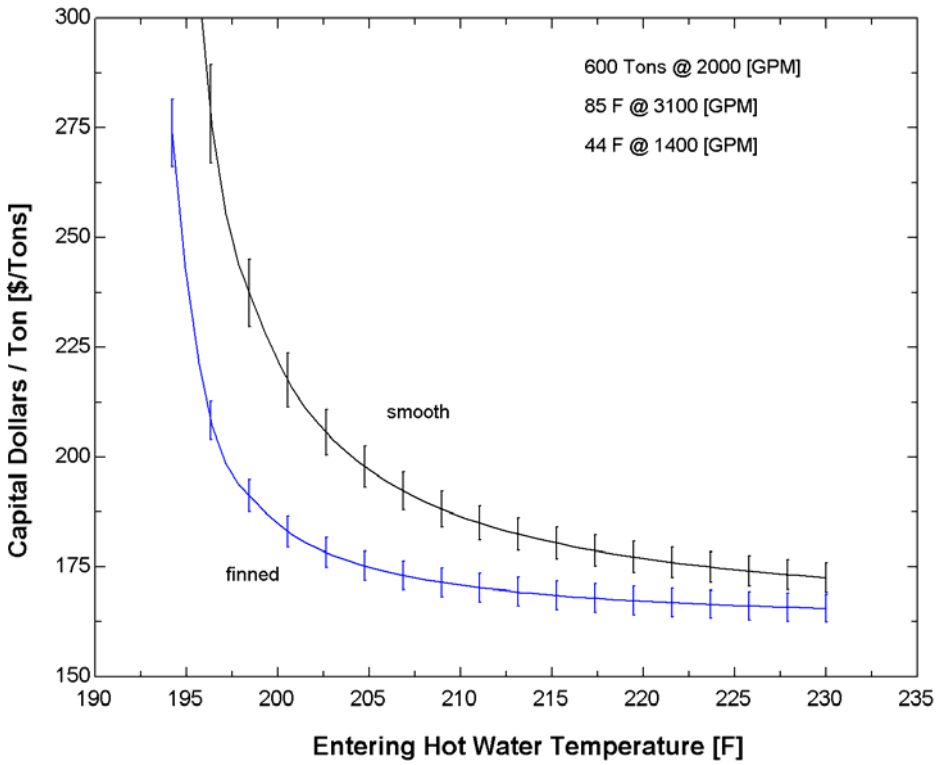

Figure 7-21. Uncertainty analysis on the cost of tubes.

Figure 7-21 shows the propagation of uncertainty on the capital dollars per ton associated with a 0.10 $/ft uncertainty in the price of all four tube components [generator, absorber, condenser, and evaporator] [Refer to Table 6-1 for tube cost]. The uncertainty increases as the entering hot water temperature decreases, which means there is a higher uncertainty in

predicting the cost of an absorption chiller at lower firing temperature. The reason for this is that at lower temperatures there is a large increase in the number of generator tubes, thus the cost of tubes is a greater percentage of the capital cost.

At 200 F the uncertainty range on capital dollars per ton is

Finned	$184.6 ± $3.6
Smoothed	$221.5 ± $6.4

Holding the capacity constant and changing the outside heat transfer coefficient requires a change in the number of tubes in the generator.

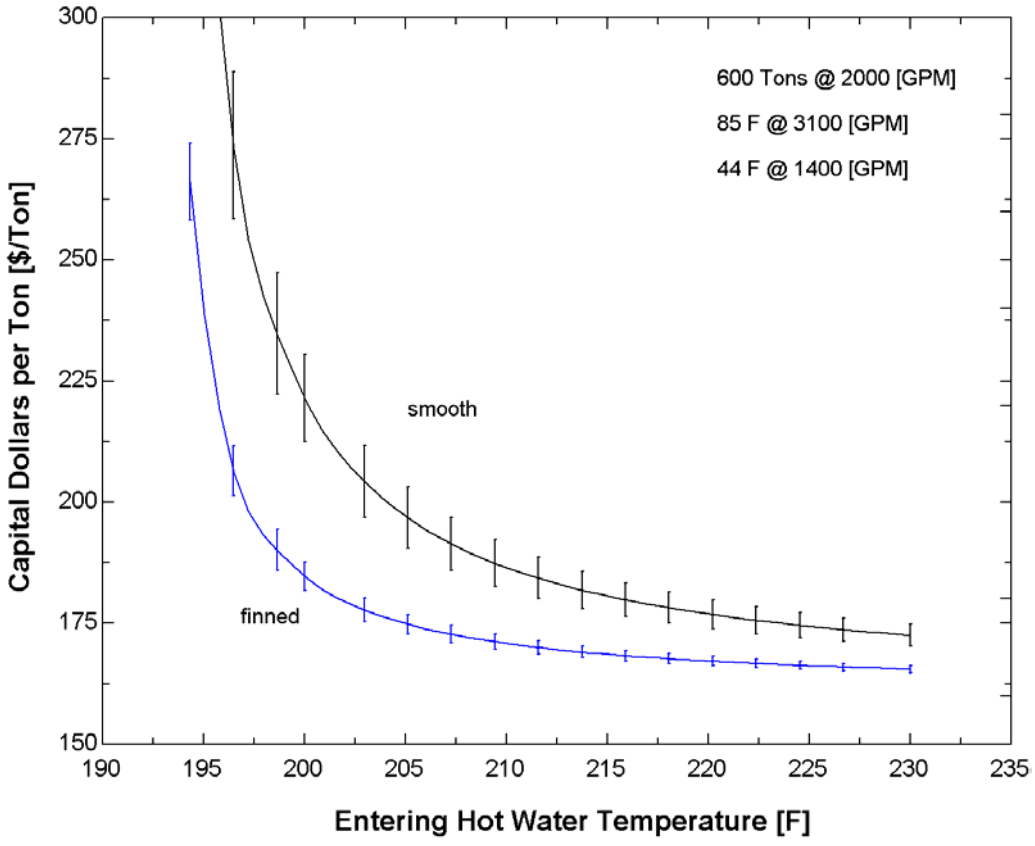

Figure 7-22. Uncertainty analysis on the generator outside heat transfer coefficient.

Figure 7-22 shows the propagation of uncertainty on the capital dollars per ton associated with a 20 % uncertainty in the generator outside heat transfer coefficient. Similar to Figure 7-21 the uncertainty increases as the hot water temperature decreases.

At 200 F the uncertainty range on capital dollars per ton is

Finned	$184.6 ± $4.2
Smoothed	$221.5 ± $12.6

The uncertainty in the outside generator heat transfer coefficient has a larger effect than the cost of the tubes, especially at lower firing temperatures. With the uncertainty in cost of tubes and generator outside heat transfer coefficient, Figure 7-21 and Figure 7-22 show that the finned tubes are still a better design because the confidence intervals do not coincide.

7.6 Life cycle savings comparison between single-effect absorption and vapor compression chillers for different heat source temperatures

A life cycle savings comparison is used to compare absorption and electric centrifugal chillers. The break-even cost of heat is determined by setting equations 6-1 and 6-2 equal to each other. Refer to section 6.2 and 6.3 for material and operating cost details of the absorption and electric centrifugal chiller. The result reveals the price at which the cost of heat must be in order for absorption to have an economic advantage over the electric centrifugal chiller. The final design absorption chiller is used [Table 7-4 finned tube], which means each component is held constant and the capacity changes with heat source temperature.

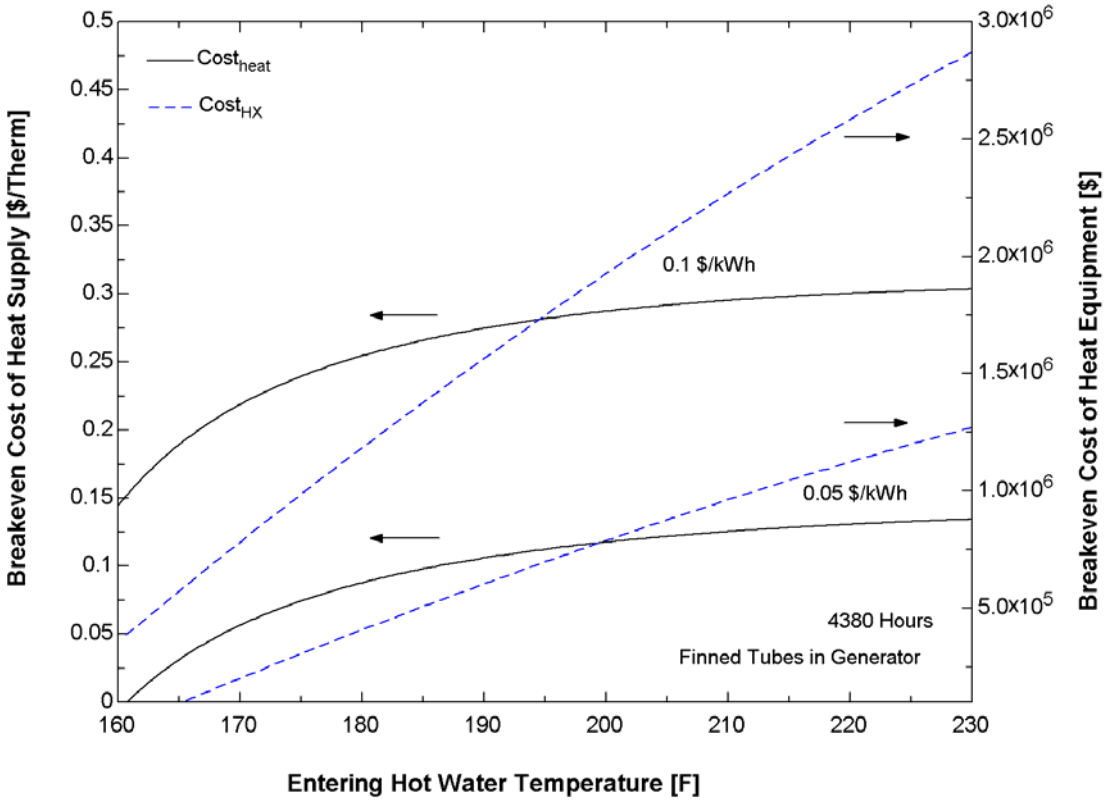

Figure 7-23. Break-even cost of supply heat to the generator or heat equipment.

Figure 7-23 demonstrates the break-even cost of supply heat for the generator to operate an absorption chiller with the same life cycle cost as an electric centrifugal chiller. For example, if the supply heat can be supplied at a cost less than or equal to approximately 0.28 $/Therm when electricity is 0.1 $/kWh, then absorption is the preferred alternative. The right hand axis shows when the supply heat is free from an industrial process or co-generation facility. The right axis determines the maximum break-even cost associated with using waste heat [refer to equation 6-5 in section 6.4]. For example, at 200^{o}F and 0.1 $/kWh, any investment made in recovering the waste heat that cost less than $2.0 million, is a viable alternative to the electric centrifugal chiller [based on a 20 year life cycle operating 4380

hours a year]. Another interesting conclusion of Figure 7-23 is that the break-even cost of heat is independent of entering hot water temperature from 190 ^{o}F and up.

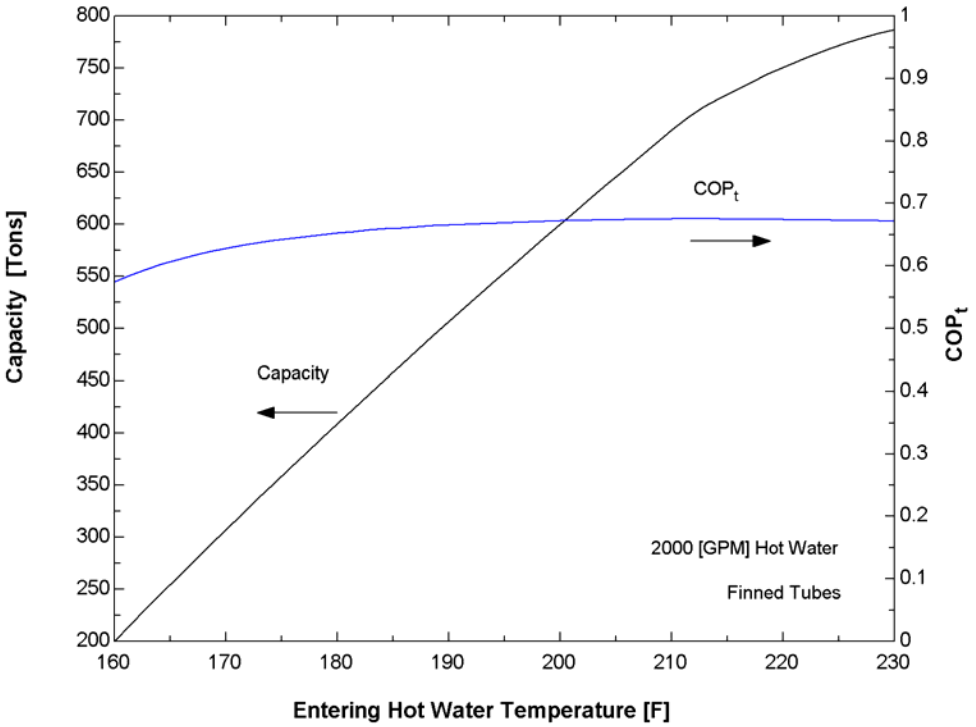

Figure 7-24. Capacity and COP as a function of heat source temperature

The main reason for this can be seen in Figure 7-24, where even though capacity is falling the COP remains constant.

The life cycle savings analysis is based on two important parameters P_1 and P_2, thus a sensitivity analysis is performed due to an uncertainty in P_1 and P_2. The uncertainty of P_1 is ± 20% of ½n where n is life cycle years. The uncertainty in P_2 is ±20% with a range of 0.8-1.2.

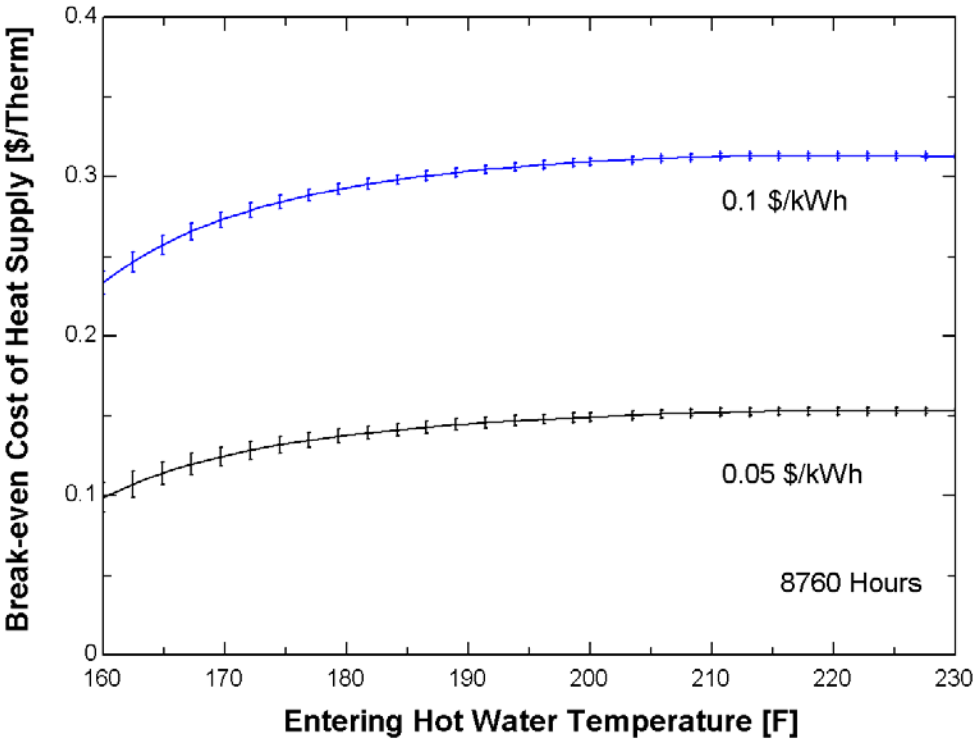

Figure 7-25. Uncertainty analysis in P_1

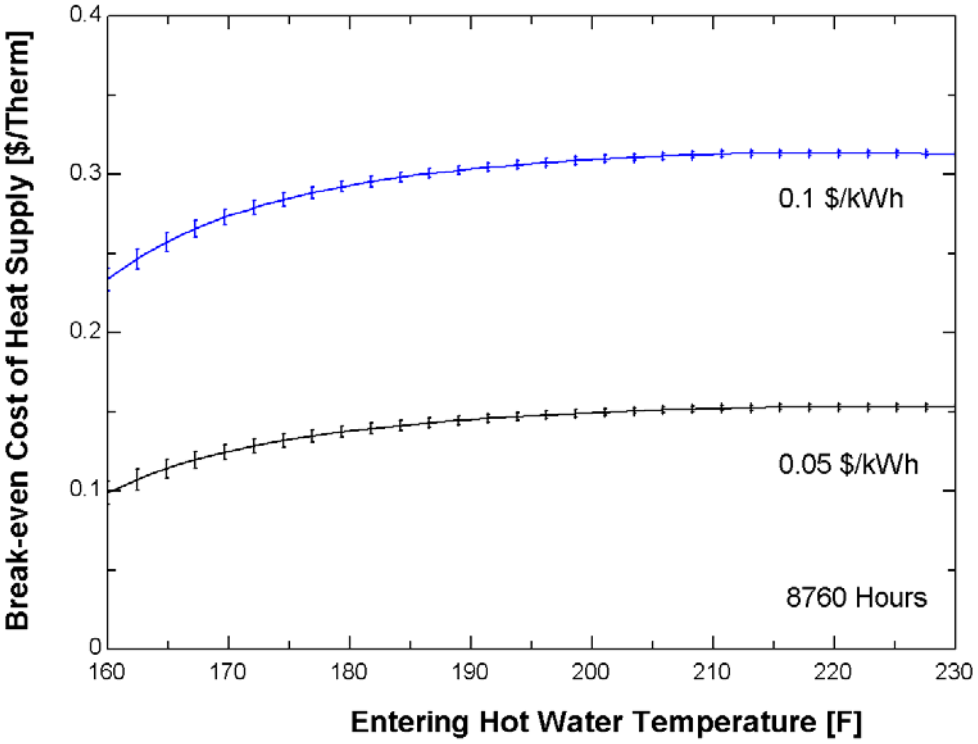

Figure 7-26. Uncertainty analysis in P_2

Figure 7-25 and Figure 7-26 shows that even with large uncertainties in P_1 and P_2 there is little effect on the solution. The above graphs are based on a full year of operation, but two interesting results occur when the absorption unit is only used for half a year. Figure 7-27 compares the uncertainty in P_2 and the cost of heat for 8760 and 4380 hours of operations.

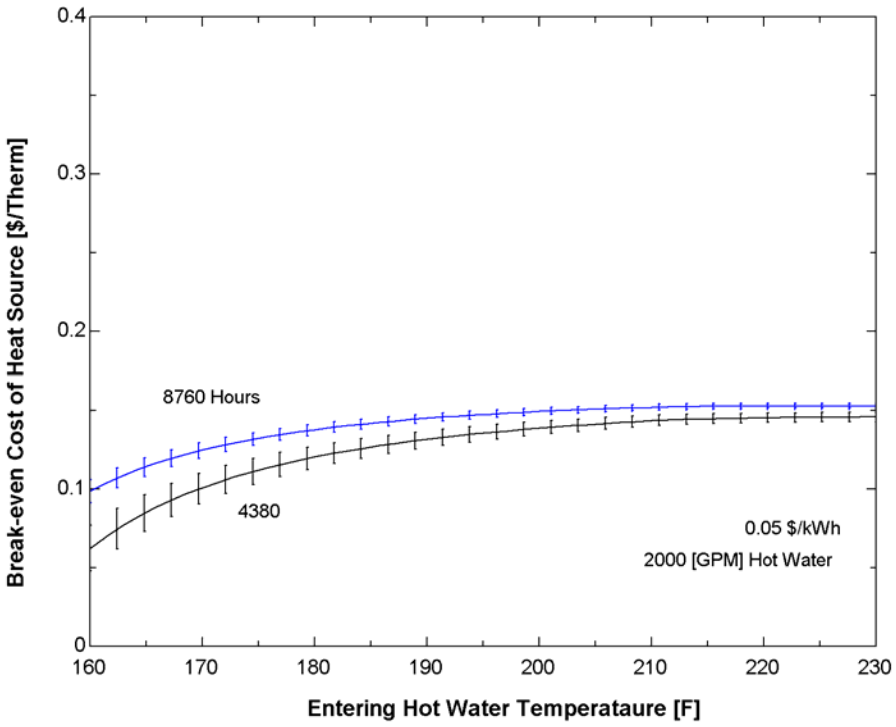

Figure 7-27. Cost of Heat Source uncertainty in P_2 for full and half a year of operation.

The scale is expanded in Figure 7-27 so that the error bars can be compared with Figure 7-26. The first result of Figure 7-27 is that the break-even cost of heat is greater for a full year of operation. This increase is due to the operating cost of the absorption chiller being less than the electric centrifugal chiller. To make use of this benefit, it is important for the absorption chiller to run as much as possible. The second result is that at 4380 hours per year of operation, the error in the cost of heat due to an uncertainty in P_2 is larger. One reason for

this is that at 4380 hours, the operating cost is lower causing the capital cost to have a larger effect on the life cycle cost.

If P_1 is less than 1 and P_2 is greater than n/2 then the break-even cost of heat increases which means a low interest rate or an increase in the economic time period.

Table 7-5. Compares the capital and operating cost between an absorption and electric centrifugal chiller for a 20 year life cycle [~600 Tons, 0.05$/kWh, 200°F Hot Water @ 2000 [gpm], 4380 Hours]

	Absorption/ Tower [finned] ~0.14 $/Therm	Electric Centrifugal / Tower
Capital Cost		
Chiller	$136,048	$117,000
Tower	$170,591	$81,046
	$306,639	$198,046
Operating Cost		
Pumps / compressor	$11,430	$783,240
Heat Source	$642,100	
Tower	$72,150	$51,030
	$725,680	$834,270
Total	$1,032,319	$1,032,316

Table 7-5 compares the capital and operating cost for the absorption chiller and the electric centrifugal chiller. The values in Table 7-5 correspond to one point on Figure 7-23. The total values in Table 7-5 are the same because the LCC costs are set equal to each other to determine the break-even cost of heat. The absorption unit is slightly more expansive than the electric centrifugal chiller but it is the cooling tower for the absorption unit that is about twice as much compared to the electric centrifugal chiller. The operating cost is not significantly lower as one would initially guess, for an absorption unit. The main operating

cost for the absorption chiller is the cost of heat. Therefore using absorption with co-generation is the only feasible situation where absorption would be more economically attractive than current centrifugal chillers, unless there are extremely high electrical costs.

7.7 Summary

Figure 7-28 compares the low temperature hot water design with the base case design. The major conclusion is an increase in capacity for a lower heat source temperature. The cost of this new design at 600 tons is 15 $/ton more.

The base case at 600 tons 227°F @ 2000 gpm is 170 $/ton
The low temperature design at 600 tons 200°F is 185 $/ton

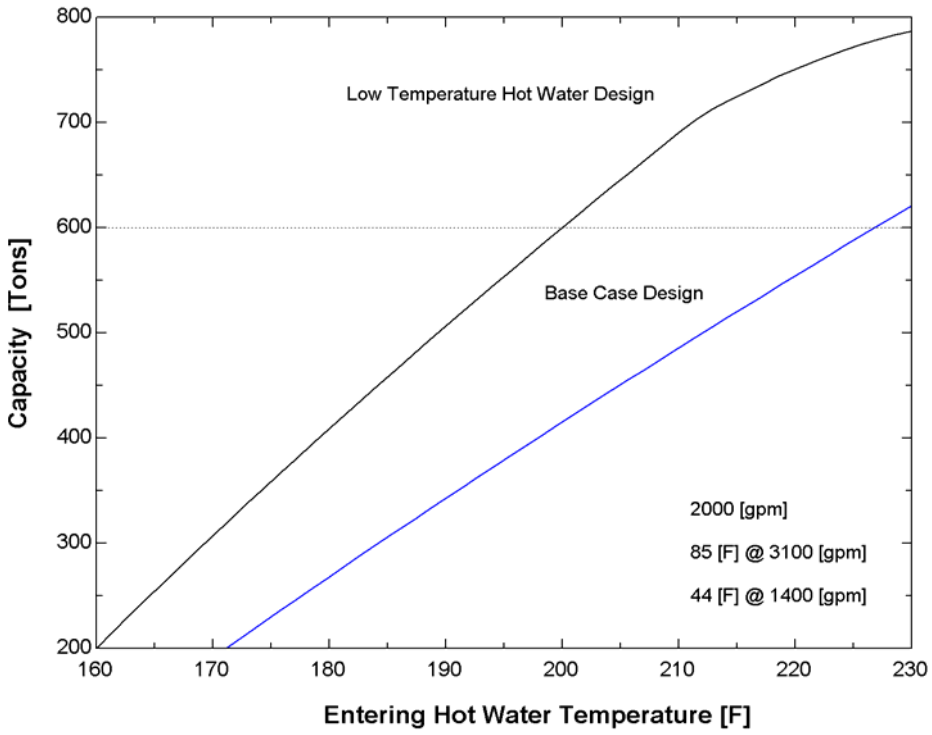

Figure 7-28. Capacity comparison between low temperature hot water design and base case design.

The following is a list of important summaries in Chapter 7

- The base case absorption unit starts to fall below design conditions [600 tons] with a hot water temperature source of 225^{o}F @ 2000 [gpm].
- Holding capacity constant [600 tons], at 205^{o}F the base case chiller size starts to change rapidly to accommodate the lower firing temperatures.
- The generator for the base case absorption unit has the largest increase in capacity cost for a unit change in UA using a low temperature heat source. Therefore any investment should first be put into the generator.
- The low temperature absorption unit was designed by increasing the number of tubes in the generator [262 $\rightarrow$ 300], using finned tubes instead of smooth tubes, increasing the number of tubes in the absorber [514 $\rightarrow$554] and increasing the low temperature heat exchanger effectiveness [0.76 $\rightarrow$ 0.8.].
- The optimum value for the cooling water flow rate is independent of the heat source temperature. The cooling water flow rate is around 3100 gpm or 5gpm/ton at 600 tons.
- Based on the assumption that finned tubes cost twice as much as smooth tubes, the reduction in generator tubes using finned tubes is enough to compensate for the higher price.
- The cost of the absorption chiller system has approximately doubled due to the cooling tower.
- If the heat source can be supplied at a cost less than or equal to approximately 0.28 $/Therm when electricity is 0.1 $/kWh then absorption is the preferred alternative [based on 600 tons capacity with 190^{o}F and up hot water at 2000 gpm].
- The break-even cost of heat source is independent of entering hot water temperature from 190^{o}F and up.
- The main operating cost for the absorption chiller is the cost of heat. Thus, using absorption with co-generation is the only feasible situation where absorption would be more economically competitive than current centrifugal chillers.

CHAPTER 8

HALF-EFFECT ABSORPTION CHILLER OPERATION

8.1 Overview

The purpose of Chapter 8 is to determine an optimum design for the half-effect cycle, evaluate the performance characteristics of the optimum design, compare this cycle with an electric centrifugal chiller, and examine different control strategies. Refer to Chapter 4 Figure 4-1 for a schematic diagram of the half-effect cycle and section 4.1 for a review of basic principals of the half-effect cycle.

8.2 Designing the Half-Effect Cycle

The design approach is to minimize cost based on decision variables of the system. The decision variables for the half-effect cycle are the number of tubes in each component and the two solution flow rates leaving the absorber.

The first step in designing the half-effect cycle is to size the components comparable to the single-effect unit to obtain a numerical solution. The condenser and evaporator are initially set to the same size as the base case unit in Table 7-1. The high and low concentration absorber sum is set equal to the absorber in the single effect unit [Table 7-1]. The single effect absorber has about 500 tubes, therefore the high and low concentration absorber will each have 250 tubes. The solution flow rates leaving the absorber are set to 230 gpm [Table 7-1]. The sizes of the generators are set equal to each other and determined by setting the capacity to 600 tons.

The half-effect cycle was designed starting with the single-effect unit until convergence on a numerical solution was reached. The convergence was not a problem of numerical difficulties but of physical limitations of the system not having enough heat exchanger area to meet the 600 tons. The procedure followed by setting the solution flow rate leaving the high concentration [HC] absorber to 200,000 lb_m /hr and the number of tubes in the absorber were changed until a solution was reached. The same procedure was implemented for the low concentration [LC] absorber, by setting the low concentration solution flow rate to 140,000 lb_m/hr and adjusting the number of tubes. Table 8-1 lists the flow rates and number of tubes for each component from this analysis.

Table 8-1. Initial Half-Effect Design

	HC Absorber	LC Absorber	HT Generator	LT Generator	Condenser	Evaporator
Tubes	300	200	306	306	128	336
Mass Flow Rate	220 [gpm]	180[gpm]				

The leaving solution flow rates from the HC and LC have very little effect on the capital dollars per ton because of the film Reynolds number. The film Reynolds number is just beyond the Nusselt number limit, thus a change in film Reynolds number does not affect the Nusselt number. [Refer to Figure 3-3 and section 3.4.3]. Therefore, increasing or decreasing the solution flow rate over a small range has little effect on the outside heat transfer ability of the two absorbers.

Figure 8-1 and Figure 8-2 were used to determine the sensitivity of each variable on the entire system. Holding each variable constant while varying the other produced the following graphs. For this analysis, the capacity is held constant at 600 tons and the number of tubes in the high temperature [HT] and low temperature [LT] generator are set equal. This procedure enables the generator size to vary due to the following different conditions. Figure 8-1 and Figure 8-2 displays the effect on dollars / ton by changing the HC and LC absorber tubes. There is a small effect on capital dollars per ton for an increase in the number of absorber tubes. The most likely reason is that since the increase in absorber tubes is small and as the absorber tubes increase, the generator tubes decrease.

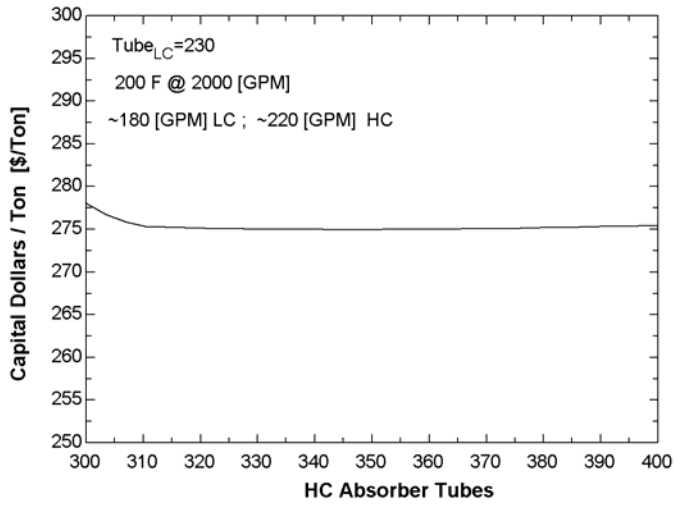

Figure 8-1. HC Absorber tubes effect on dollars per ton.

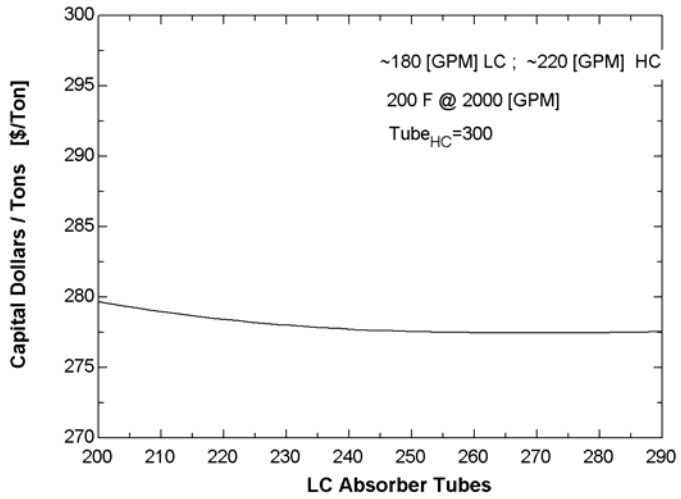

Figure 8-2. LC Absorber tubes effect on dollars per ton.

Because both the mass flow rates have a small effect on the system, and the tube counts of the evaporator and condenser remain constant there are four variables left that need to be optimized. The four variables are $LT_{tubes,}$ $HT_{tubes,}$ $LC_{tubes,}$ and HC_{tubes}. Using a ratio to represent the portion of tubes in the HC and LC absorber and HT and LT generator provides

limits that are between 0 and 1. For example, the ratio of LC to HC absorber tubes is optimized instead of the number of tubes. The 2 ratios are f_{abs}, f_{gen}.

$$f_{abs} = \frac{LC_{tubes}}{(HC_{tubes} + LC_{tubes})},\ f_{gen} = \frac{LT_{tubes}}{(HT_{tubes} + LT_{tubes})}$$

Specifying capacity allows for HT_{tubes} or LT_{tubes} not be specified. A value of 350 tubes for the HC_{tubes} absorber will be used for the initial optimization, thus the two remaining variables to be optimized are f_{abs} and f_{gen}

The objective function is

$$\min(\$/Ton) = f(f_{abs}, f_{gen}) \qquad [\ 8\text{-}1\ ]$$

Where the decision variables are constrained by

$$0. < f_{abs} < 1.$$
$$0. < f_{gen} < 1$$

The variables can not equal the constraints because that would result in one of the components to have zero tubes, which is physically impossible.

The first attempt to solve the optimization problem was to use EES to minimize the dollars per ton based on f_{abs} and f_{gen}. The problem with using EES is that within the constrained variables, the program would take a step that did not have a solution, thus stopping the program. In order to circumvent this problem, EES would have to know that a solution does not exist and return to the previous step, solve, and then take a smaller step or change

direction. Since the optimization only contains two variables, a contour plot can be used to find the minimum. The advantage of the contour plot is that the user can control the variation of f_{abs} and f_{gen}. Figure 8-3 is a contour plot of capital dollars per ton for different variations of f_{abs} and f_{gen}.

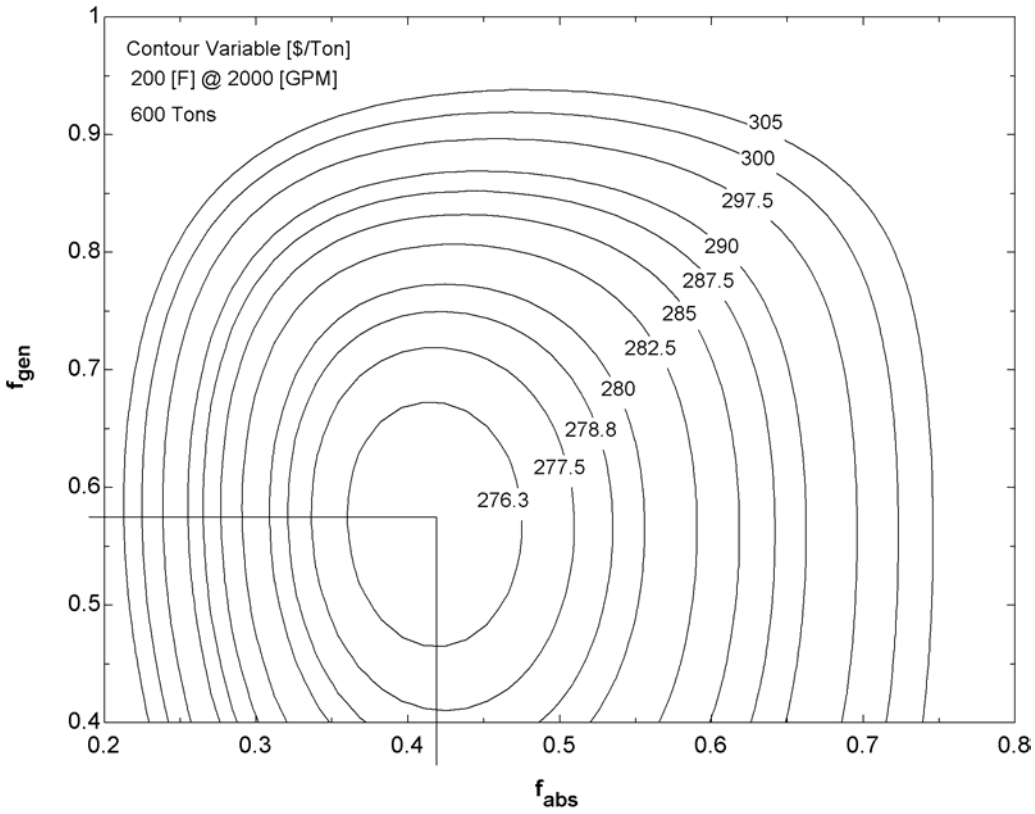

Figure 8-3. Contour plot of capital dollar per tons for series flow.

The optimum fractions from Figure 8-3 are

$f_{abs} = .41$

$f_{gen} = .57$

Table 8-2 lists the optimum solution for the half-effect cycle using 200°F hot water at 2000 gpm in series flow.

Table 8-2. Optimum Half-Effect Design [600 Tons, 200°F @ 2000 gpm]

	HC Absorber	LC Absorber	HT Generator	LT Generator	Condenser	Evaporator
Tubes	350	243	192	255	128	336
UA [Btu/hr-F]	375285	327870	246966	283976	882375	1.354e6
Internal Solution Flow Rate	240 [gpm]	210 [gpm]				

Since the design was based on series flow through the two generators, the same analysis was performed for parallel flow through the generators.

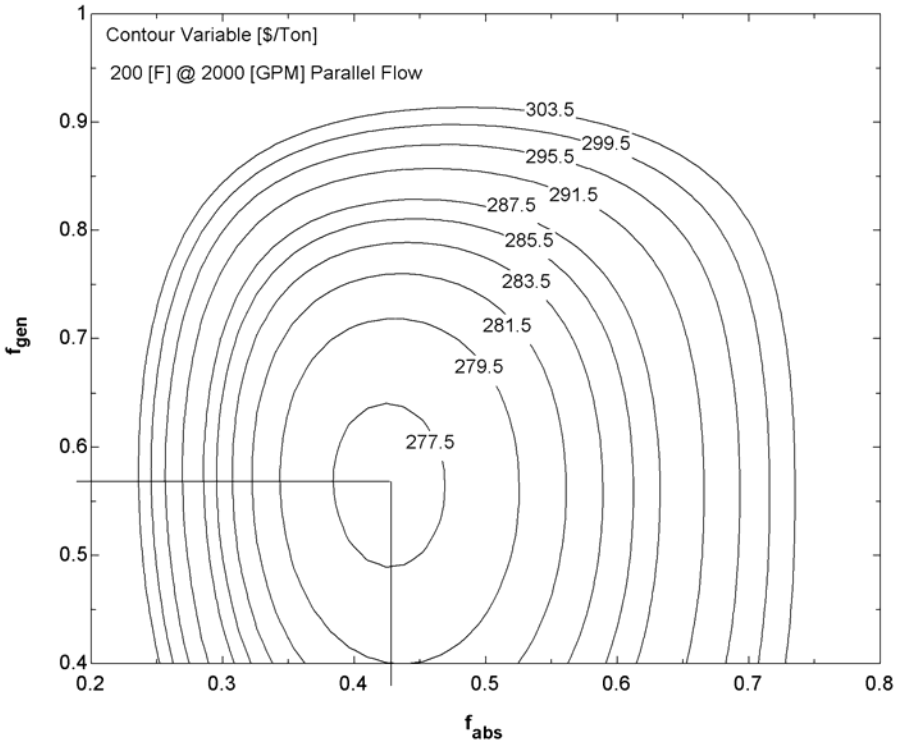

Figure 8-4. Contour plot of capital dollar per tons for parallel flow.

Figure 8-4 is a contour plot of capital dollars per ton for different fractions. The main result of Figure 8-4 is that the same optimum solution exists regardless of flow arrangement with the two generators.

Figure 8-5 examines the effect on the optimum fraction by lowering the heat source temperature to 185°F. At lower hot water temperatures the f_{abs} is greater than 0.5, which means the LC absorber is now larger than the HC absorber. On the contrary, the f_{gen} did not change.

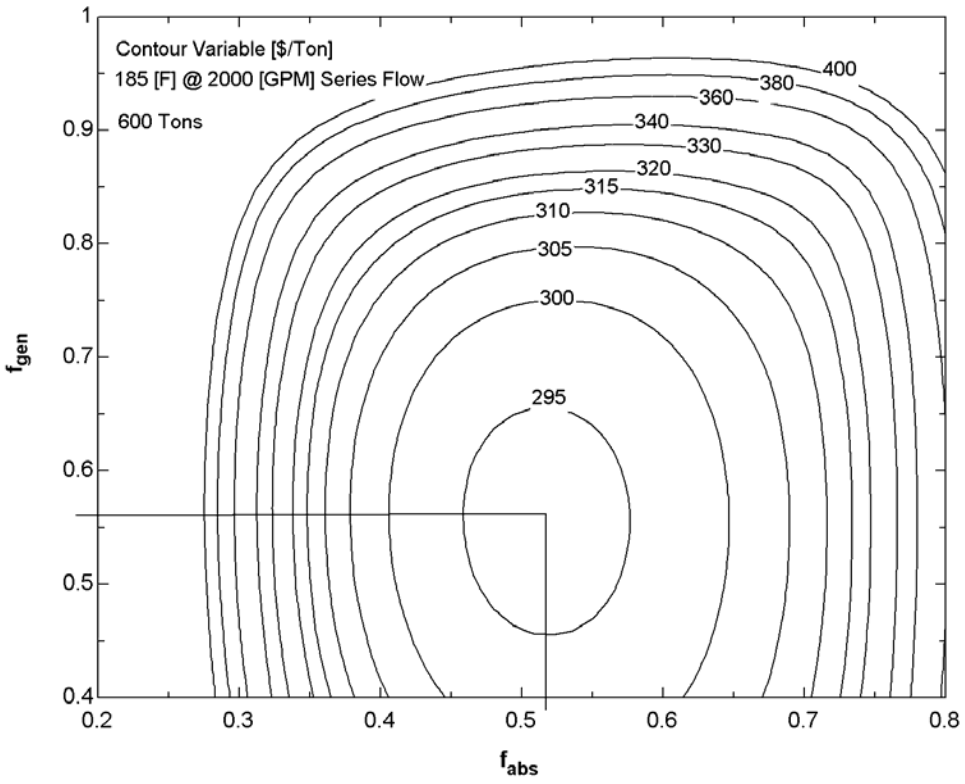

Figure 8-5. Contour plot of capital dollars per ton for series flow [185°F heat source].

The next step in the design is to determine the sensitivity of the design sizes. For example, if the condenser size is increased will this decrease the capital cost. Figure 8-6 displays a graph

of the sensitivity of each component with regard to capital cost. The capacity is held constant and a factor is used to increase or decrease one component at a time, which also effects the size of the generators based on the solved ratio of 0.57.

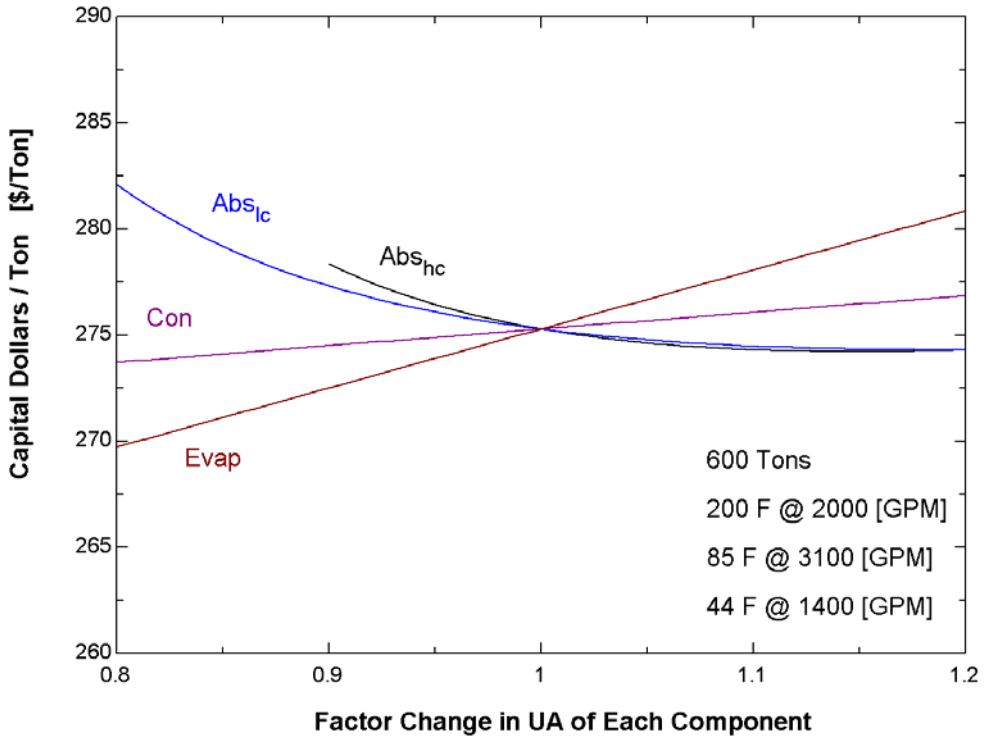

Figure 8-6. Effect on capital cost due to changing the size of each component.

Figure 8-6 demonstrates that the half-effect cycle is properly designed since there are small changes in capital cost for a change in UA of each component. Decreasing the size of the HC absorber below 90% resulted in a design that did not have enough UA to meet the 600 ton capacity. One possible reason for this result is that as the HC absorber decreases in size, the leaving concentration increases. Small changes in concentration result in large changes in solution flow rate, however since solution flow rate is constant, no solution is possible.

Figure 8-6 also shows that the evaporator is over designed because the same capacity can be met with a lower UA for the evaporator.

8.3 Effect of Heat Source Temperature

Figure 8-7 and Figure 8-8 describes the effect on the generator UA for varying hot water temperatures. The capacity is held constant and the two generators change in size with the varying hot water temperature. The optimum half-effect fractions are still used but the number of tubes in each generator is allowed to vary. The UA for the LT generator is slightly higher than that of the HT, which is a result of the LT generator having more tubes than the HT generator. Figure 8-9 shows the change in capital dollars per ton for varying entering hot water temperatures.

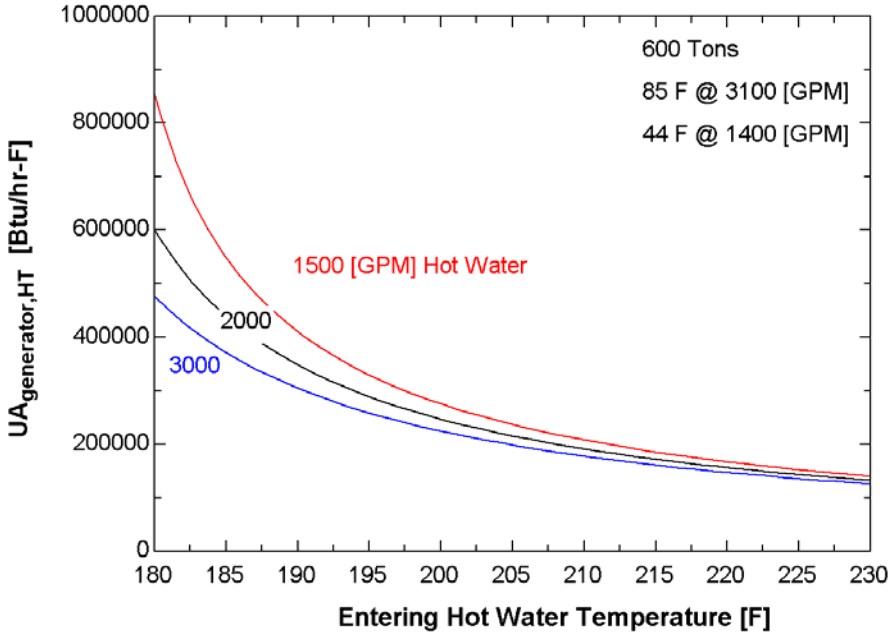

Figure 8-7. HT generator UA as a function of entering hot water temperature.

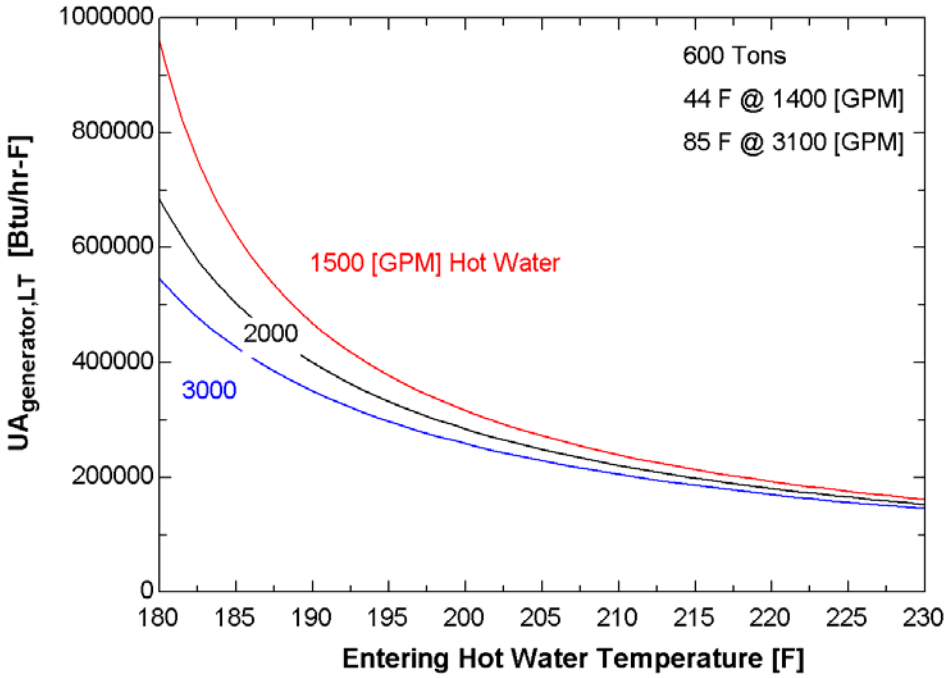

Figure 8-8. LT generator UA as a function of entering hot water temperature.

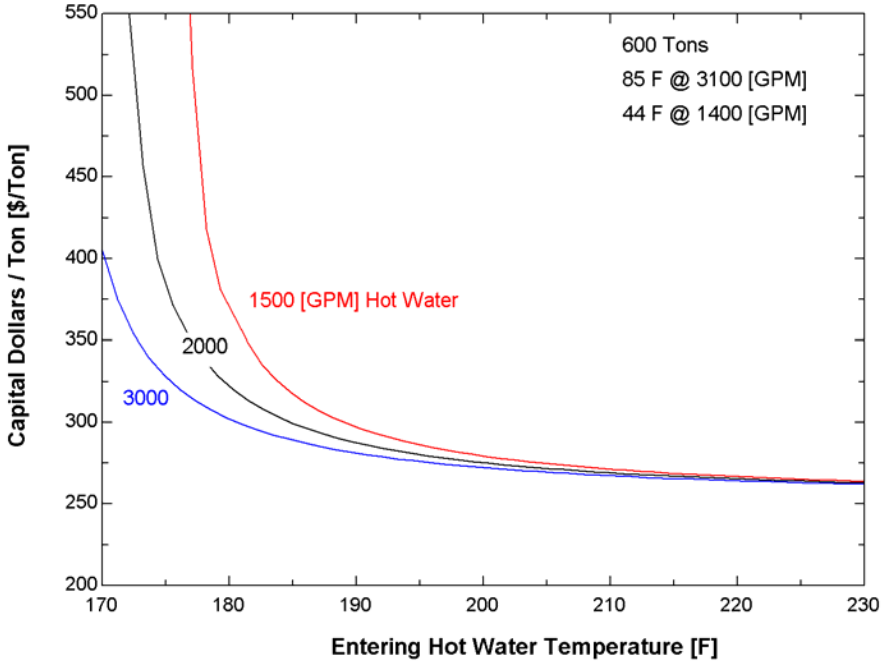

Figure 8-9. Capital dollars per ton for varying entering hot water temperature.

As the hot water flow rate increases, the required capital investment decreases. This is the same conclusion as the single-effect cycle. Figure 8-10 compares the capital cost between an absorption chiller and the absorption chiller and cooling tower.

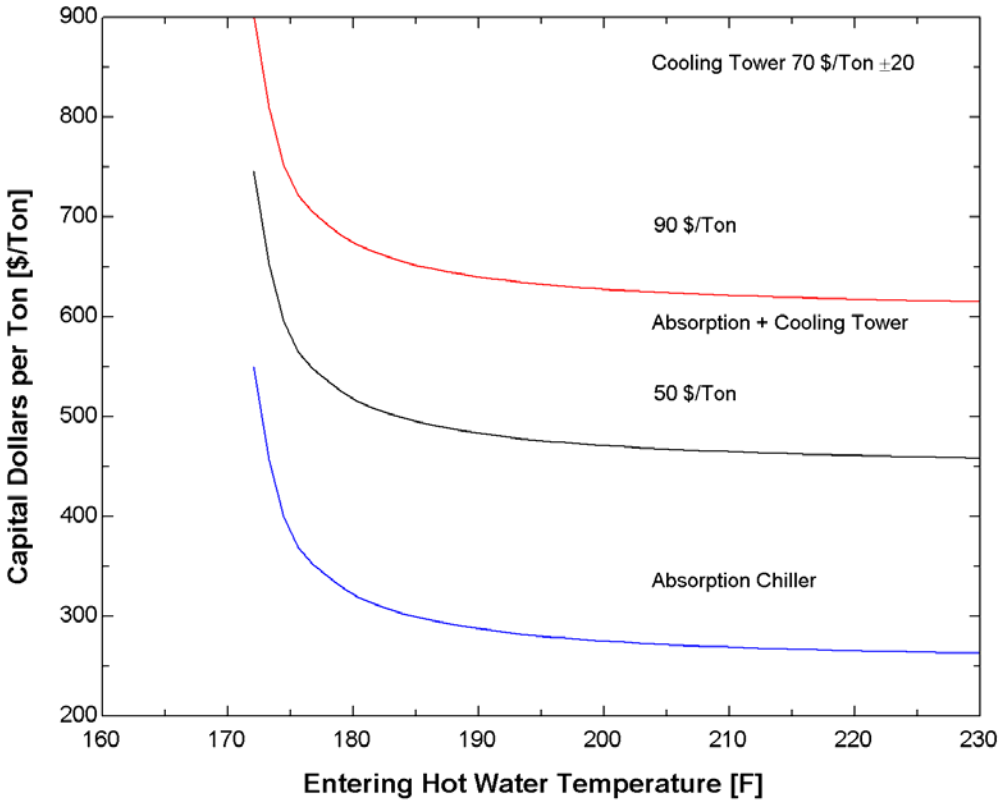

Figure 8-10. Capital dollars comparison between half-effect absorption chiller and system

At 200°F and 2000 gpm the half-effect absorption chiller and system cost is

275 $/ton 550 $/ton ± 78 $/ton

The plus and minus is based on the cooling tower cost range. The important result is that the cost of the system has approximately doubled due to the cooling tower.

8.4 Dollars per ton effect due to split or continuous heat source flow rate into the generators

The above analysis has assumed that the hot water source passes through the HT generator followed by the LT generator. The following figures were drawn to determine if it is better to use series flow or parallel flow with half the flow rate. For example, is it more economical to pass 2000 gpm of hot water first through the HT and then the LT, or pass 1000 gpm each to both generators? Figure 8-11 and Figure 8-12 compares the two different types of flow arrangements. The higher the hot water flow rate the lower the entering hot water temperature can go before there is a difference between series and parallel flow arrangement. At approximately 190 ^{o}F is it more economical to use series flow rather than parallel flow. One must keep in mind that the half-effect cycle was designed for 200^{o}F water series flow and Figure 8-3 and Figure 8-4 shows no difference in the optimum fraction. In order for parallel flow to be as economical as series flow it is best to redesign the half-effect chiller for a lower-temperature parallel flow arrangement.

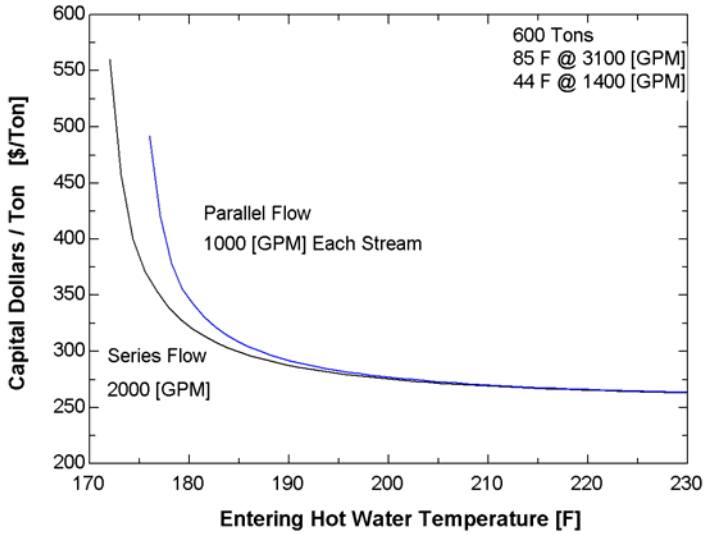

Figure 8-11. Effect on capital cost for different flow arrangement 2000 [gpm].

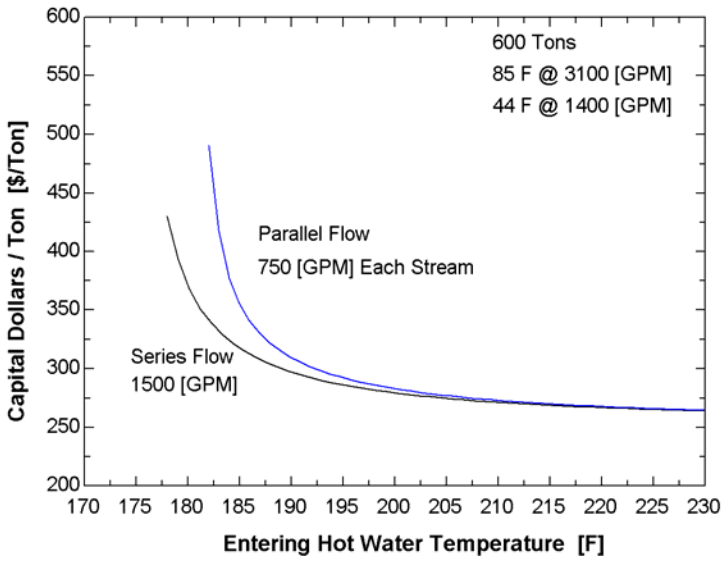

Figure 8-12. Effect on capital cost for different flow arrangement 1500 [gpm].

8.5 Life cycle savings comparison between half-effect absorption and vapor compression chillers

Figure 8-13 displays the break-even cost of the heat source from setting the life cycle savings equations for a half-effect absorption chiller and an electric centrifugal chiller [equation 6-1 and 6-2] equal to each other. The economic analysis for the comparison between the half-effect and electric centrifugal chiller is based on the same assumptions in Chapter 6. The only difference is that the constant price of $20,000, which takes into account the brine solution, piping, purging system, control system, etc. is doubled due to the extra components of the half-effect cycle. Similar to the single effect cycle section 7.6, any cost of heat below the line signifies that the half-effect cycle is economically favored over an electrical centrifugal chiller. At higher electrical cost the half-effect cycle has the advantage because of

lower electrical operating costs. Figure 8-13 shows that the half-effect cycle requires a cheap source of fuel to overcome the higher capital cost and larger cooling tower.

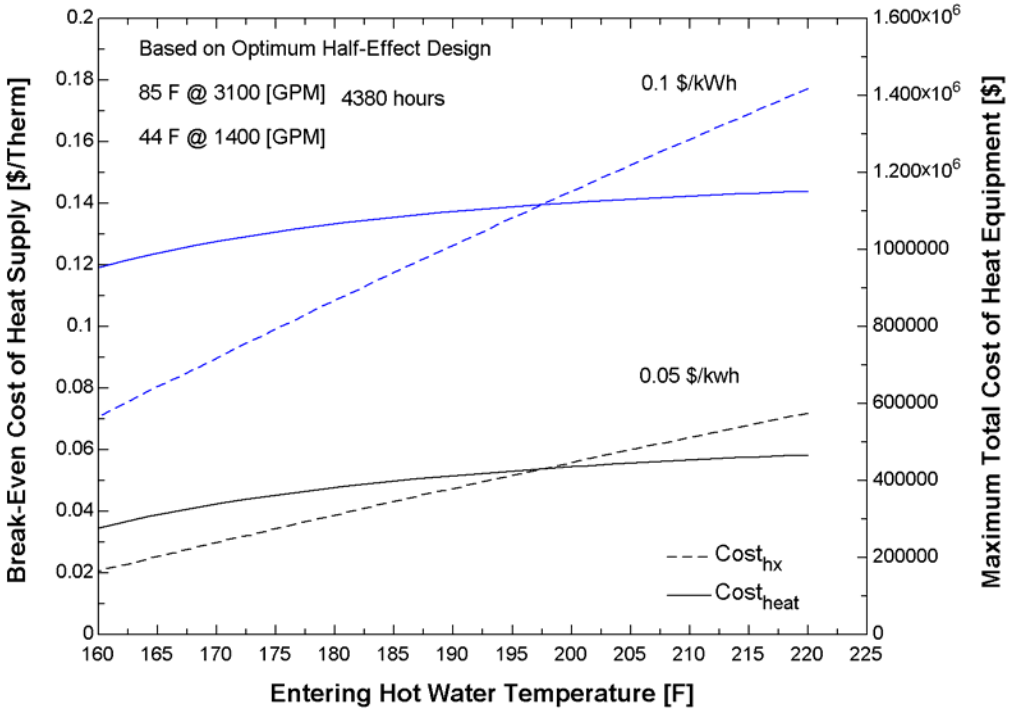

Figure 8-13. Comparison between half-effect cycle and electric centrifugal chiller.

At 200°F and 0.1 $/kWh the break-even cost of heat is approximately 0.13 $/therm.

The right axis on Figure 8-13 depicts if the heat source were free, what the heat recovery equipment would have to cost in order to provide the energy [refer to equation 6.5 in section 6.4]. For example, at 0.1 $/kWh and 200°F, the heat recovery equipment must cost less than $1.2 million in order for the project to be feasible [20 year life cycle 4380 hours of operation per year]. The term "heat recovery equipment" encompasses all the equipment needed to transfer the waste heat into a form that can be used by the absorption chiller.

The break-even cost of heat is constant for 180°F hot water temperatures and higher. The reason for this is depicted in Figure 8-14, which shows the COP and capacity as a function of heat source temperature.

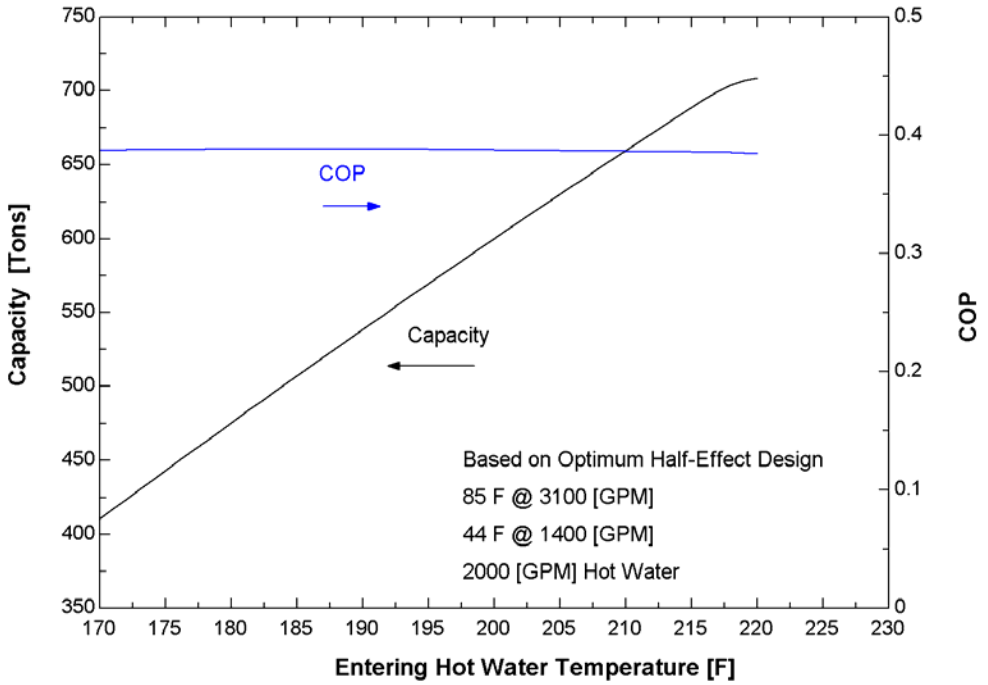

Figure 8-14. Change in capacity and COP as a function of entering hot water firing temperature.

Even though capacity is decreasing, the COP remains constant because the amount of heat input is also decreasing.

8.6 Variation of Capacity due to different operating conditions and designs.

The half-effect was designed for 200°F at 2000 gpm, but how does the performance change if the temperature of hot water flow rate is varied? Figure 8-15 displays a graph of the capacity due to different hot water flow rates. The change in the capacity is gradual due to a decrease in hot water flow rate. As the temperature of the hot water decreases so does the capacity. Therefore, an increase in UA for the generator or absorber is needed to achieve 600 tons for hot water temperatures less than °F.

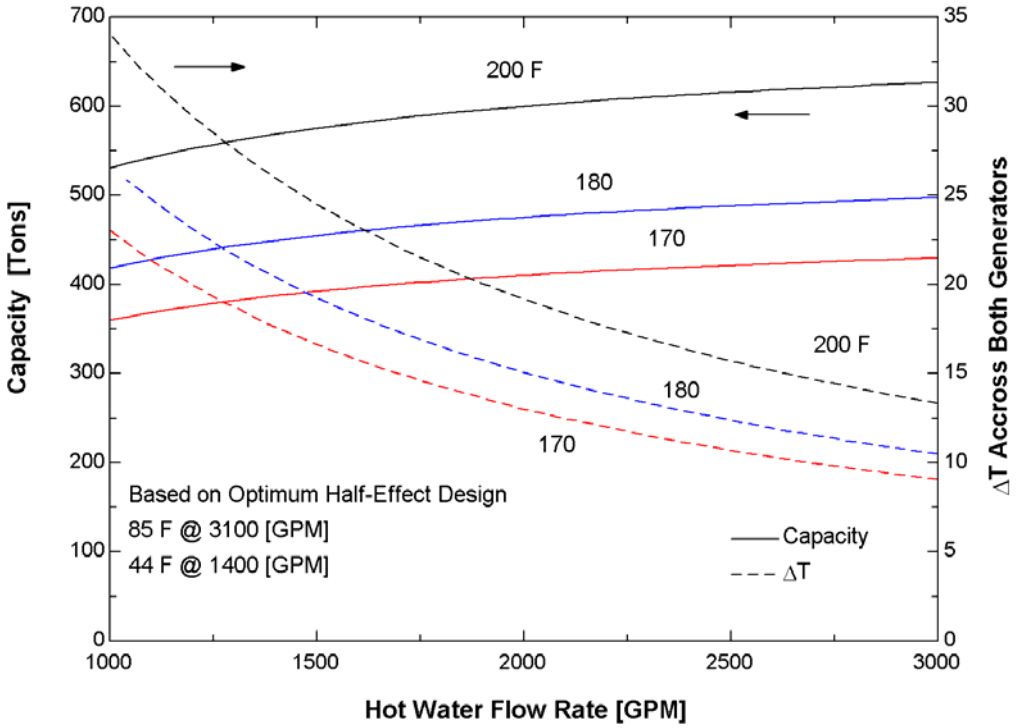

Figure 8-15. Capacity effect due to different hot water flow rates.

The right axis in Figure 8-15 represents the temperature drop across both generators. For example, at 200°F and 2000 gpm the temperature leaving the LT generator would be approximately 180°F, which corresponds to a 20°F drop across both generators.

The cooling water flow rate first enters the HC absorber, then the LC absorber and finally the condenser. In Figure 8-16 the first number represents the flow rate through the absorbers and the second number is the flow rate through the condenser. Figure 8-16 shows the effect of changing the flow arrangement by splitting the flow into two streams, one stream enters the absorber combination and the goes directly to the condenser.

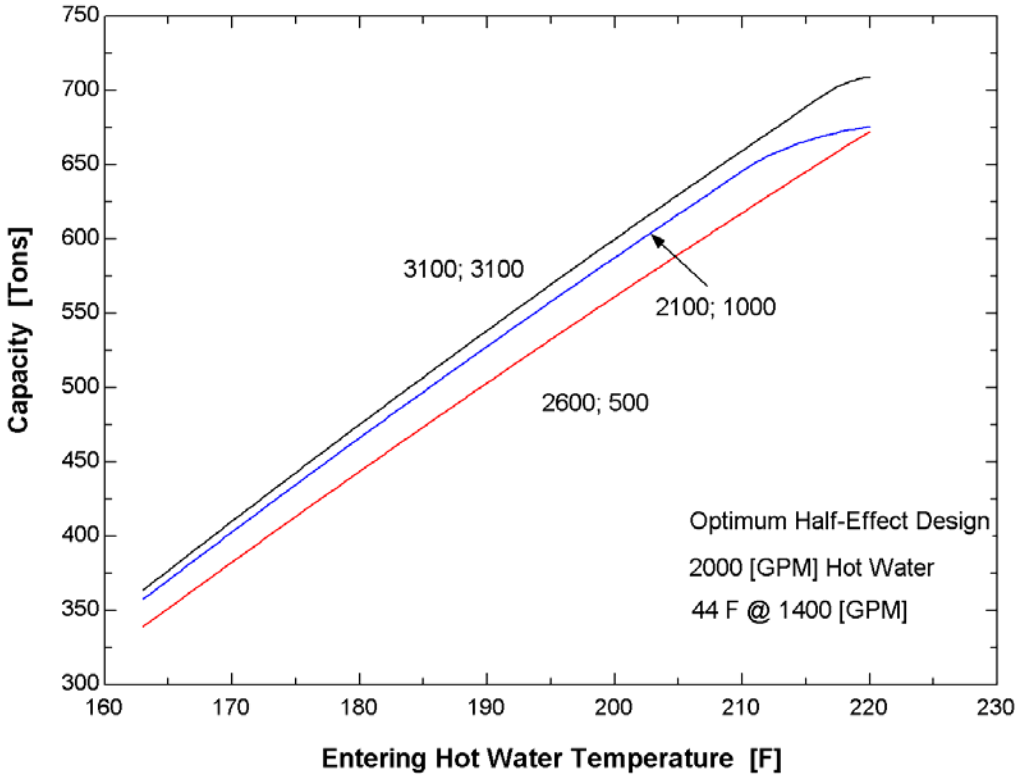

Figure 8-16. Comparison of different cooling water flow arrangements.

The base case is 85°F at 3100 gpm and the two split cases are 2100 and 2600 gpm into the absorber and 1000 and 500 gpm into the condenser. According to Figure 8-16 the best design is the base case in which the water flows in series through all three components.

The internal solution flow rate leaving the absorber can be adjusted using a variable speed pump to control capacity at part load conditions. The reason for this adjustment instead of decreasing the hot water flow rate or temperature is because the absorption chiller may be connected in a co-generation system where the heat source has a constant waste heat flow rate and requires a certain temperature on the return. Figure 8-17 and Figure 8-18 displays the effect on capacity for decreasing and increasing the flow rate leaving the absorbers.

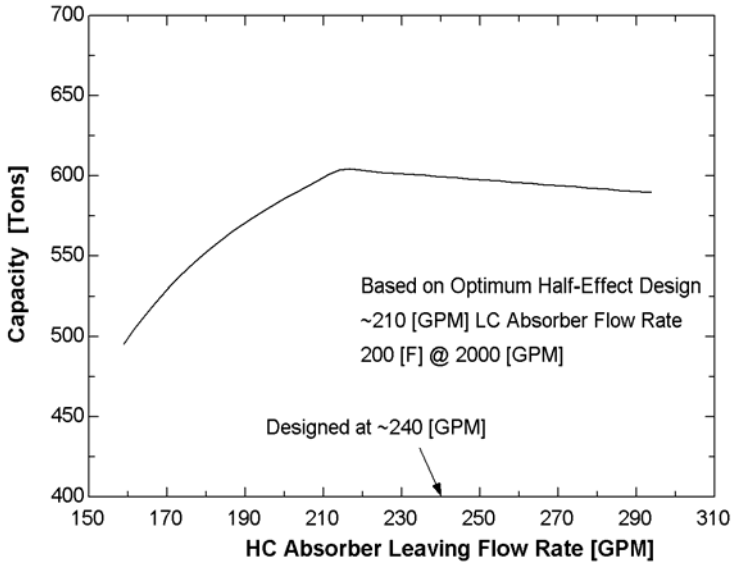

Figure 8-17. Effect on Capacity due to varying HC absorber solution flow rate.

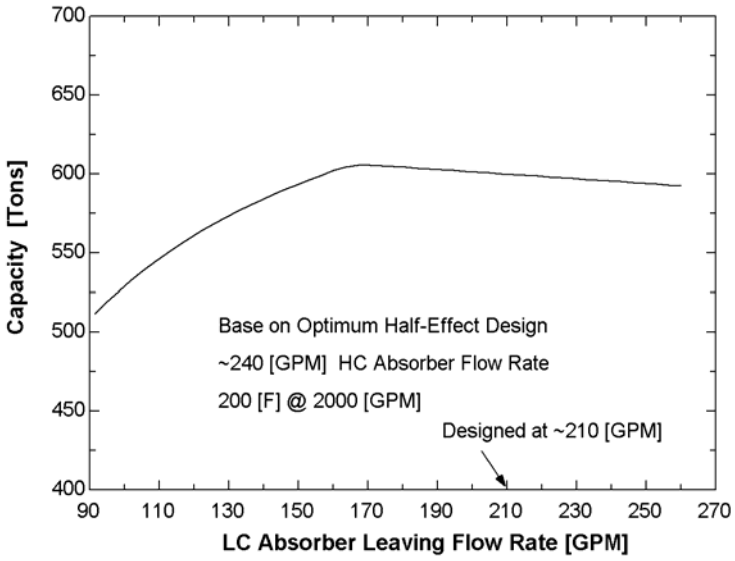

Figure 8-18. Effect on Capacity due to varying HC absorber solution flow rate.

The discontinuity in the slope in Figure 8-17 and Figure 8-18 is due to the outside heat transfer is being set to a specific value at and above a certain film Reynolds number [refer to section 3.4.3] . The left of the knee represents a heat transfer coefficient that is decreasing with film Reynolds number and the right is a constant heat transfer coefficient with an increase in film Reynolds number. Figure 8-17 and Figure 8-18 demonstrates the effect on capacity for independent changes in solution flow rate. Figure 8-19 shows the effect of reducing both internal solution flow rates by the same percentage.

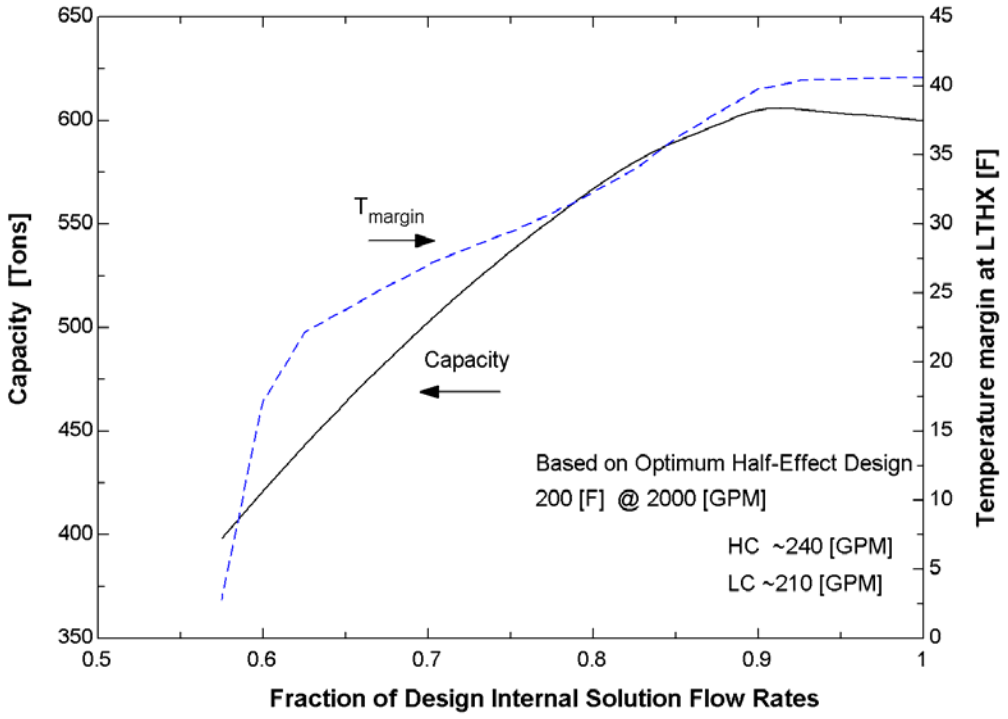

Figure 8-19. Simultaneous reduction in both internal solution flow rate.

The x-axis of Figure 8-19 is the fraction that is multiplied by the design solution flow rate. For example at 0.7 the HC solution flow rate is 168 gpm instead of 240 gpm. Reducing both flow rates did not produce a large change in the reduction of capacity compared to Figure 8-17 and Figure 8-18. For example, in Figure 8-17 at 170 gpm, the capacity is approximately 525 tons. Whereas in Figure 8-19 at 0.7 fraction, the capacity is approximately 500 tons. The only advantage of reducing both flow rates is that the HC solution flow rate could be reduced more than if the LC was held constant. An important parameter to keep track of when reducing flow rate is the temperature margin. The right axis displays the change in temperature margin as both flow rates are reduced. Operating the absorption unit with a small [5-10 ^{o}F] temperature margin is not an appropriate design because of potential problems with crystallization.

Even though the capacity is reduced in Figure 8-17 and Figure 8-18, it may not be enough for part load conditions. Another option is to increase the temperature of the cooling water to the absorber. This will have two effects: it will reduce capacity for part load and reduce fan power at the cooling tower. The different lines in Figure 8-20 represent different cooling water flow rates. By increasing the cooling water temperature, capacity can be reduced to about 450 tons. Another advantage of this technique is that the temperature margin for this analysis did not fall below 30°F.

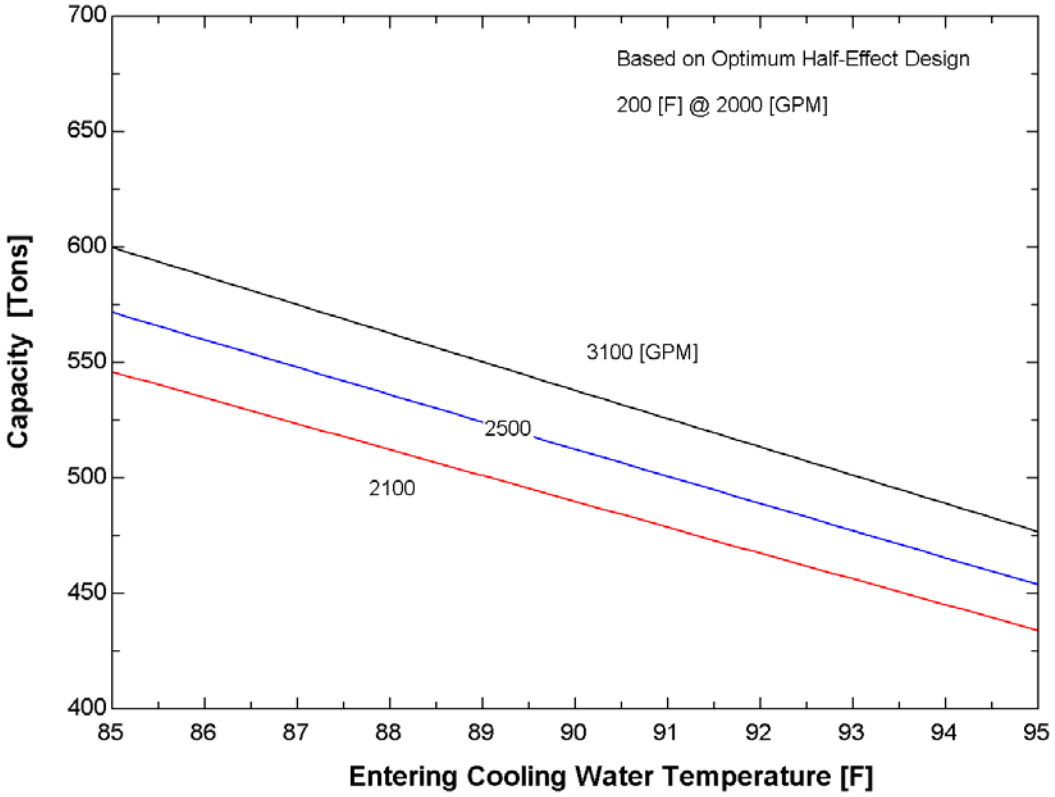

Figure 8-20. Effect on capacity due to varying cooling water temperature.

8.7 Summary

The following is a list of major conclusions regarding the analysis of the half-effect cycle in Chapter 8.

- The same optimum solution of tube fraction in the generator and absorber exists regardless of series or parallel flow arrangement with 200 ^{o}F water at 2000 gpm. If the hot water temperature is lowered, the f_{abs} changes from 0.41 to a number greater than 0.5, which means that the LC absorber is now larger than the HC absorber. On the contrary, the f_{gen} did not change.

- Similar to the findings for the single-effect cycle as the hot water flow rate increases less capital investment is required.

- The higher the hot water flow rate the lower the entering hot water temperature can go before there is a difference between series and parallel flow arrangement. At approximately 190 ^{o}F it is more economical to use series flow rather than parallel flow in the generator design.

- The addition of the cooling tower doubles the cost of the absorption chiller system.

- The half-effect cycle requires a cheap source of fuel to overcome the high capital cost and larger cooling tower. At 200 ^{o}F and 0.1 $/kWh, the break-even cost of heat is approximately 0.13 $/therm.

- The best design for cooling water flow arrangement is to have the water flow in series through the HC, followed by the LC, and then finally the condenser.

- Reducing both internal solution flow rates out of the HC and LC absorber did not produce a large change in the reduction of capacity compared to the reduction in the individual flow rates. The capacity can be reduced by 150 tons before there are problems with the temperature margin becoming to low.

- Another option to reduce capacity is to increase the temperature and/or decrease the solution flow rate of the cooling water. This will have two positive effects: it will reduce capacity for part load conditions and reduce fan power at the cooling tower, which lowers operating cost.

CHAPTER 9

COMPARISON BETWEEN HALF-EFFECT AND SINGLE-EFFECT ABSORPTION CHILLERS

9.1 Overview

The purpose of Chapters 7 and 8 were to examine the single and half-effect cycle. Chapter 9 compares the two cycles based on economics and capacity. The process is based on finding what operating conditions are favorable in the single-effect cycle compared to the half-effect cycle.

9.2 Dollar per ton for different heat source temperatures.

Figure 9-1 and Figure 9-2 compare the capital cost between the single and half-effect absorption chiller unit and system cost. The system cost consists of the absorption chiller and cooling tower. The analysis was based on holding capacity constant and allowing the generator size to vary with entering hot water temperature. Both figures demonstrate that the single-effect unit has a lower price per ton at firing temperatures above 200^{o}F.

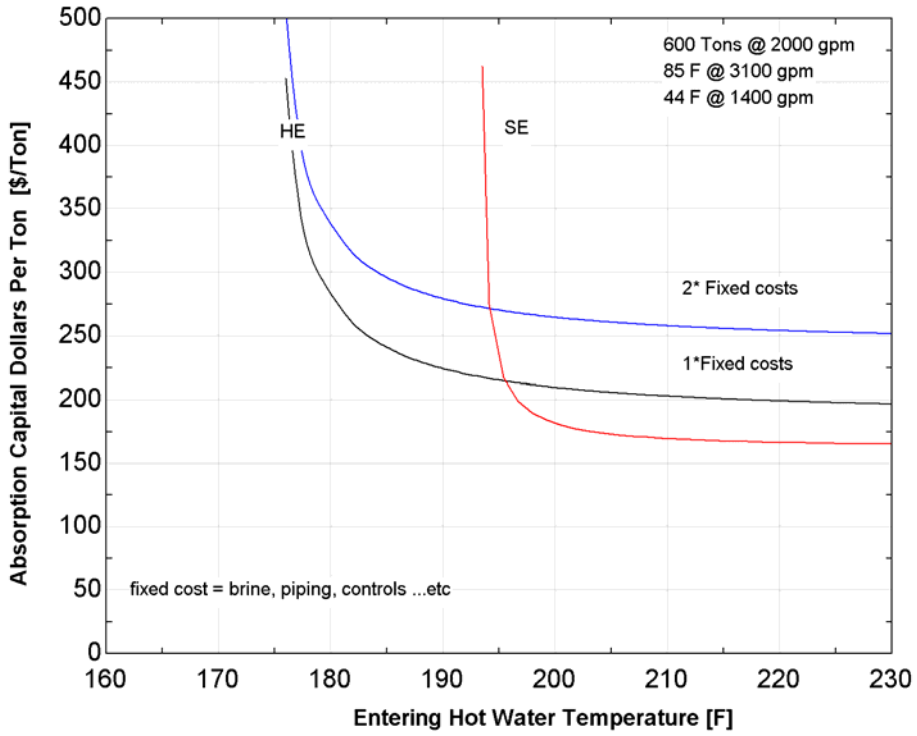

Figure 9-1. Capital dollars per ton cost comparison between single and half-effect chiller.

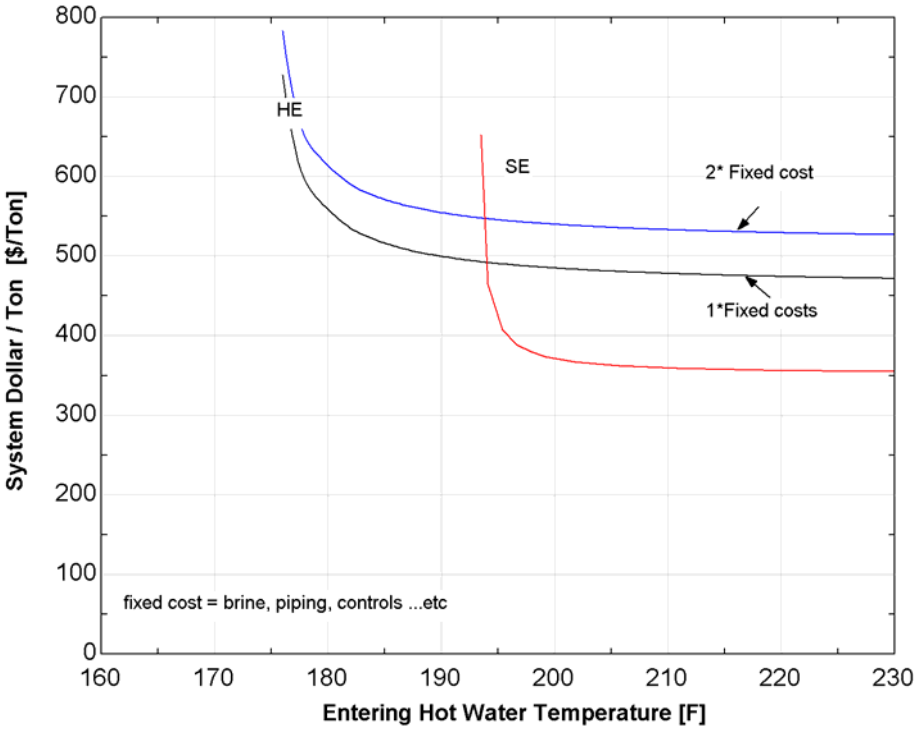

Figure 9-2. System dollars per ton cost comparison between single and half-effect chiller.

The capital cost is based on material, labor, and overhead. At around 220^{o}F, Figure 9-1 has a cost difference of about 90 $/ton for 2 times the fixed price and 30 $/ton for the equal fixed price. The system cost difference in Figure 9-2 is 180 $/ton for 2 times the fixed price and 120 $/ton for equal fixed price. An important result of Figure 9-1 and Figure 9-2 is that in the range of 195-200^{o}F at 2000 gpm, there is a transition as to which type of unit one would want to install. The assumption of fixed price does not change the transition temperature because of the steep slope for the SE unit. The lower limit based on economics for the half-effect cycle is about180^{o}F at 2000 gpm and 200^{o}F for the single-effect unit. Table 9-1 compares the capital cost between the single, half, and electric centrifugal chiller.

Table 9-1. Capital cost comparison between single-effect, half-effect, and electric centrifugal chiller [600 tons, 200^{o}F, 2000 gpm heat source]

Chiller	$/Ton Chiller	$/Ton System	Cost range of Cooling Tower	Fraction of Cooling Tower Cost
Single-Effect [Base Case]	170	363	±55	0.53
Single-Effect [finned]	185	374	±54	0.51
Single-Effect [smooth]	222	411	±54	0.46
Half-Effect	275	550	±78	0.50
Electric Centrifugal	150	285	±39	0.47

The cooling tower cost for the electric centrifugal chiller is approximately 47% of the total system cost whereas the cooling tower is about 50% of the total system cost for the absorption unit. Even for the electric centrifugal chiller the cooling tower is a major cost for

the system but the capital cost is lower. The cost range for the cooling tower is used to compare a galvanized or stainless steel constructed cooling tower.

Figure 9-3 and Figure 9-4 compares the capital and system cost for various hot water flow rates. The main conclusion from both graphs is that as the hot water flow rate is decreased, the transition to the half-effect cycle occurs at higher hot water firing temperatures. For example, at 2000 gpm the transition temperature to the half-effect is 195°F, but at 1000 gpm the temperature is 205°F.

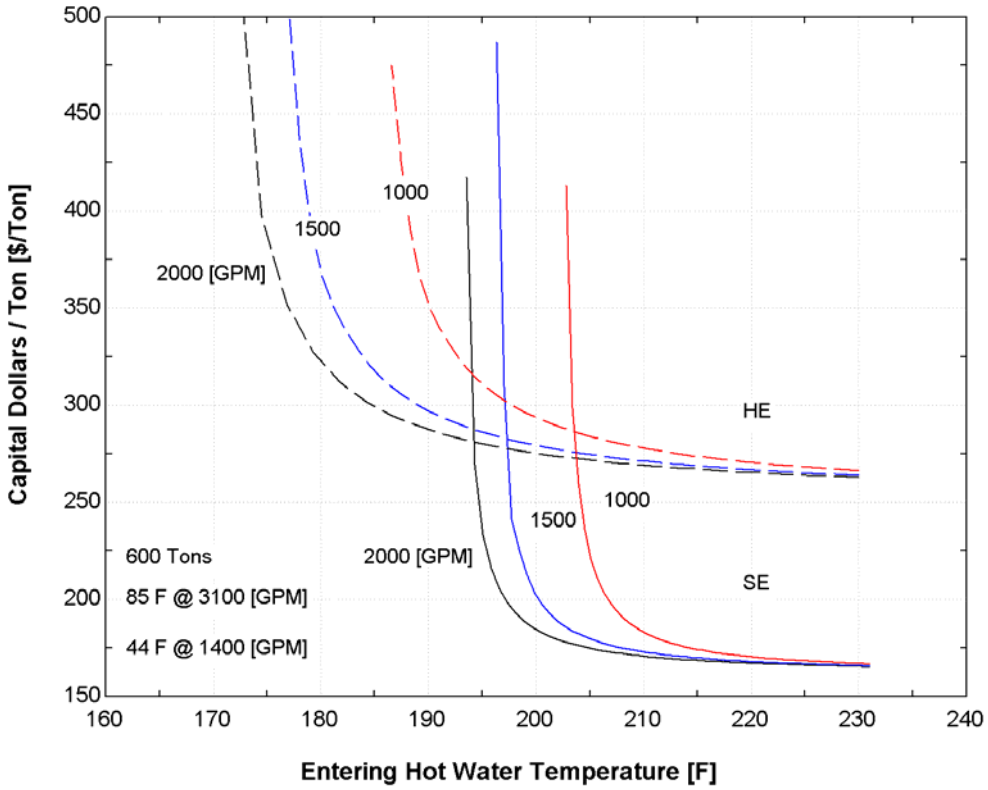

Figure 9-3. Capital dollars per ton for different hot water flow rates.

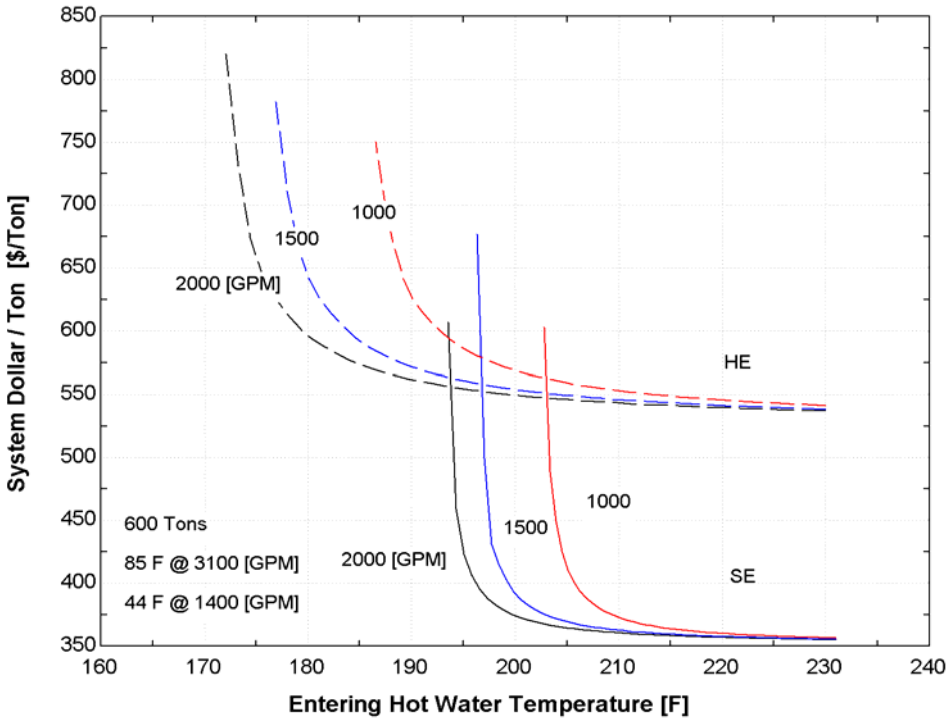

Figure 9-4. System dollars per ton for different hot water flow rates.

Figure 9-5 compares the capacity between the SE and HE cycle designs for various hot water flow rates and temperatures. Both the HE and SE at 200°F and 2000 gpm have a capacity of 600 tons. As the heat source flow rate is lowered, the temperature at which the transition to the HE having a higher capacity occurs at higher temperatures. This means the HE can achieve a higher capacity than the SE over a larger range of low-temperature and low flow rate applications.

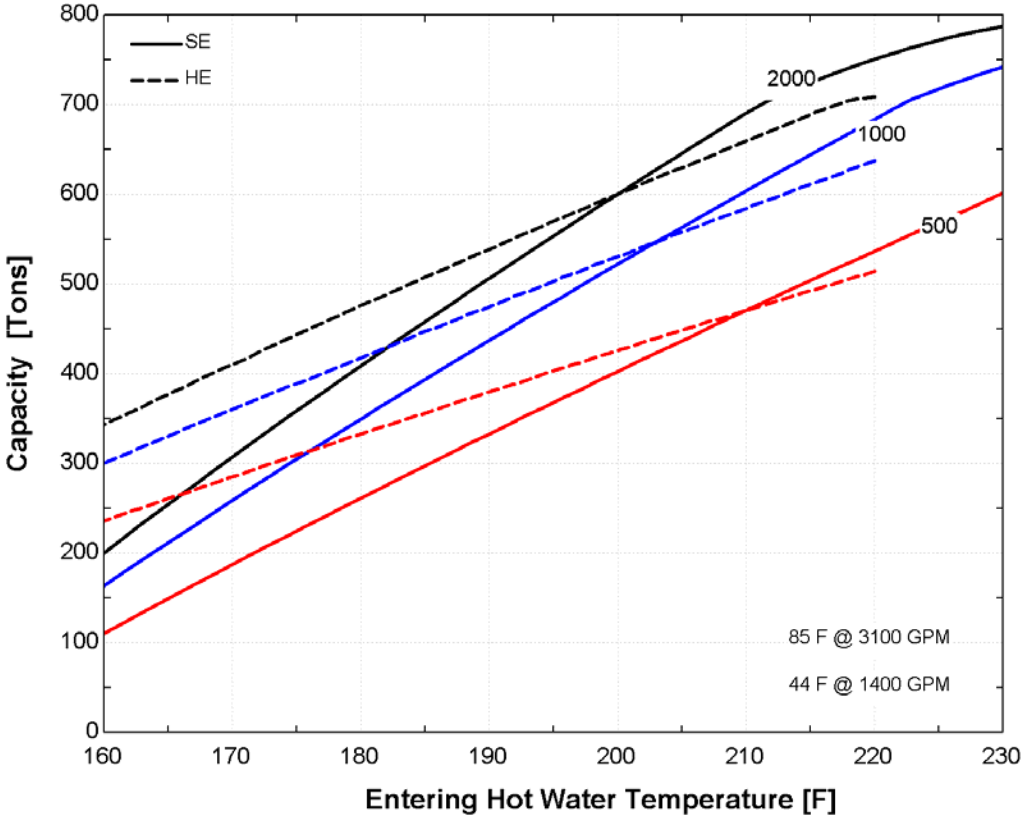

Figure 9-5. Capacity comparison between SE and HE cycle.

In other words, the HE cycle can maintain a higher capacity compared to the SE unit at lower operating temperatures and flow rates.

9.3 Break-even cost comparison.

Figure 9-6 compares the capacity and COP for the single and half-effect unit. At 200°F there is a transition to the half-effect unit having a higher capacity, which corresponds to the results in Figure 9-1. The COP for the half-effect unit is linear in the temperature range of 160-220°F, whereas at 185°F the COP starts to decrease for the SE unit.

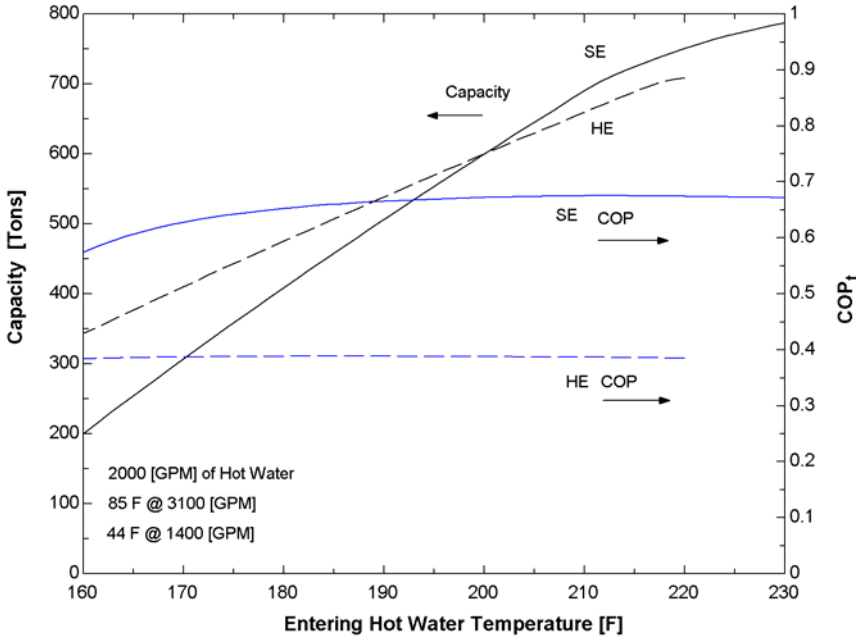

Figure 9-6. Comparison of capacity and COP for the single and half-effect absorption unit.

Another important result of Figure 9-6 is that the COP for the half-effect unit is about ½ of the single-effect. This result was seen in Figure 9-2, due to the larger cooling tower and is also present in Figure 9-7.

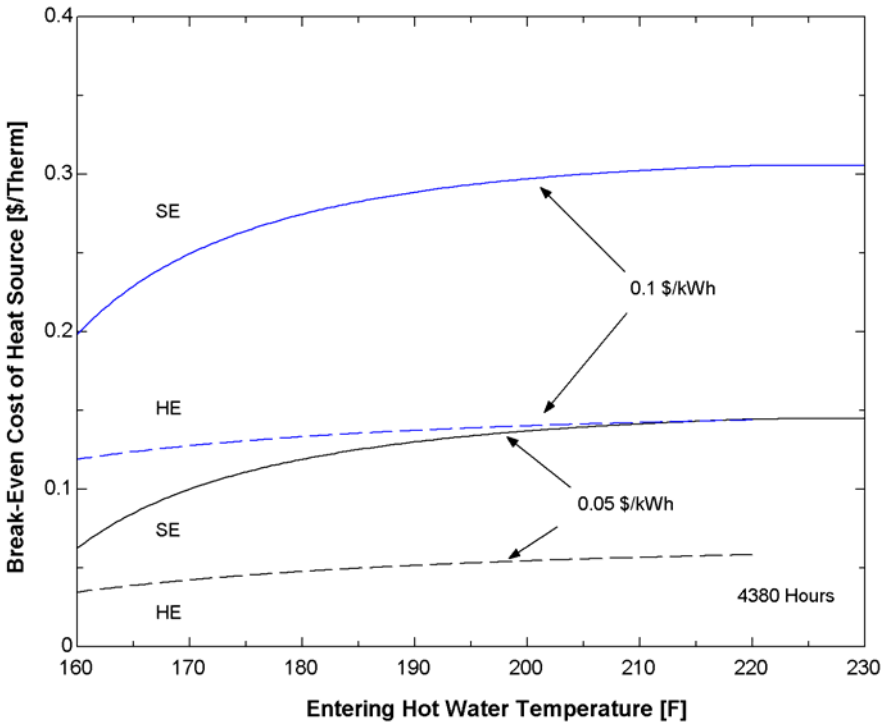

Figure 9-7. Comparison of cost of heat for the single and half-effect absorption unit.

The break-even cost of heat for the half-effect cycle is about ½ of the single-effect for the same entering hot water temperature. For example, at 200°F and 0.1$/kWh, if heat can be supplied at approximately 0.13 $/Therm then half-effect cycle has an economic advantage over the electric centrifugal chiller, whereas it is approximately 0.28 $/Therm for the single-effect cycle.

Table 9-2. Compares the life-cycle cost between the single and half-effect absorption unit. [20 year life cycle , 600 Tons, 0.05$/kWh, 200°F Hot Water @ 2000 gpm, 4380 Hours].

	SE Absorption/ Tower ≈0.14 $/Therm	HE Absorption/ Tower ≈0.05 $/Therm
Capital Cost		
Chiller	$136,048	$206,526
Tower	$170,591	$248,654
	$306,639	$455,180
Operating Cost		
Pumps	$11,430	$19,600
Heat Source	$642,100	$447,360
Tower	$72,150	$115,360
	$725,680	$582,320
Total	$1,032,319	$1,037,500

The only reason the total cost is nearly the same is that the break-even cost of heat is different. Table 9-2 demonstrates the higher capital cost required for the half-effect cycle: the main disadvantage of the half-effect cycle is that it is approximately 1.5 times more than the single-effect, the cooling tower for the half-effect is also about 1.5 times more than the single-effect, and the half-effect has a higher operating cost if the heat source were supplied at the same price. The only situation in which the half-effect cycle has an advantage is if the heat source is free and it is lower than 200°F or has a low flow rate.

Table 9-3 examines the difference in UA and tube count for each component of the single and half effect design. The main difference in the design is the number of generator tubes. The half-effect cycle is able to produce the same cooling effect with two smaller generators and a slight increase in the absorber. The total area is less for the half-effect cycle, however t the capital cost is still greater [Figure 9-1] because of the extra solution pump, heat exchanger, brine solution, increase in controls due to extra components, etc.

An interesting aspect is that the half effect cycle is able to generate the same cooling effect with approximately twice as much heat input with smaller generators to transfer the heat. The smaller generators are interesting, but twice as much heat is still needed. Even if it is free from co-generation, it still puts a burden on the system. Table 9-3 also shows that twice as much heat must be rejected to the absorber, which explains the need for a larger cooling tower.

Table 9-3. Tube and UA comparison between half and single effect unit. [600 Tons, 200°F hot water at 2000 gpm.]

	Tubes	UA [Btu/hr-F]	Energy [Mbtu/hr]	Internal solution flow rate[gpm]
Absorber SE	554	558751	9.9	230
Absorber HC, HE	350	375285	9.3	240
Absorber LC, HE	243	327870	8.9	210
Generator SE	1133 / 300	993439	10.7	
Generator HE, LT	255	283976	9.7	
Generator HE, HT	192	246966	8.9	
Condenser SE	128	882375	8.0	
Condenser HE	128	852738	7.6	
Evaporator SE	336	1.354e6	7.2	
Evaporator HE	336	1.35e6	7.2	

The ability to have smaller generators transferring the same amount of heat compared to the SE generator is due to the LT generator operating at a mid-pressure and the HT generator operating at a lower concentration. In summary, a mid pressure with a smaller surface area is as effective as a high pressure with a larger surface area.

9.4 Summary

The following is a summary of the comparison between the single and half effect absorption chiller system

- The single-effect unit has a lower price per ton at firing temperatures above 200^{o}F.
- In the range of 195-200^{o}F at 2000 gpm there is a transition from the single-effect unit to the half-effect unit being installed.
- For all systems including the electric centrifugal chiller, the cooling tower is about 50% of the total system cost. The disadvantage for absorption unit is that the capital cost is higher because of the lower COP.
- The half-effect cycle can achieve a higher capacity compared to the single-effect over a larger range of low temperature and low flow rate applications.
- The only way in which the half-effect cycle is advantageous compared to over the single-effect cycle is if the heat source is relatively free and it is lower than 200^{o}F or has a low flow rate.
- The break-even cost of heat for the half-effect cycle is about ½ the cost of the single-effect for the same entering hot water temperature.
- Desorption is most effective at lower pressures and lower concentrations, which explains why the half-effect cycle can operate with smaller generators compared to the single-effect unit.

CHAPTER 10

CONCLUSIONS AND RECOMMENDATIONS

10.1 Conclusions

The following is a list of important conclusions from the study of low-temperature absorption chiller systems.

- From examining the published literature, the single-effect unit finds applications in co-generation, geothermal energy, and combined heating and cooling plants. The best method for designing a single-effect unit to operate on low heat source temperatures is to examine the heat exchanger area of all components.

- Holding capacity constant [600 tons], at 205^{o}F the base case chiller size starts to change rapidly in generator heat exchanger area to accommodate the lower firing temperatures.

- Based on the assumption that finned tubes cost twice as much as smooth tubes, the reduction in generator tubes using finned tubes is enough to compensate for the higher price.

- The new low temperature single-effect absorption unit was designed by increasing the number of tubes in the generator [262 $\rightarrow$ 300], using finned tubes instead of smooth tubes, increasing the number of tubes in the absorber [514 $\rightarrow$554], and increasing low temperature heat exchanger effectiveness [0.76 $\rightarrow$ 0.8.].

- The new low temperature single-effect hot water design has an increase of 15 $/ton to obtain a capacity of 600 tons with 200^{o}F, compared to 227^{o}F hot water at 2000 gpm.

- The optimum value for the cooling water flow rate is independent of the heat source temperature.

- The cost of the absorption chiller system for the single and half-effect has approximately doubled due to the cooling tower. This is also true for an electric centrifugal chiller but the capital investment for the cooling tower in the SE is $170,000 compared to $80,000 for the electric chiller.

- If the heat source can be supplied at a cost less than or equal to approximately 0.28 $/Therm when electricity is 0.1 $/kWh then absorption is the preferred alternative [based on 600 tons capacity with 2000 gpm hot water].

- The half-effect cycle requires a cheap source of fuel to overcome the high capital cost and larger cooling tower. At 200^{o}F and 0.1 $/kWh, the break-even cost of heat is approximately 0.05 $/therm.

- The cost of heat for the absorption chiller is 90% of the total operating cost over one year. Thus, using absorption with co-generation is one of the only feasible situations where it would be more economically competitive than current centrifugal chillers. The other situation is high electrical cost.

- The best design for the cooling water flow arrangement in the half-effect cycle is to have the water flow in series through the HC, followed by the LC, and finally then the condenser.

- One option to reduce capacity in the half-effect cycle is to increase the temperature and/or decrease the solution flow rate of the cooling water. Using cooling water at 95 ^{o}F, 2100 gpm reduces the capacity to 450 tons. This technique will have two positive effects: it will reduce capacity for part load conditions and reduce fan power at the cooling tower, which lowers operating cost. Another option is to use variable speed pumps for the HC and LC absorber solution flow rates. Decreasing both solution flow rates can lower the capacity to 450 tons without the temperature margin decreasing below 10 ^{o}F.

- The single-effect unit has a lower price per ton compared to the half-effect cycle for firing temperatures above 200^{o}F.

- In the range of 195-200^{o}F at 2000 gpm there is a transition from the single-effect unit to the half-effect unit being installed.

- The half-effect cycle can achieve a higher capacity compared to the single-effect cycle over a larger range of low temperature and low flow rate applications.

- The only advantage of the half-effect cycle over the single-effect cycle occurs if the heat source is free and it is lower than 200^{o}F or has a low flow rate.

- The break-even cost of heat for the half-effect cycle is about ½ the cost for the single-effect for the same entering hot water temperature.

- The total number of tubes for the half-effect cycle is less then the single-effect cycle even though the heat transfer in the generator and absorber is twice as much. This result is due to the fact that desorption is most effective at lower pressures and lower concentrations. The half-effect unit cost more because it requires at minimum one additional pump, another brass plate heat exchanger, additional brine solution, additional control equipment, piping…etc.

10.2 Recommendations

Each component was modeled based on an inside and outside heat transfer coefficient. One detail of further study would be to examine the effect of changing the tube arrangement in each component. This analysis would involve determining the dependence of tube arrangement on the outside heat transfer coefficient. For example, in the condenser, as the fluid condenses on the pipes, there is an increase in the thickness of the liquid as it falls down the pipe. This has the effect of decreasing the heat transfer coefficient along a tube column.

With the completion of designing the single and half-effect cycle for low temperature applications, an analysis with case studies would give another perspective on possible applications. The analysis of this paper involved looking at constant cooling loads for 8760 hours per year and 4380 hours per year. A case study involving a building with a cooling and electrical load would help determine the viability of an absorption unit for co-generation. Another approach would be to contact industries to determine their waste heat output and if there is a need for cooling in the area.

REFERENCES

Electrical Research Association, (1967). 1967 Steam Tables, Thermodynamic Properties of Water and Steam; Viscosity of Water and Steam, Thermal Conductivity of Water and Steam, Edward Arnold Publishers, London.

Beckman W. A., and Duffie J. A. (1991). Solar Engineering of Thermal Processes, John Wiley & Sons.

Braun J. E., Klein S. A., and Mitchell J. W. (1989). "Effectiveness models for cooling towers and cooling coils." ASHRAE Trans., 96, 164-174.

Bruno J.C., Fernandez F., and Castells F. (1996). "Absorption Chillers Integration in a Combined Heat and Power." Ab-Sorption, 2, 759-767.

Marley Cooling Tower Company, (1998). "UPDATE [Unitary Product Data and Thermal Evaluation]." , Overland Park.

Cosenza F., and Vliet G.C. Ph.D. (1990). "Absorption in Falling Water/LiBr Films on Horizontal Tubes." ASHRAE Transaction, 96, 693-701.

Erickson D.C., (1995). "Waste-Heat-Powered Icemaker for Isolated Fishing Village." ASHRAE Transactions, 101(Part 1), 1185-1188.

Fairchild M., (2000). "Marley Cooling Tower Company."

ASHRAE Handbook, (1989). "Fundamentals I-P." , American Society of Heating, Refrigerating, and Air-Conditioning Engineers, Inc., Atlanta.

Herold K.E., Radermacher R., and Klein S.A. (1996). Absorption Chillers and Heat Pumps, CRC Press.

Homma R., Nishiyama N., and Wakimizu H. "Simulation and Experimental Research of Single-Effect Absorption Refrigerators Driven by Waste Hot Water." Proceedings of the International Absorption Heat Pump Conference, New Orleans, Louisiana, 273-278.

IEA District Heating and Cooling (1999). "District Cooling, Balancing the Production and Demand in CHP." Novem, Netherlands, 1-180.

RS Means Co. Inc., (1998). Mechanical Cost Data HVAC & Controls, .

Incropera F.P., and DeWitt D.P. (1996). Fundamentals of Heat and Mass Transfer, John Wiley & Sons.

Kececiler A., Acar H., and Dogan A. (1999). “Thermodynamic analysis of the absorption refrigeration system with geothermal energy: an experimental study.” Energy Conversion and Management, 41(1), 37-48.

Koeppel, E. A. (1994). “The Modeling, Performance, and Optimal Control of Commercial Absorption Chillers,” MS, UW Madison, Madison.

Lamp P., and Ziegler F. (1996). “Comparison of different liquid and solid sorption systems with respect to low temperature driving heat.” Ab-Sorption, 1, 269-276.

MA W.B., Xia H.W., and Deng S.M. “Industrial Application of a Two-Stage, Half Effect LiBr/H20 Absorption Chiller.” Ab-Sorption, Montreal, Quebec, Canada, 679-683.

U.S Chiller Manufacturer, (2000).

Meloche N., Larsson I., and Snoek C. (1996). “Integrating District Cooling with Combined Heat and Power.” Ab-Sorption, 2, 795-802.

Plzak, B. “Absoprtion Cooling Demonstration and Application.” Ab-Sorption, Montreal, Quebec, Canada, 67-74.

Rohensenow W.M., Hartnett J.P., and Cho Y.I. (1998). Handbook of Heat Transfer, McGraw-Hill Handbooks.

Schweigler C., Demmel S., and Ziegler F. “Single-Effect/Double-Lift Chiller: Operational Experience and Prospect.” Proceedings of the International Sorption Heat Pump Conference, Munich, Germany, 533-539.

Thornbloom M.D., and Nimmo D.G. “Modification of the Absorption Cycle for Low Generator Firing Temperatures.” Solar Engineering, San Francisco, CA, 367-372.

Wang C., Zhen Lu, and Zhou J. “Enhancement of Heat and Mass Transfer in Lithium Bromide Falling Film Generator.” Proceedings of the International Sorption Heat Pump Conference, Munich, Germany, 301-305.

APPENDIX A CD-ROM FILES

EES Code

The folder EES code contains the model for the single and half-effect absorption chiller. The folder also contains the component subroutines that the single and half-effect model calls.

Functions

Tseq.txt	Equilibrium temperature of LiBr-water solution
Tveq.txt	Equilibrium temperature of Water
reynolds_dg.txt	Reynolds number
libr_cp.txt	Specific heat for LiBr-water solution
libr_con.txt	Conductivity for LiBr-water solution
libr_den.txt	Density for LiBr-water solution
libr_vis.txt	Viscosity for LiBr-water solution
xeq.txt	Equilibrium concentration for LiBr-water solution
libr_Tc2.txt	Crystallization temperature using Trane UCP2 controller
libr_Tcry.txt	Crystallization temperature using Foote Mineral Co. correlation
hfo_abs.txt	Outside heat transfer coefficient for absorber
UALTHX.txt	Brass plate heat exchanger model
massflow.txt	Internal mass flow rate leaving the absorber control
generatorNTU.txt	Calculates NTU for cross or counter flow heat exchanger
CoolingTowerSelection.txt	Different cooling tower parameters.
Generatortype.txt	Control for generator type, steam or hot water.
tubetype.txt	Control for generator tube type, smooth or finned tube

Modules

CoolingTowerMod.txt	Cooling tower model for absorption unit
CoolingTowerModVC.txt	Cooling tower model for electric chiller
generator.txt	Absorption generator UA model
absorber.txt	Absorption absorber UA model
condenser.txt	Absorption condenser UA model
evaporator.txt	Absorption evaporator UA model
vaporcompression.txt	Vapor compression model, not used but still good
pump.txt	Pump model used to calculate the pump power

Cooling Tower Performance Curves

In the Marley folder there is a program named Update.exe that provide performance curves for a specific cooling tower. The program can also be used to determine the fan power required for a specified capacity.

Electronic Word Document

An electronic copy of the master's thesis is provided.

Miscellaneous Folder

The folder contains EES, Excel and Word programs. For example an EES program to produce Dühring plots.